Recombinant Lysine:N^6-Hydroxylase: Conformational Response to Cys→Ala Substitutions and Interaction with its Ligands

by

Scott Dick

A thesis
presented to the University of Waterloo
in fulfillment of the
thesis requirement for the degree of
Doctor of Philosophy
in
Chemistry

Waterloo, Ontario, Canada, 2001

The University of Waterloo requires the signatures of all persons using or photocopying this thesis. Please sign below, and give address and date.

Abstract

Recombinant lysine:N^6-hydroxylase (*r*IucD) catalyses the conversion of L-lysine to its N^6-hydroxy derivative and requires flavin adenine dinucleotide (FAD) and the reduced form of nicotinamide adenine dinucleotide phosphate (NADPH) for its catalytic function. Previous studies had revealed that, of the five cysteine residues present in *r*IucD, two of them were susceptible to alkylation with iodoacetate and three such residues were amenable to modification by 5,5'-dithiobis-(2-nitrobenzoic acid), DTNB, with the concomitant loss of lysine monooxygenase function. Furthermore, two of *r*IucD's alkylatable cysteine residues, Cys51 and Cys158, could be replaced, by alanine, without adverse effect on the catalytic function (L. Marrone and T. Viswanatha, *Biochim. Biophys. Acta* **1343**, 263-277, 1997).

In the current investigations, the effect of individual replacement of *r*IucD's Cys31, Cys146, and Cys166 with alanine on the protein's structural integrity and catalytic function was examined by monitoring T_M using differential scanning calorimetry and lysine:N^6-hydroxylase activity respectively. Each of these substitutions appeared to lead to a slight decrease in the stability of the protein, as indicated by a lower T_M relative to that of the parent protein. Interestingly, the Cys166→Ala substitution, which was found to be accompanied by the largest decrease in T_M (-2.4 K), had no significant effect on the protein's catalytic function. In contrast, Cys146→Ala replacement, which results in a relatively much lower decrease in T_M (-0.8 K), was accompanied by profound conformational changes as indicated by approximately 50% reduction in monooxygenase activity and the ready accessibility of the remaining cysteine residues to chemical modification.

Ligand-induced conformational changes in *r*IucD were assessed by monitoring its CD spectra, DSC profile, and susceptibility to both endo- as well as exopeptidases. The first two methods indicated the absence of any significant conformational change in *r*IucD, while the last approach revealed that FAD, and its analog ADP, can protect the protein from the deleterious action of proteases. NADPH was partially effective and L-lysine was ineffective in this regard. Deletion of the C-terminal segment, either by treatment with carboxypeptidase Y or by mutagenesis of *iucD*, results in the loss of *r*IucD's monooxygenase activity. These findings demonstrate the crucial role of the C-terminal segment in maintaining *r*IucD in its native conformation.

Acknowledgements

I would like to express my deepest gratitude to Dr. T. Viswanatha for his astute guidance, encouraging support and tireless spirit throughout the duration of my research in his laboratory. I would also like to express my appreciation to Dr. J.F. Honek, Dr. G.I.. Dmitrienko, Dr. J.R. Lepcok, and Dr. R.A.B. Keates for their time and advice.

I would like to thank Dr. P. Frey (L-β-lysine), Dr. N.L. Benoiton (α-N-methyllsyine), Dr. B.A.K. Chibber (synthesis of C-peptide), Dr. B. M. Martin (amino acid analysis), Dr. H.E. Frey (DSC), Dr. H. Duewel (synthesis of DL-*cis*-4,5-dehydrolysine, K_D determination), Dr. P. Sampson and Dr. J.F. Honek (methionine analogs), Ms. J. McCourt (Western blotting) and Dr. J.G. Guillemette (for CD and thermocycler as well as helpful discussions). Thank are also due to Dr. E. Daub and Sue Clugston for their advice in many different areas. Many thanks to Dr. S. Siemann for his advice and interesting discussions. Special thanks to Dr. L. Marrone for teaching and guiding me through the initial phases of this research and for the technical assistance and invaluable discussions.

I would also like to thank Dr. E.M. Meiering, Dr. J.F. Honek and Dr. J.G. Guillemette for the use of equipment in their laboratories. Thanks to the members of the Meiering (Joe, Jessica, Scott, and Chengsong), Honek (Sue, Pete, Mark, and Jen), and Guillemette (Heather and Elena) groups and members of the Viswanatha group (Dr. M. Beecroft, Dr. H. Duewel, and Jen McCourt), for their camaraderie and assistance during the course of this work.

To my parents who have supported me in every respect without question, my debt of gratitude is beyond measure. I wish to express my thanks and best wishes to Jeff, my brother, and his new family for providing me with a welcome distraction now and then.

Finally, I would like to express my heartfelt appreciation to Tracy Kerr for her constant support, understanding and devotion for all these years. Thank-you.

Table of Contents

List of Figures

List of Schemes

List of Tables

Abbreviations Used

ADP	adenosine diphosphate
BSA	bovine serum albumin
C31A *r*IucD	Cys31Ala recombinant lysine:N^6-hydroxylase mutein
C51A *r*IucD	Cys51Ala recombinant lysine:N^6-hydroxylase mutein
C146A *r*IucD	Cys146Ala recombinant lysine:N^6-hydroxylase mutein
C158A *r*IucD	Cys158Ala recombinant lysine:N^6-hydroxylase mutein
C166A *r*IucD	Cys166Ala recombinant lysine:N^6-hydroxylase mutein
C31A/C51A *r*IucD	Cys31Ala/Cys51Ala recombinant lysine:N^6-hydroxylase mutein
C51A/C158A *r*IucD	Cys51Ala/Cys158Ala recombinant lysine:N^6-hydroxylase mutein
C51A/C166A *r*IucD	Cys51Ala/Cys166Ala recombinant lysine:N^6-hydroxylase mutein
CD	circular dichroism
CPDA	carboxypeptidase A
CPDB	carboxypeptidase B
CPDY	carboxypeptidase Y
DFP	diisopropylfluorophosphate
DNA	deoxyribonucleic acid
DNAase	deoxyribonuclease I
dNTP	deoxynucleotide triphosphate
DPIP	2,6-dichlorophenol indophenol
DSC	differential scanning calorimetry
DTNB	5,5'-dithiobis(2-nitrobenzoic acid)
DTT	DL-dithiothreitol
EDTA	ethylenediamine tetraacetic acid
ε_M	molar extinction coefficient
FAD	flavin adenine dinucleotide (oxidised form)
$FADH_2$	flavin adenine dinucleotide (reduced form)
G-6-P	glucose-6-phosphate
GDP	guanosine diphosphate
HEPES	N-(2-hydroxyethyl)piperazine-N'-(2-ethanesulfonic acid)
*iuc*A and *iuc*C	genes encoding for aerobactin synthase
*iuc*B	gene encoding for acetyl transferase
*iuc*D	gene encoding for lysine:N^6-hydroxylase
IucD	lysine:N^6-hydroxylase, *iuc*D gene product
K_D	dissociation constant
lacZ	gene encoding for β-galactosidase
mutein	protein containing amino acid replacement(s)
$NADP^+$	nicotinamide adenine dinucleotide phosphate (oxidised form)
NADPH	nicotinamide adenine dinucleotide phosphate (reduced form)
pAT5	plasmid bearing *r*IucD
PIPES	piperazine-N,N^6-bis(2-ethanesulfonic acid)
PMSF	phenylmethanesulfonyl fluoride
RNAase	ribonuclease A
*r*iucD	recombinant gene encoding for lysine:N^6-hydroxylase
*r*IucD	recombinant cytoplasmic lysine:N^6-hydroxylase

*r*lucD Δ8	Leu418ter recombinant lysine:N^6-hydroxylase mutein
*r*lucD Δ11	Pro415ter recombinant lysine:N^6-hydroxylase mutein
*r*lucD Δ14	Leu412ter recombinant lysine:N^6-hydroxylase mutein
*r*lucD Δ17	Leu409ter recombinant lysine:N^6-hydroxylase mutein
SBTI	soybean trypsin inhibitor
SDS-PAGE	sodium dodecylsulfate polyacrylamide gel electrophoresis
SOD	superoxide dismutase
TAE	Tris/acetic acid/EDTA buffer
TCA	trichloroacetic acid
TFA	trifluoroacetic acid
TLCK	N-tosyl-L-lysine chloromethyl ketone
TPCK	N-tosyl-L-phenylalanine chloromethyl ketone
Tris (Trizma base)	Tris(hydroxymethyl) aminomethane
*wt*lucD	wild type (membrane associated) lysine:N^6-hydroxylase

1.0 Introduction

The dependence of all forms of life on iron, regardless of their status in evolutionary development, hardly needs to be stressed. Iron, by virtue of its presence in a number of biologically active substances is involved in multiple functions (DNA replication, O_2 transport, electron transfer, detoxification reactions, etc.) that are vital both to the sustenance as well as to the propagation of life. Although the fourth most abundant element on our planet, its bioavailability is highly restricted due to its presence predominantly in the Fe(III) oxidation state, as $Fe(OH)_3$. In this form it is virtually insoluble ($K_{sp} \approx 10^{-38}$ M^4) under physiological conditions. The equilibrium concentration of free iron at physiological pH is $\approx 10^{-18}$ M and this level is far too low to support growth of even the simplest microorganism (1-4). Hence, it is not surprising to find that living systems have developed novel mechanism(s) not only for sequestering this element from their environment, but also for minimising its loss following uptake.

When confronted with iron starvation, miccroorganisms respond with elegant strategies to fulfil their requirement for the metal. One such strategy for iron acquisition involves the production of siderophores, compounds of low molecular weight and high affinity for ferric iron (5). The primary function of these siderophores concerns the retrieval of iron from the environment for fulfilling the requirement of the parent organisms. In general, the uptake of iron bound to siderophores is a receptor mediated and an energy dependent process (6).

The identification of siderophore mediated iron uptake in microorganisms was made possible by the initial finding of ferrichrome in the culture fluids of *Ustilago sphaerogena* (7,8). This pioneering contribution by Neilands in 1952 set the stage for research endeavours

which have resulted in the isolation and characterisation of siderophores with diverse structural features from a wide variety of microorganisms (9-11). Chemical syntheses of many of these siderophores have been accomplished (12-19). Based on the functional groups that serve as ligands for the metal, the siderophores would appear to fall into three distinct categories. These are: (i) hydroxamates; (ii) catecholates; and (iii) the mixed type with more that one kind of ligand for the metal. Structures of some of these are presented in Figures 1A and 1B.

1.1 Aerobactin

Aerobactin, a mixed type siderophore, is of particular interest to our investigation. As shown in Figure 2, this siderophore comprises two residues of N^6-acetyl-N^6-hydroxylysine which are condensed to the distal carboxyl functions of citric acid (20). It forms a 1:1 octahedral complex with ferric iron (Figure 2). The observation that aerobactin mediated iron uptake system encoded by pColV plasmids forms the basis for virulence in the invasive strains of *Escherichia coli* provided an impetus for further investigations on the genetic basis governing the phenomenon (21,22). The ability of this siderophore, upon release, to retrieve iron from the environment and even from transferrin would appear to be responsible for its functioning as a virulence determinant in pathogenic organisms (23).

Elegant work by both Braun and co-workers (24,25) as well as by Neilands and his colleagues (26,27) has led to the identification of five genes in the aerobactin operon, of which four encode for enzymes participating in the biosynthesis of aerobactin, while the fifth encodes for the protein involved in the transport of the ferric iron-siderophore complex. These genetic investigations and the biochemical studies in this laboratory (28) provided insights into the sequence of events in the biosynthesis of the siderophore (Figure 3). Thus, the initial step in aerobactin biosynthesis concerns the N^6-hydroxylation of

Figure 1A: **Structures of some representative hydroxamate siderophores** (10)

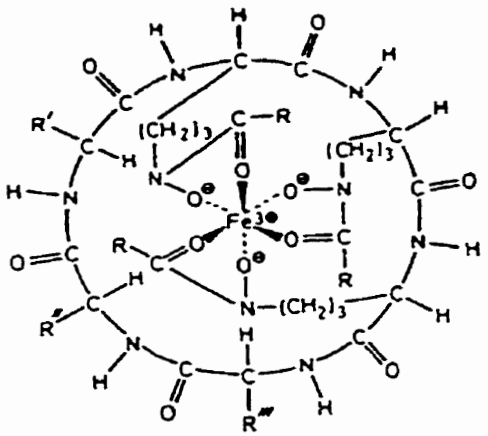

Ferrichrome
(R=CH_3, R'=R"=H)

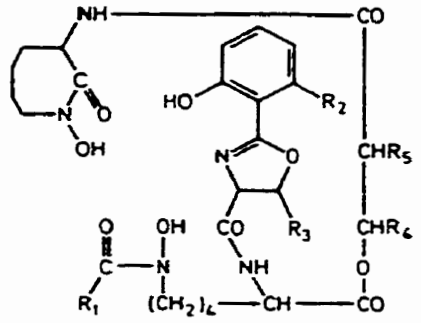

Mycobactin
$R_1=C_nH_m$, $R_2=R_5=CH_3$, $R_4=C_2H_5$ (n≥12)

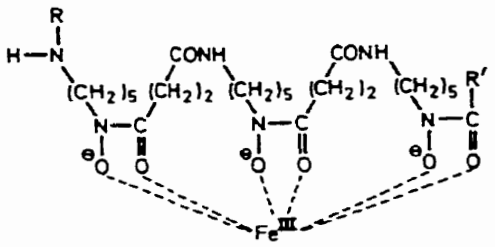

Ferrioxamine B
R=H, R'=CH_3

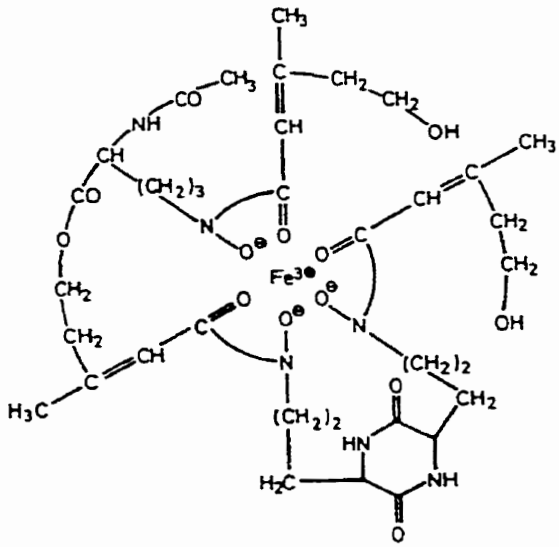

Coprogen

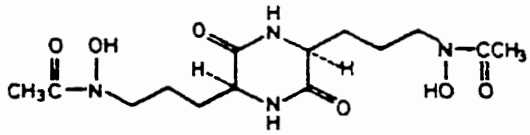

Rhodotorulic acid

Figure 1B: **Structures of some representative catecholate and mixed type siderophores** (10)

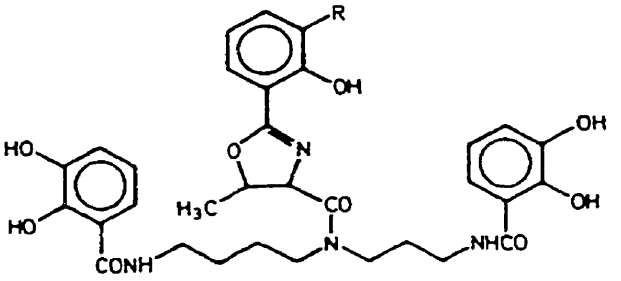

Agrobactin (R=OH)
Parabactin (R=H)

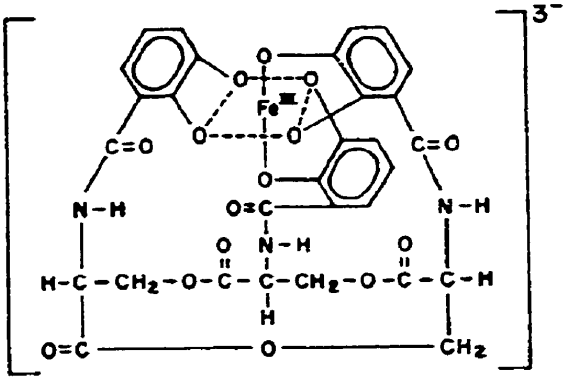

Enterobactin

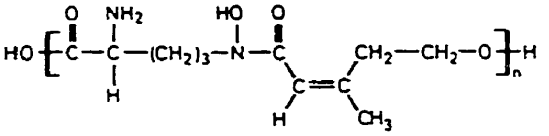

Fusarinine C (n=3)

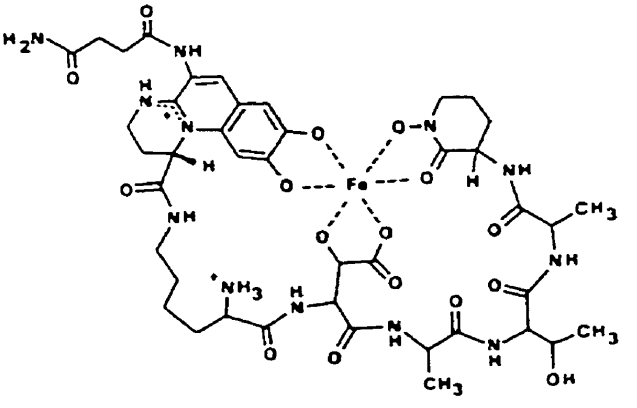

Pseudobactin

Figure 2: **Structure of aerobactin and ferric aerobactin**

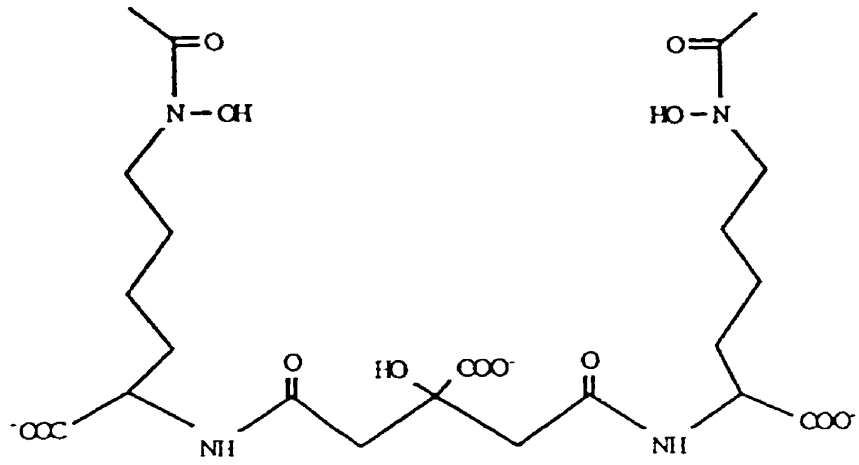

Aerobactin

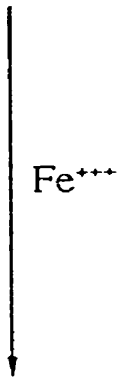

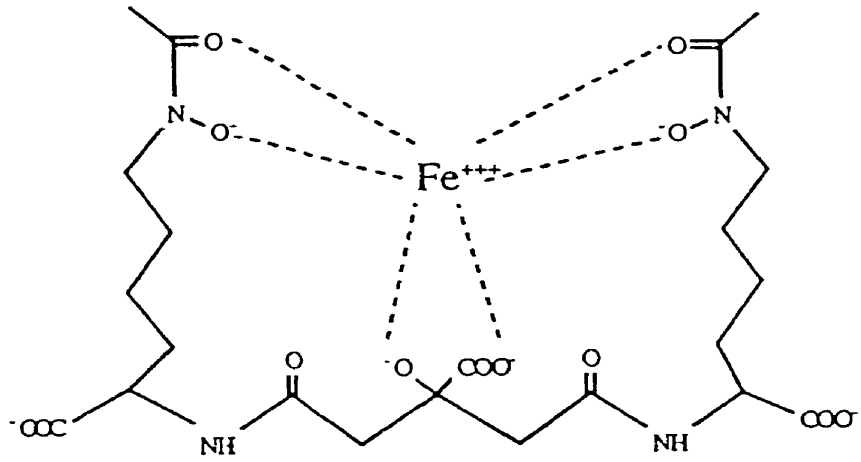

Ferric-aerobactin

Figure 3: **Genes in the aerobactin operon and the enzyme catalysed reactions in the biosynthesis of aerobactin**

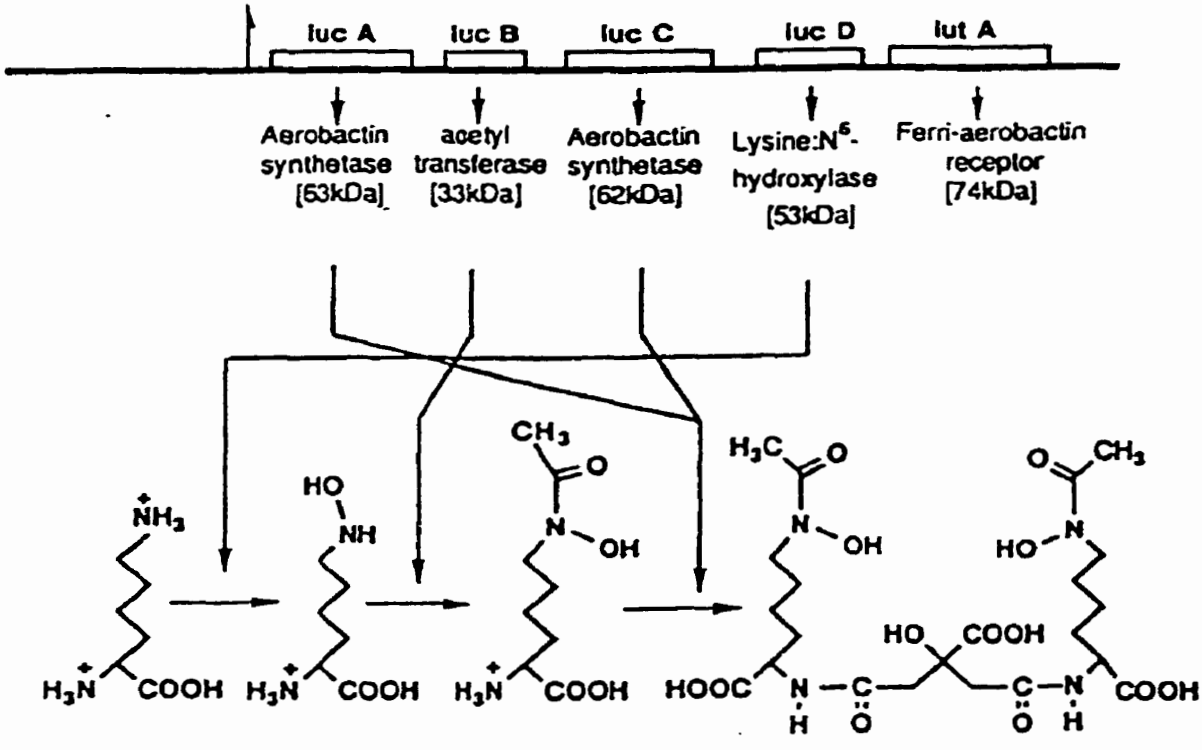
iuc A
iuc B
iuc C
iuc D
iut A
Aerobactin synthetase [63kDa]
acetyl transferase [33kDa]
Aerobactin synthetase [62kDa]
Lysine:N6-hydroxylase [53kDa]
Ferri-aerobactin receptor [74kDa]
NH3
HO
NH
CH3
O
N
OH
H3C
HO
COOH
HOOC
H3N
H
C

L-lysine, which, in the subsequent step, is converted to its N^6-acetyl derivative. The final two steps pertain to the condensation of the N^6-acetyl-N^6-hydroxylysine residues to the distal carboxyls of citric acid. Furthermore, these studies have shown lysine:N^6-hydroxylase, IucD, (E_1) and the acetyl transferase (E_2) to be membrane associated while the cytosolic enzymes (E_3 and E_4) catalyse the terminal steps of peptide bond formation resulting in the production of aerobactin (29).

1.2 Regulation of aerobactin biosynthesis

The biosynthesis of aerobactin in *E. coli* is regulated by a ferrous iron binding protein, Fur, the product of the *fur* (*f*erric *u*ptake *r*egulation) gene and the protein occurs in the dimeric form. This protein has been found to control transcription of iron dependent promoters in many prokaryotes (30). Fur is a zinc containing, Fe(II) binding protein that represses the transcription of the genes implicated in the response to iron deprivation when the metal is abundant in the medium (31). Interestingly, Fur appears to play a role in a variety of cell functions unrelated to iron acquisition (Figure 4). Such processes include: (i) the production of a number of virulence determinants (32); (ii) defence against oxygen radicals (33,34); (iii) chemotaxis (35); and (iv) metabolic pathways (36). The interaction of Fur-Fe^{2+} complex with its operator, referred to as the "iron box' has been characterised with the following nucleotide sequence: 5'-(GATAATGATAATCATTATC)3' (31). The binding of Fe^{2+} to the C-terminal domain of Fur has been found to be accompanied by conformational changes in the protein's N-terminal region, promoting its interaction with the operator (37). The mode of binding of Fur repressor to the operator has been shown to result in a helical wrapping of protein around the DNA helix. Recent studies have revealed Fur to contain 2 moles of Zn(II) per monomer. Of these two Zn(II), one is tightly bound to the protein and plays a structural role, while the other would appear to be replaceable by

Figure 4: **Functions affected in the *fur* regulon of *E. coli* K12** (38)

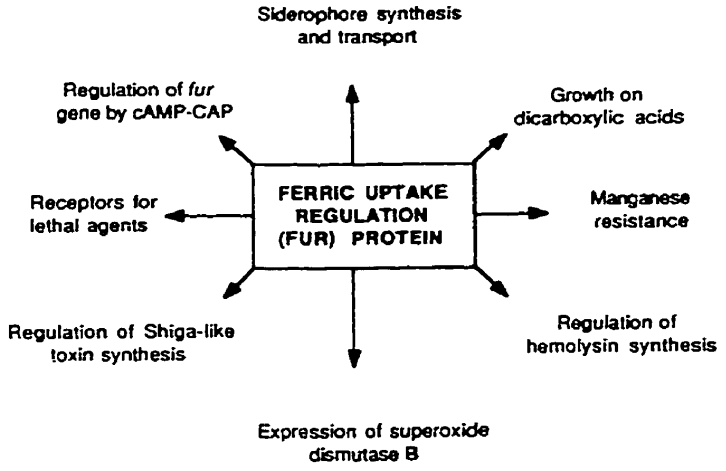
Siderophore synthesis and transport
Regulation of *fur* gene by cAMP-CAP
Growth on dicarboxylic acids
Receptors for lethal agents
FERRIC UPTAKE REGULATION (FUR) PROTEIN
Manganese resistance
Regulation of Shiga-like toxin synthesis
Regulation of hemolysin synthesis
Expression of superoxide dismutase B

Fe(II). Both Fur-Zn_1 and Fur-Zn_2 complexes have been found to be capable of tight interaction with the operator DNA (the iron box). These observations suggest the need for a re-examination of the role of Fe(II) as a corepressor in the regulation of iron-responsive genes (39).

1.3 Lysine:N^6-hydroxylase (IucD)

As noted earlier, lysine:N^6-hydroxylase, IucD, was found to be associated with the membrane component of the cell-free system (28,40). Furthermore, since the cell-free system was obtained by osmotic shock of the lysozyme treated cell preparations, the membrane vesicles would be expected to retain their normal RSO (right side out) orientation (28,40,41). Lysine:N^6-hydroxylation catalysed by these RSO vesicular enzyme preparations was found to by stimulated by pyruvate, which appeared to serve both as a source of reducing equivalents required for O_2 activation, as well as for the acetyl moiety needed for the conversion of N^6-hydroxylysine to its hydroxamate derivative (28,40,41). The process of pyruvate oxidation and lysine:N^6-hydroxylation mediated by the vesicular enzyme preparation appeared to be tightly coupled since pyruvate analogs (fluoropyruvate, methylacetyl phosphonate, and cinnamylidene) were found to inhibit not only the former, but also the latter reaction (41,42). Although none of the amino acids other than L-lysine served as a substrate, both L-glutamic acid and L-glutamine were found to both stimulate as well as activate the N-hydroxylase activity of the enzyme preparation (40,43).

Further evidence for the location of IucD in a membrane environment was provided by the observations recorded in the studies with *iuc*D´-`*pho*A and *iuc*D´-`*lac*Z constructs (44). These investigations have revealed the presence, in IucD, of at least two domains of attachment to the inner side of the cytoplasmic membrane. The first such membrane attachment domain has been noted to occur within the first twenty four amino acid residues

of the protein and the sequence of this segment resembles that of the signal peptide (44). IucD's association with the membrane was further confirmed by the continued presence of lysine:N^6-hydroxylase activity in ISO (inside out) vesicular enzyme preparations (45).

Repeated efforts to achieve membrane free preparations of IucD were futile (46). To circumvent this problem, recombinant IucD proteins with modified amino termini were produced by performing three in frame gene fusions of IucD to the amino terminal amino acids of the cytoplasmic protein β-galactosidase as shown in Figure 5. Two of these constructs involved the addition, to the *iuc*D coding region, of a hydrophilic leader sequence. In one, the attached leader sequence results in the addition of 13 amino acid residues (construct pAT5 that would result in the production of *r*IucD439) and in the second, the appended leader segment would lead to a gain of 30 amino acids (construct pAT2). The third construct, pAT3, involved the addition of 19 N-terminal amino acid residues from β-galactosidase to the C-terminal fragment of *iuc*D (obtained by the deletion of the nucleotide sequence encoding for the first 47 amino acids) and this allowed for the production of *r*IucD398. *E. coli* DH5α transformed with pAT5 or pAT3 were found to produce cytoplasmic forms of *r*IucD. In the case of pAT2, lysine:N^6-hydroxylase activity could be either cytoplasmic when expressed in *sup*K strain of *E. coli*, or membrane bound when expressed in *E. coli* DH5α. This observation lends further evidence for IucD being normally located in a membrane environment (46).

Recombinant forms of IucD are produced as apoproteins and require NADPH and FAD for their catalytic function, with L-lysine functioning as the preferred hydroxylatable substrate (46,47). Neither pyruvate nor L-glutamine has any effect on the reactions catalysed by the *r*IucD preparations. Although the membrane bound and the cytoplasmic (recombinant) forms of IucD are similar in their function and many other properties, they

Figure 5: **Details of the pUC19-*iuc*D gene fusions** (46)

The DNA sequences of the fusion endpoints in pAT2, pAT3, and pAT5 were deduced from the published sequences of pUC19 and *iuc*D (44,48). Shadowed amino acids indicate the portion of the recombinant polypeptide segment contributed by the β-galactosidase α-peptide encoded by pUC19. Double underlined amino acids denote the IucD sequence. Underlined regions of the DNA sequence in pAT2 and *iuc*D denote the leader sequence that contains the ribosome binding site of the wild-type *iuc*D gene and two UGA stop codons (asterisks). Shaded bases in the *iuc*D sequence indicate the Shine-Dalgarno sequence as reported by Herrero *et. al.* (44)

pAT2 (*iuc*D456)

pAT3 (*iuc*D398)

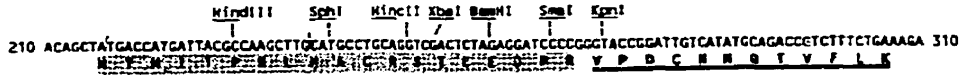

pAT5 (*iuc*D439)

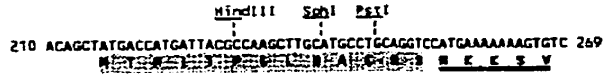

***iuc*D**

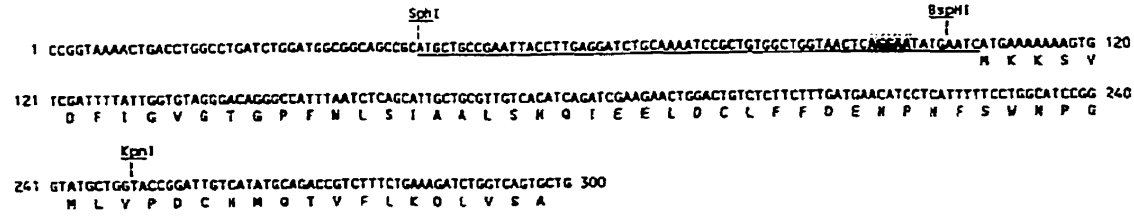

do differ with respect to their cofactor requirements as indicated in Table 1. The basis for such a difference is not apparent at the present time.

The primary structure of IucD, deduced from the nucleotide sequence of *iuc*D, has revealed the presence of two potential nucleotide binding domains, one comprising the first 27 amino acid residues at the N-terminus and the other in the segment comprising residues 183-213 of the protein. However, the availability of the former for cofactor occupancy appears remote in view of its involvement in the protein's attachment to the cytoplasmic membrane. This view is further supported by the observation that deletion of this domain, as in *r*IucD398, has no deleterious effect on the protein's catalytic functions. Consequently, the latter domain, which fulfils the fingerprint requirements (49) more effectively than the former, has been assigned as the flavin cofactor binding domain (47). The situation with respect to the NADPH binding domain would appear to be analogous to that in the case of *p*-hydroxybenzoate hydroxylase, which has no identifiable domain in its primary structure for this obligatory cofactor (50). However, the exact locations of the nucleotide binding domains for NADPH and FAD in the primary structure of IucD remains to be firmly established (51-53). Besides the determination of crystal structures of *r*IucD-cofactor complexes, studies with photolabile cofactor analogs (54,55) may prove helpful in an unambiguous assignment of ligand binding domains in the protein.

Purification and physico-chemical characterisation of *r*IucD439 and *r*IucD398 has been achieved (46,47,56,57). Chemical modification of thiol functions of the proteins has been found to result in a loss of their lysine monooxygenase function, an observation that led to further studies on the role of cysteine residues in *r*IucD's catalytic functions. Treatment of *r*IucD with either ICH_2COO^- or DTNB under denaturing conditions consistently indicated the presence of 5 moles of cysteine residues per mole of protein (58)

Table 1: **Enzymatic activity of membrane bound and cytoplasmic IucD preparations under conditions of various effectors** (56)

Effector	Relative enzymatic activity[a]	
	Cytoplasmic IucD	Membrane bound IucD
None	100	100
-70°C	0[b]	0
L-Glutamine (1 mM)	100	200
Pyruvate (1 mM)	100	100 (22)[c]
Acetaldehyde (1 mM)	100	120 (22)[c]
Cinnamylidene (400 µM)	8	25
Gramicidin S (100 µM)	100	19
CCCP (100 µM)	6	10
FCCP (100 µM)	11	15
Phenyl hydrazine (500 µM)	0	27

[a] In the case of cytoplasmic IucD, the assay (final volume of 5 mL) comprised enzyme (100 µg), L-lysine (1 mM), FAD (40 µM), NADPH (80 µM, regenerated using 1 mM G-6-P and 1 unit G-6-P deH_2), and potassium phosphate (50 mM, pH 7.2). Incubation: 15 min at 37°C. In the case of the membrane bound enzyme, the assay (final volume of 10 mL) comprised membrane vesicles (1 mL), L-lysine (1 mM), pyruvate (1 mM), and potassium phosphate (50 mM, pH 7.2). Incubation: 1 h at 37°C. These served as controls and the activity of each was set at 100 in the assessment of the influence of effectors indicated.

[b] Lability at subzero temperatures noted in the case of enzyme preparations in buffer media containing NaCl (≥ 500 mM). The enzyme is stable at subzero temperatures when maintained in 200 mM potassium phosphate, pH 7.0 in the absence of NaCl. The membrane bound enzyme preparation is labile at temperatures < 0°C regardless of the nature of the medium of its maintenance.

[c] The activity in the absence of pyruvate or acetaldehyde.

instead of the 6 such residues predicted by the nucleotide sequence of *iucD* (44). Consequently, the nucleotide sequence has been redetermined leading to a revised version which predicted the presence of 5 cysteines in IucD, a finding in agreement with the experimentally observed value (58,59). Examination of the number of cysteine residues accessible to modification in the native conformation of *r*IucD indicated that two residues were susceptible to alkylation with ICH_2COO^- while three were amenable to modification by DTNB (59). Of these three cysteine residues accessible to DTNB, two reacted "fast" while the third was "slow" to undergo modification (Note: for convenience, the terms "fast" and "slow" are used in the presentation; "fast", reaction time ≤ 20 sec; "slow", reaction time ≥ 150 sec). The two cysteine residues of *r*IucD alkylatable by ICH_2COO^- have been identified as Cys51 and Cys158 of the protein (59). Interestingly, replacement of these alkylatable cysteine residues, either individually or in combination, has been noted to have no adverse effect on IucD's lysine monooxygenase function. Furthermore, analysis of results of the reaction of *r*IucD muteins with DTNB indicated that Cys51 as one of the "fast" reacting residues and Cys158 as the "slow" one to undergo modification (59).

Both *r*IucD and its thiol modified preparations have been found to promote the NADPH-dependent DPIP reduction. However, the unmodified *r*IucD preparation has been noted to rapidly lose its ability to accommodate the flavin cofactor in the process due to the inherent ability of the dye to effect covalent modification of protein's thiol functions (60-62). In contrast, *r*IucD preparations with prior modification of its cysteine residues can still allow for the participation of FAD in the electron transfer process, since such covalent labelling is precluded due to the nonavailability of thiol function(s) (58). Thus *r*IucD preparations, with their thiol groups modified are devoid of monooxygenase activity, but can still participate in

NADPH oxidation, with the process leading to the production of H_2O_2 or reduction of exogenous electron acceptor.

1.4 Xanthine oxido-reductase

Regulation of catalytic function(s) of enzymes based on changes in the red-ox state of their cysteine residue(s) is not uncommon. Xanthine oxido-reductase serves as an excellent example of such phenomena (63). This enzyme, which has been isolated from a wide range of organisms, catalyses the hydroxylation of a variety of purine, pyrimidine, pterin and aldehyde substrates. The enzymes from different sources have similar molecular weight and composition of red-ox centres (64,65). The mammalian enzyme catalyses hydroxylation of hypoxanthine and xanthine, the last two events in the production of urate. This enzyme is a dimer, with each subunit containing one molybdopterin cofactor, two distinct [2Fe-2S] clusters and one FAD cofactor. Each of the subunits is catalytically functional. The oxidation of xanthine occurs at the molybdopterin centre and the electrons introduced are distributed in other centres by an intramolecular electron transfer process, resulting in the 6 electron reduced species of the enzyme (Scheme 1). In contrast to other hydroxylases, xanthine oxidase utilises water as the source of oxygen incorporated into the product (Scheme 2).

Interestingly, the enzyme is synthesised as a dehydrogenase (XDH) and is converted to an oxidase (XO) by oxidation or chemical modification of its cysteine residues or by proteolysis (66-68). XDH shows a preference for NAD^+ as an electron acceptor and the reduction occurs through the FAD cofactor. Conversion of XDH to XO is accompanied by a loss of ability to bind NAD^+ with a concomitant increase (4-fold) in the affinity for molecular oxygen. In XO, the reduced form of the flavin cofactor ($FADH_2$) reacts exclusively with dioxygen which serves as the ultimate electron acceptor. The reactions

Scheme 1: **Generation of 6 electron reduced xanthine oxidase** (67)

X = xanthine; U = urate

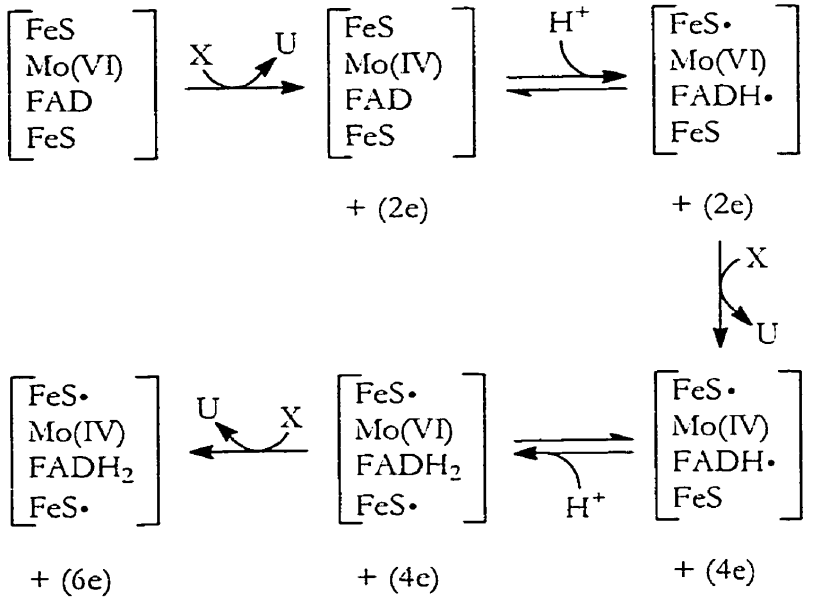
FeS
Mo(VI)
FAD
FeS
X
U
FeS
Mo(IV)
FAD
FeS
H+
FeS•
Mo(VI)
FADH•
FeS
+ (2e)
+ (2e)
X
U
FeS•
Mo(IV)
FADH2
FeS•
U
X
FeS•
Mo(VI)
FADH2
FeS•
H+
FeS•
Mo(IV)
FADH•
FeS
+ (6e)
+ (4e)
+ (4e)

Scheme 2: **The mechanism of xanthine oxidase**

The reduced enzyme is subsequently reoxidized by O_2, yielding H_2O_2.

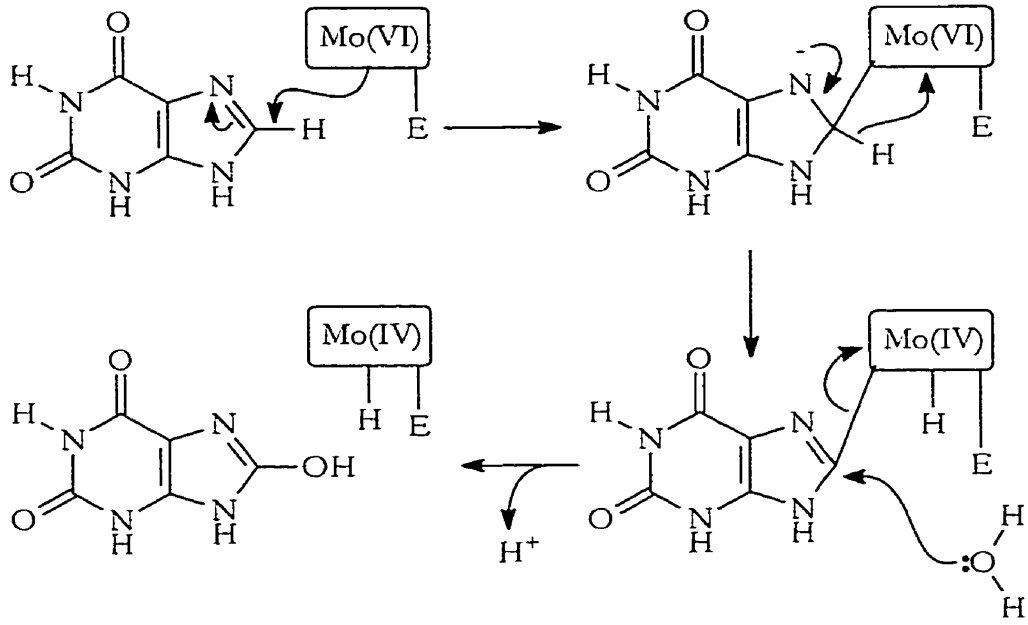
Mo(VI)
E
H
Mo(VI)
E
H
Mo(IV)
H
E
Mo(IV)
H
E
OH
H+
H
H

catalysed by XDH and XO are illustrated in Scheme 3. Although Scheme 3 depicts exclusive formation of H_2O_2 in the reaction between $FADH_2$ and dioxygen, studies with cytochrome c as electron acceptor have revealed the process is actually accompanied by the generation of both the superoxide anion, $O_2^{\bullet}$ (the product of one electron transfer) and peroxide, O_2^{2-} (the product of two electron reduction). The process can be visualised as follows:

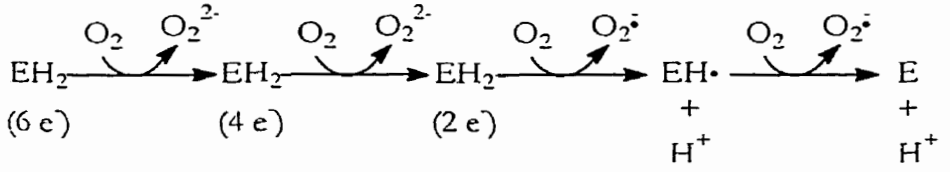

The generation of 3 equivalents of $O_2^{\bullet}$ during the process has also been reported (63).

In light of the control of xanthine oxidoreductase function via the red-ox state of its cysteine residues, it may be pertinent to reassess the role of cysteine thiol functions in IucD. The maintenance of lysine monooxygenase activity in the *r*IucD muteins, developed by the substitution of two of the alkylatable cysteine residues, would appear to rule out their participation in the protein's catalytic mechanism. And, this may indeed hold true in the case of the *wt-iuc*D gene product. However, the possibility of the cysteine residues being involved in an *in vivo* post-translational regulation of the protein's ability to function as a monooxygenase needs to be considered. In this connection, the narrow window observed in the manifestation of the lysine:monooxygenase activity in cultures producing aerobactin (28,43) may be a reflection of the control exercised in the regulation of the activity of this enzyme. *In vivo*, modulation of the protein's lysine:monooxygenase function by a change in the red-ox state of its cysteine residue(s) may provide one such control mechanism. If the above situation were to prevail, it would mean that the monooxygenase activity of *r*IucD muteins

Scheme 3: **Reaction catalysed by xanthine dehydrogenase (XDH) and xanthine oxidase (XO)**

X = xanthine; U = urate

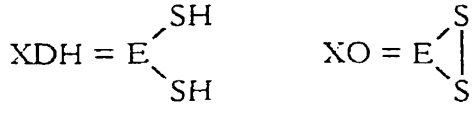

XDH to XO conversion can also be achieved by chemical modification of the cysteine residues.

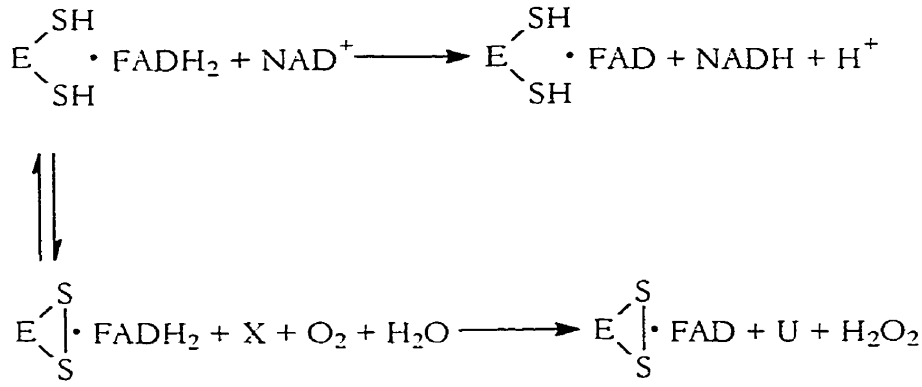
SH
E
SH
· FADH2 + NAD+
SH
E
SH
· FAD + NADH + H+
S
E
S
· FADH2 + X + O2 + H2O
S
E
S
· FAD + U + H2O2

with cysteine substitution(s) (with alanine in this study) may not be subject to such *in vivo* post-translational regulation.

As noted above, the transition of XDH to XO is accompanied by a change in the protein's preference for its electron acceptor from NAD^+ to dioxygen. As a consequence, the products of the electron transfer reactions catalysed by the two forms of the protein are distinct, with the formation of the reduced form of nicotinamide adenine dinucleotide (NADH) in the case of XDH and that of peroxide (H_2O_2) and superoxide anion ($O_2^{\bullet}$) from XO. The situation in the case of *r*lucD is distinct from that noted above in that the enzyme with its cysteines intact functions as a monooxygenase while that with such residues oxidised is capable of mediating electron transfer to artificial electron acceptors. Thus, it would appear that O_2 serves as an electron acceptor in both the parent and the modified *r*lucD preparations, the difference being that in the former case, the activated oxygen species is utilised for the hydroxylation of substrate, while in the latter instance it may be channelled towards the production of H_2O_2 and/or the reduction of exogenous electron acceptors.

1.5 Objectives

In light of considerations cited above, current studies were initiated to address aspects that yet remained to be resolved in order to gain an insight into the mechanism(s) operative in *r*lucD catalysed processes. These are: (i) the basis for the loss of *r*lucD's monooxygenase activity upon chemical modification of its accessible cysteine residues; (ii) the role of the cysteine residues inaccessible to chemical modification in the protein's catalytic function(s); (iii) the factor(s) contributing to the anomaly in the number of *r*lucD's cysteine residues susceptible to modification by thiol modifying agents, namely iodoacetate and DTNB; and (iv) evaluation of approaches employed for monitoring the ligand (substrate or cofactor) induced conformational changes in *r*lucD.

2.0 Materials

Chemical	Supplier
Dyematrex Orange A gel Centricon 50 kDa concentrators Centriprep 50 kDa concentrators	Amicon Corporation Beverly, MA
cis-1,4-dichloro-2-butene diethyl acetamidomalonate L-glutamine Imidazole DL-norleucine L-norleucine Phthalimide, potassium derivative Sodium Azide *cis*-1,2,3,6-tetrahydrophthalimide	Aldrich Chemical Company Milwaukee, WI
Polyclonal anti-*r*IucD antibodies (from rabbit)	Alpha Diagnositcs International San Antonio, TX
Ampicillin trihydrate	Amersham Life Sciences Arlington Heights, IL
Aminopeptidase M Calcium chloride dihydrate DPIP Guanidine hydrochloride, ultrapure bioreagent HEPES, ultrapure bioreagent Hydrochloric acid Isopropylthiogalactoside (IPTG) Magnesium sulphate heptahydrate ($MgSO_4 \cdot 7H_2O$) Potassium phosphate, dibasic (K_2HPO_4) Potassium phosphate, monobasic (KH_2PO_4) Potassium thiocyanate	J.T. Baker Chemical Company Phillipsburg, NJ
trans-4,5-dehydro-L-lysine Furylacryloyl-L-Phe-Ala	Bachem, Biosciences Inc. King of Prussia, PA
Acetic Acid Ethanol Glycine Iodine α-Naphthylamine Sodium bicarbonate Sodium chloride	BDH Chemical Company Toronto, Ontario

Sodium hydroxide N,N,N',N'-tetramethylehylenediamine (TEMED) Trichloroacetic acid Trifluoroacetic acid Urea	BDH Chemical Company Toronto, Ontario
Acrylamide Ammonium persulphate AP conjugate substrate kit BioGel p4 (200-400 mesh) Bisacrylamide Coomassie brilliant blue R-250 Dowex 50W-X8 and X16 (200-400 mesh, H^+ form) Goat anti-rabbit IgG-AP conjugate Kaleidoscope prestained standards Protein Assay Dye Reagent Concentrate SDS-PAGE low molecular weight standards (97.4 kDa, 66.2 kDa, 45 kDa, 31 kDa, 21.5 kDa, 14.4 kDa) Sodium dodecylsulphate (SDS) Trans blot transfer medium Tween-20	Bio-Rad Laboratories Richmond, CA
λ-DNA Agarose LE Carboxypeptidase B *Bam*H I restriction endonuclease and reaction buffer *Eco*R I restriction endonuclease and reaction buffer *Kpn* I restriction endonuclease and reaction buffer Proteinase K *Pwo* DNA polymerase and reaction buffer	Boehringer Manheim Manheim, Germany
Isopropyl alcohol, HPLC grade	Caledon Laboratories Ltd. Georgetown, Ontario
Carboxypeptidase Y	Carlbiotech Copenhagen, Denmark
Ethanol Methanol	Commercial Alcohols Brampton, Ontario
DTT	Diagnostic Chemicals Ltd. Charlottetown, PEI
Bacteriological agar Casamino acids Tryptone Yeast Extract	Difco Laboratories Detroit, MI

Methanol, HPLC grade	EM Science Gibbstown, NJ
T4 DNA ligase	Fermentas Burlington, ON
Iodine Sulfanilic acid	Fisher Scientfic Toronto, Ontario
Ampicillin Carboxypeptidase A (PMSF treated) DTT Glucose-6-phosphate dehydrogenase Leucine aminopeptidase Trifluoroacetic acid	Fluka Biochemika Switzerland
E. coli DH5α [F$^-$ ϕ80d*lac*ZΔM15 Δ(*lac*ZYA-*arg*F) U169 *end*A1 *rec*A1 *hsd*R17(r_k^- m_k^+) *deo*R *thi*-1 *pho*A *sup*E44 λ$^-$ *gyr*A96 *rel*A1]	Gibco BRL Gaithesburg, MD
Ammonium sulphate, ultrapure PMSF	ICN Biochemicals Cleveland, OH
Oligonucleotide primers DNA sequencing	MOBIX McMaster University, Hamilton, Ontario
Carnation instant skim milk powder	Nestlé Don Mills, Ontario
Dpn I restriction endonuclease with reaction buffer *Hin*D III restriction endonuclease with reaction buffer BSA, molecular biology grade	New England Biolabs Mississauga, Ontario
E. coli BL21(DE3) [F$^-$ *omp*T *hsd*S_B(r_B^- m_B^-) *gal dcm* (DE3)]	Novagen, Inc. Madison, WI
dNTPs, ultrapure MAbTrap GII kit SDS-PAGE low molecular weight standards (94 kDa, 67 kDa, 43 kDa, 30 kDa, 20.1 kDa) Thrombin	Pharmacia Baie d'Urfe, Quebec
Qiagen plasmid midi kit QIAquick gel extraction kit QIAprep miniprep kit	Qiagen Inc. Chatsworth, CA

ADP ADP-agarose BSA Chymotrypsin (3x crystallised) Cyclophilin Cytochrome C Diamide DNAase DTNB EDTA Ethidium bromide EZMix™ LB broth Ferrous ammonium sulphate FAD GDP D-(+)-glucose Glucose-6-phosphate Glucose-6-phosphate dehydrogenase L-glutamine Glycine Hippuryl-Arg Hippuryl-Phe Iodoacetate L-lysine Lysozyme β-mercaptoethanol $NADP^+$ NADPH PIPES Potassium thiocyanate Protease X (thermolysin) RNAase SBTI N-succinyl-Ala-Ala-Pro-Phe-*p*-nitroanilide TLCK-Chymotrypsin TPCK-Trypsin Trizma base (Tris)	Sigma Chemical Company St. Louis, MO
Spectra/Por® membrane (MWCO 6,000-8,0000)	Spectrum Gardena, CA

3.0 Methods

A list of buffers used in these investigations is provided below, along with the buffer composition when available.

Buffer Name	Composition
Qiagen®	(69-71)
P1	50 mM Tris·Cl, pH 8.0; 10 mM EDTA; 100 µg/mL RNAase A
P2	200 mM NaOH, 1% SDS
P3	3.0 M potassium acetate, pH 5.5
QBT	750 mM NaCl; 50 mM MOPS, pH 7.0; 15% isopropanol; 0.15% Triton® X-100
QC	1.0 M NaCl; 50 mM MOPS, pH 7.0; 15% isopropanol
QF	1.25 M NaCl; 50 mM Tris·Cl, pH 8.5; 15% isopropanol
TE	10 mM Tris·Cl, pH 8.0; 1 mM EDTA
PB	Supplied Buffer (Qiagen®)
PE	Supplied Buffer (Qiagen®)
EB	Supplied Buffer (Qiagen®)
QG	Supplied Buffer (Qiagen®)
N3	Supplied Buffer (Qiagen®)
MabTrap™ G II	(72)
Buffer EQ	Supplied Buffer (Pharmacia)
Buffer EL	Supplied Buffer (Pharmacia)
Buffer NE	Supplied Buffer (Pharmacia)
General	(73,74)
buffer CC	60 mM $CaCl_2$; 15% glycerol; 10 mM PIPES, pH 7.0
buffer DS	0.25% bromophenol blue, 0.25% xylene cyanol FF, 30% glycerol in water

3.1 Molecular biology protocols

3.1.1 Preparation of competent cells

3.1.1.1 Preparation of competent cells by treatment with $CaCl_2$ (75,76)

The desired bacterial cell culture was grown overnight in a 5 mL starter culture at 37°C in LB medium with constant shaking. This culture was used to inoculate 100 mL of LB medium and was allowed to grow, at 37°C with constant shaking, until it reached an O.D. at 600 nm of about 0.3. The culture was chilled to 4°C in an ice bath for 15 minutes prior to its transfer to sterile centrifuge tubes for centrifugation (2,000 x g) for 5 minutes at 4°C. The cell pellet was washed in 80 mL of sterile, ice-cold buffer CC and allowed to sit in an ice-bath for 30 minutes prior to centrifugation (2,000 x g) for 5 minutes at 4°C. After a second washing, the cell pellet was resuspended in 6-8 mL of sterile, ice-cold buffer CC containing 15% glycerol (v/v). Aliquots of the cell suspension (100-150 µL) were transferred to sterile Eppendorf tubes, snap-frozen in liquid nitrogen and stored at –80°C until needed.

3.1.1.2 Preparation of competent cells for electroporation (77)

The desired bacterial cell culture was grown overnight in a 5 mL starter culture at 37°C in LB medium with constant shaking. The starter culture was used to inoculate 1L of LB medium, which was grown at 37°C with continuous shaking until reaching an O.D. at 600 nm of ~0.5. At this point, the culture was cooled in an ice bath for 10 minutes before harvesting by centrifugation (4,000 x g) for 15 minutes at 4°C. The supernatant was removed and the cells were washed in 1L of ice-cold sterile 10% glycerol and centrifuged (4,000 x g) for 15 minutes at 4°C. The washing cycle was repeated with 500 mL and 250 mL of ice-cold sterile 10% glycerol. Following removal of the supernatant the cell pellet was resuspended in

3 mL of ice-cold sterile 10% glycerol. The competent cells were divided into 100 µL aliquots, frozen in liquid nitrogen and stored at –80°C.

3.1.2 Transformation protocol

3.1.2.1 Procedure for competent cells prepared by $CaCl_2$ treatment (75,76)

Approximately 1 µg (in 5 µL) of the appropriate plasmid preparation was added to a suspension of competent cells (100-150 µL) and allowed to sit in an ice-bath for 30-45 minutes. The cells were heat shocked in a 42°C water bath for 2 minutes, LB medium (500 µL) was then added to the suspension and the culture was incubated at 37°C for 2-3 hours with no shaking. This suspension was streaked on LB agar plates containing ampicillin (100 µg/mL) and incubated for ~20 hours at 37°C for the selection of ampicillin resistant colonies.

3.1.2.2 Procedure for competent cells prepared for electroporation (77)

Competent cells were thawed and cooled in an ice-bath along with the cuvette holder. An aliquot (2 µL) of the desired plasmid was added to 100 µL of competent cells and let stand for 1 minute in an ice-bath. Following transfer to an electroporation cuvette and its placement in the holder, voltage (250 kV) was applied for 3 seconds. This was immediately followed by the addition of 1 mL of SOC medium and transfer to a sterile Eppendorf tube in an ice-bath. The transformed cells were incubated at 37°C with gentle shaking for 1 hour. The suspension was streaked on LB agar plates (containing ampicillin, 100 µg/mL) and incubated for 20 hours at 37°C for the selection of ampicillin resistant colonies.

3.1.3 Isolation and purification of plasmids

The procedures followed and described below are those recommended by Qiagen (69,70).

3.1.3.1 Miniprep

E. coli DH5α transformed with the plasmid of interest was grown in 5 mL of LB medium, containing ampicillin (100 μg/mL), at 37°C with constant shaking for ~16 hours. The cells were harvested by centrifugation (6,000 x g) for 15 minutes and the culture supernatant was discarded. The pellet was resuspended in ice-cold P1 buffer (250 μL) and transferred to an Eppendorf tube. P2 lysis buffer (250 μL) was added and the reaction allowed to proceed for no longer than 5 minutes before the addition of neutralising N3 buffer (350 μL). The lysis mixture was centrifuged (16,110 x g) for 10 minutes. The supernatant was removed and applied to a Qiaquick column, placed in a 2-mL collection tube. The column was centrifuged (16,110 x g) for 1 minute and the collection tube emptied. PB buffer (750 μL) was added and the column centrifuged (16,110 x g) for 1 minute. The collection tube was emptied and the column centrifuged again (16,110 x g) for 1 minute to remove all liquid. The column was then allowed to air dry for 5 minutes. Subsequent to air drying, the column was placed in a sterile Eppendorf tube followed by the addition of sterile water or TE buffer (50 μL) to the column. After standing for 1 minute, the column was centrifuged for the last time (16,110 x g) for 1 minute, the Eppendorf sealed and stored at –20°C until needed.

3.1.3.2 Midiprep

E. coli DH5α transformed with the plasmid of interest was grown in 5 mL of LB medium containing ampicillin (100 μg/mL) at 37°C with constant shaking for ~16 hours. Alternatively, a single colony was picked from a streak plate and was grown in 5 mL of LB medium containing ampicillin (100 μg/mL) at 37°C with constant shaking for ~8 hours. This culture was used to inoculate 100 mL of LB medium, containing ampicillin (100 μg/mL), and

incubated at 37°C with constant shaking. After achieving a cell density of ~3 x 10^9 cells/mL (A_{600} of 1.4) the cells were harvested by centrifugation (6000 x g) for 15 minutes at 4°C. Cell pellets were resuspended thoroughly in Buffer P1 (4 mL). Buffer P2 (4 mL) was then added, the suspension mixed by inversion and then incubated at room temperature for no longer than 5 minutes. Ice cold Buffer P3 (4 mL) was added, the suspension mixed by inversion and incubated on ice for 15-20 minutes. Precipitated proteins and chromosomal DNA were removed by centrifugation (35,000 x g) for 30 minutes at 4°C. The supernatant was then promptly removed and filtered through glass wool prior to its application, by gravity flow, onto a Qiagen Tip 100 column that had previously been equilibrated with Buffer QBT (4 mL). The Tip 100 column was then washed with Buffer QC (2 x 10 mL), which was followed by elution of the DNA using Buffer QF (5 mL). The DNA was precipitated by the addition of 0.7 volumes (3.5 mL) of isopropanol at room temperature. Following mixing, the solution was allowed to sit at –20°C for 15-20 minutes prior to centrifugation (28,000 x g) for 30 minutes at 4°C. Pelleted DNA was washed with 70% ethanol (2 mL) and maintained at –20°C for 15-20 minutes prior to centrifugation (28,000 x g) for 15 minutes. The pellet was air dried for 15 minutes and then redissolved in sterile H_2O to achieve a final concentration of ~200-300 ng/μL. The plasmid solution was stored at –20°C until needed.

3.1.4. Digestion of plasmid DNA with restriction endonucleases

Plasmid DNA (0.5-1.0 μg) was digested with the appropriate restriction endonuclease using conditions described by the manufacturer. A typical reaction mixture is shown below using *Bam*H I:

H_2O	4 μL
SuRE/Cut buffer B (10X), for *Bam*H I	1 μL
BSA, 10X	1 μL

plasmid DNA (200-300 ng/μL)	3 μL
*Bam*H I (10 U/μL)	1 μL

3.1.5 Electrophoretic analysis of DNA fragments (78)

Plasmids and DNA fragments were separated and visualised by electrophoresis on agarose gels. A suspension of agarose (0.7 %) in TAE was heated in a microwave for ~40 seconds in order to obtain a clear solution. This solution was mixed with an aliquot of ethidium bromide (20 μL of 10 mg/mL) and cooled to luke warm temperature prior to being poured into the horizontal gel casting chamber to achieve a gel thickness of ~ 5 mm. A comb, with the appropriate number of lanes, was placed at one end of the gel prior to the setting of the agarose to produce the necessary wells. The comb was removed and the set agarose gel placed into the horizontal electrophoresis chamber and covered with TAE buffer (200 mL). The DNA samples and standards, final amount of 100-500 ng in buffer DS, were then added to the wells and the electrophoresis conducted at constant 80 volts for 2 hours at room temperature. DNA bands were visualised under ultra-violet light and the gel was photographed using a Polaroid photographic transilluminator system (Bio/Can Scientific, Mississauga, Ontario).

3.1.6 Extraction and purification of DNA fragments from agarose gels (71)

The DNA band of interest was excised from the agarose gel using a clean, sharp razor blade, weighed, and transferred to an Eppendorf. Buffer QG (3 volumes to 1 volume of agarose, where 100 mg of agarose = 100 μL Buffer QG) was added to the Eppendorf and the mixture heated at 50°C for 2-3 minutes, or until the agarose was completely dissolved. (Buffer QG contains a pH indicator to ensure that the pH of the solution was below 7.5. If the solution is pink, the pH must be adjusted until the solution turns yellow.) Isopropanol (1 volume) was added to the Eppendorf, the solution mixed and then applied to a QIAquick

column and centrifuged (16,110 x g) for 1 minute. The flow-through was discarded, Buffer PE (750 µL) was added, and the column was washed by centrifugation (16,110 x g) for 1 minute. The flow-through was discarded and the column was re-centrifuged (16,110 x g) for 1 minute to remove residual ethanol from Buffer PE. The QIAquick column was then placed in a clean Eppendorf tube and the DNA was eluted by adding H_2O, or Buffer EB, (30-50 µL) to the centre of the membrane, waiting for 1 minute, and centrifuging (16,110 x g) for 1 minute. This DNA was stored at –20°C until needed.

3.1.7 Complementary primers

The *iuc*D gene present in pAT5 was selected for site-directed mutagenesis to achieve the desired single Cys→Ala replacement(s) in IucD. The site-directed mutagenesis of *iuc*D was accomplished by the use of complementary primers with the triplet for cysteine having been changed to that of alanine. The plasmid preparation containing *iuc*D encoding for C31A *r*IucD was employed to effect the second desired Cys→Ala replacement. The sequence of mutagenic complementary primers for achieving replacement of cysteine residues in *r*IucD is shown in Table 2.

This approach was also employed to achieve deletion of C-terminal segments at specified locations in *r*IucD. The *iuc*D gene in pAT5 was targeted for deletion of segments encoding for the C-terminal region of IucD by site-directed mutagenesis employing complementary primers with the triplet for the desired amino acid changed to that for termination. The nucleotide sequence of the mutagenic complementary primers employed to generate truncated versions of *r*IucD are shown in Table 3.

Table 2: **Nucleotide sequence of complementary mutagenic primers used for Cys→Ala mutagenesis of *iucD***

Plasmid	Complementary Primers Used	Mutation in *r*IucD
pAT5	5'd(ATCGAAGAACTGGAC**GCT**CTCTTCTTTGATGAA)3' 5'd(TTCATCAAAGAAGAG**AGC**GTCCAGTTCTTCGAT)3'	C31A
pAT5	5'd(GGGTATGCTG*GTT*CCGGAT**GCT**CATATGCAGACCGTC)3' 5'd(GACGGTCTGCATATG**AGC**ATCCGG*AAC*CAGCATACCC)3'	C51A
pAT5	5'd(TTTGCCCGCATATCG**GCC**CTTGGTACAGGAAAA)3' 5'd(TTTTCCTGTACCAAG**GGC**GATATTGCGGGCAAA)3'	C146A
pAT5	5'd(CCTTATTTACCACCC**GCT**GTGAAG*CAC*ATGACACAATCC)3' 5'd(GGATTGTGTCAT*GTG*CTTCAC**AGC**GGGTGGTAAATAAGG)3'	C158A
pAT5	5'd(CATATGACACAATCC**GCT**TTCCATGCCAGTGAA)3' 5'd(TCACTGGCATGGAA**AGC**GGATTGTGTCATATG)3'	C166A
C31A-pAT5[a]	5'd(GGGTATGCTG*GTT*CCGGAT**GCT**CATATGCAGACCGTC)3' 5'd(GACGGTCTGCATATG**AGC**ATCCGG*AAC*CAGCATACCC)3'	C31A/C51A
C158A-pAT5[b]	5'd(GGGTATGCTG*GTT*CCGGAT**GCT**CATATGCAGACCGTC)3' 5'd(GACGGTCTGCATATG**AGC**ATCCGG*AAC*CAGCATACCC)3'	C51A/C158A

The plasmid pAT5 (46) was used to effect the desired mutations. The incorporation of the desired site-specific mutation(s) was achieved by the use of complementary primers containing the mutation(s) of interest. Cys→Ala mutations are denoted in bold underline; silent mutations, for restriction analysis, are denoted in gray, bold and italicised lettering. The plasmid containing *iucD* encoding for C31A-*r*IucD was employed to effect the second mutation..

[b] The plasmid containing *iucD* encoding for C158A-*r*IucD was employed to effect the second mutation.

Table 3: **Nucleotide sequence of complementary primers used for C-terminal mutagenesis of *iucD***

Plasmid	Complementary Primers	Mutation in *r*IucD	Protein
pAT5	5'd(GTAATGGGACGTGAT**TAA**TTCGATCTCAGTATG)3' 5'd(CATACTGAGATCGAA**TTA**ATCACGTCCCATTAC)3'	L409-ter	*r*IucD Δ17
pAT5	5'd(CGTGATTTATTCGAT**TAG**AGTATGCCGCCCGCC)3' 5'd(GGCGGGCGGCATACT**CTA**ATCGAATAAATCACG)3'	L412-ter	*r*IucD Δ14
pAT5	5'd(TTCGATCTCAGTATG**TAG**CCCGCCCTGATTCAG)3' 5'd(CTGAATCAGGGCGGG**CTA**CATACTGAGATCGAA)3'	P415-ter	*r*IucD Δ11
pAT5	5'd(CTCAGTATGCCGCCCGCC**TAG**ATTCAGTGCCGCAGC)3' 5'd(GCTGCGCCACTGAAT**CTA**GGCGGGCGGCATACTGAG)3'	L418-ter	*r*IucD Δ8

The plasmid pAT5 (46) was used to effect deletion at the desired location. The incorporation of the termination triplet at the desired location was achieved by the use of complementary primers containing the deletion codon (bold underline).

3.1.8 Conditions for Quick Change™ mutagenesis (79)

The parent plasmid, pAT5 containing the *iuc*D gene and the ampicillin resistant gene, served as the template for *Pwo* polymerase. In order to effect a second cysteine replacement in IucD, the plasmid containing *iuc*D encoding for C31A *r*IucD served as the template for *Pwo* polymerase. The following reagents were added to a PCR tube in order:

Pwo reaction buffer (10X)	5 µL
pAT5 (5 ng/µL)	10 µL
complementary primer 1 (125 ng/µL)	10 µL
complementary primer 2 (125 ng/µL)	10 µL
dNTP mixture (10 mM of all four dNTPs)	1 µL
sterile H_2O	13 µL
Pwo DNA polymerase (5 U/µL)	1 µL

The reaction mixture was kept at 4°C until ready for thermocycling using an Ampligene II thermocycler. The temperature cycling was programmed as follows:

jumpstart 85°C, 2 minutes

16 x { 95°C, 30 seconds; 55°C, 1 minute; 68°C, 10 minutes }

The cycle, excluding the jumpstart, was repeated an additional 15 times followed by a dwell period of 15 minutes at 68°C to allow for the extension of any incomplete replications. The reaction products were either used immediately or stored at –20°C until needed.

The PCR reaction mixture was treated with *Dpn* I (20 U) for 1 hour at 37°C in order to degrade the parent plasmid and the mutant plasmid product (15 µL) was used to

transform competent *E. coli* DH5α. Transformants were selected from LB agar plates on the basis of ampicillin resistance. The transformed cells were grown in LB media (100 mL) and the cells were harvested and used for the isolation of the plasmid as described in section 3.1.3.2. The incorporation of the desired mutation was established by analysis of the nucleotide sequence of the *iucD* gene in the plasmid.

3.2 Growth of *Escherichia coli* cultures

3.2.1 *Escherichia coli* DH5α and BL21 (DE3)

The *E. coli* DH5α and BL21 (DE3) cells were grown and maintained on LB agar plates at 4°C. A typical starter culture was prepared by inoculating 5 mL of LB medium with the bacterial cells and growing at 37°C with continuous shaking for 10-12 hours.

3.2.2 Growth of *E.coli* transformants

E. coli DH5α was transformed with the plasmid pAT5, or its variants, (~1 μg) and allowed to sit in an ice bath for 30-45 minutes. The suspension was then heat shocked at 42°C for 2 minutes. LB medium (500 μL) was added and the suspension was incubated at 37°C for 2-3 hours with no shaking. This growth was used to inoculate 5 mL of LB medium with ampicillin (100 μg/mL), which was incubated at 37°C for 12-16 hours with continuous shaking. The cells were transferred to 1.5 L of minimal medium (Monod M9), with yeast extract (1 g/L) and casamino acids (1 g/L), supplemented with ampicillin (100 μg/mL) and grown at 37°C for 24-28 hours with constant shaking. Cells were harvested (6,000 x g) for 15 minutes at 4°C.

3.3 Isolation and purification of *iucD* and its muteins

3.3.1 Preparation of cell-free extract

Cell-free extracts were obtained by rupturing cells under high pressure (French press) similar to the procedure described previously (41,45,46). The cells were first harvested by centrifugation (6,000 x g) for 15 minutes at 4°C. The pellets were washed with a NaCl solution (0.85%) and centrifuged (6,000 x g) for 15 minutes at 4°C. The cells were resuspended in ~40 mL of an ice-cold potassium phosphate buffer (10 mM, pH 7.0) containing L-glutamine (1 mM) and DTT (1 mM). This suspension was ruptured by a single passage through a prechilled (4°C) French press chamber at 10,000-12,000 psi. The cell-free extract was incubated at room temperature with DNAase (10 µg) and RNAase (10 µg) for 10 minutes prior to centrifugation (113,612 x g) for 60 minutes at 4°C.

3.3.2. Purification of lysine:N^6-hydroxylase (46)

Ammonium sulphate was added to the cell-free extract to achieve 40% saturation and the suspension was allowed to stand at 4°C overnight. The suspension was centrifuged (48,384 x g) for 15 minutes at 4°C, the supernatant discarded and the pellet resuspended in ~10 mL of potassium phosphate (10 mM, pH 8.0), containing NaCl (300 mM) and DTT (1 mM), and dialysed against 1 L of the same buffer for 12-16 hours. To the dialysed material, ammonium sulphate was added to 30% saturation and the suspension was allowed to stand at 4°C overnight. The suspension was centrifuged (48,384 x g) for 15 minutes at 4°C and the supernatant removed. The pellet was resuspended in ~10 mL of potassium phosphate (10 mM, pH 7.0), containing NaCl (250 mM) and DTT (1 mM), and dialysed against 1 L of the same buffer for 12-16 hours. The material was finally dialysed against a solution (1L) containing potassium phosphate (10 mM, pH 7.0) for 2 hours prior to its application onto the Orange A Dyematrex column, equilibrated with the same buffer. Protein was recovered by elution with potassium phosphate (10 mM, pH 7.0) buffers containing stepwise increases in NaCl concentration (0 mM, 250 mM, 500 mM, 750 mM, 1000 mM). Two ~30 mL

fractions (elution rate ~1 mL/min) of each of the elution media were collected and examined for the presence of protein by measuring their absorbance at 280 nm and by SDS-PAGE. Lysine:N^6-hydroxylase activity was most often found in the second 500 mM and the two 750 mM NaCl fractions. Fractions showing lysine:N^6-hydroxylase activity were pooled and concentrated using Centriprep 30 kDa membrane to achieve a final protein concentration of 20 - 50 μM. The buffer was changed by dialysis against potassium phosphate (200 mM, pH 7.0) containing DTT (1 mM) for 12-16 hours. The protein solution was divided into 1 mL aliquots, frozen in liquid N_2 and stored at –80°C until needed.

With repeated use of the Orange A column, the lysine:N^6-hydroxylase activity was found to elute in buffer media containing NaCl < 500 mM.

3.3.3 Preparation of S-carboxymethyl-*r*IucD (58)

In a typical experiment, a solution of *r*IucD (100 nmoles) in 3 mL of potassium phosphate (200 mM, pH 7.0) containing DTT (2 mM) was treated with an aliquot (50 μL) of an aqueous solution of ICH_2COO^- (1 M) to achieve an approximately 20-fold excess of the reagent over that of thiol functions present in the protein and DTT. After 20 minutes at 25°C, the reaction was terminated by the addition of DTT equivalent to that of ICH_2COO^- and allowed to stand for 30 minutes at 25°C. The reaction mixture was finally dialysed extensively against potassium phosphate (200 mM, pH 7.0) and the dialysed material stored at -20°C. The concentration of S-carboxymethyl-*r*IucD was estimated using an ε_M of 6.2 x 10^4 $M^{-1}cm^{-1}$.

3.3.4 Synthesis and purification of the decapeptide (C-peptide)

The decapeptide Pro-Ala-Leu-Ile-Gln-Trp-Arg-Ser-Gly-(D)-Thr, the amino acid sequence corresponding to that of the C-terminal segment of *r*IucD except for the change in configuration of the terminal threonine residue, was synthesised by Dr B.A.K. Chibber

(Central Bio-core Facilities, University of Notre Dame, IN). The material was purified by HPLC on a 0.8 x 10 cm Bondapak C_{18} RCM column employing a solvent system comprising water (0.1% TFA) and CH_3CN (01.% TFA) with the latter being brought to 25% and 90% after 40 and 50 minutes respectively, subsequent to the initiation of the procedure at a flow rate of 1 mL/min and at 25°C. The material was characterised by ESMS analysis. Calculated 1128.3; Found 1127.4.

3.3.5 Synthesis and characterisation of DL-*cis*-4,5-dehydrolysine

The methods used were essentially as those described previously in the literature (80,81).

(1) Synthesis of 1-chloro-4-phthalamido-2-butene. To a flask equipped with a water condenser, was added 1,4-*cis*-dichloro-2-butene (15 g, 120 mmol) that was heated to 130-140°C. Potassium phthalimide (11.1 g, 60 mmol) was added in portions over 20 min and the mixture was heated at 150°C for 45 min. The viscous material was allowed to cool and then extracted with ether (100 ml). The ether extract was concentrated *in vacuo* and the beige precipitate was collected and recrystallised from hot ethanol yielding 2.9 g (21%) of off-white crystals. Melting point - 80-81.5°C (literature value - 75-76°C).

(2) Synthesis of DL-*cis*-4,5-dehydro lysine hydrochloride. Sodium metal (washed in hexane, 0.56 g, 24 mmol) was added over a 5 min period in small portions to anhydrous ethanol (30 ml) cooled on ice under argon. When all the sodium had dissolved, diethyl acetamidomalonate (3.2 g, 15 mmol) was added at once and allowed to dissolve with mild heating. To the solution was added 1-chloro-4-phthalamido-2-butene (2.9 g, 12 mmol) in portions and the mixture was refluxed for 6 hr. After cooling, the solvent was removed *in vacuo* and the solid taken up in methylene chloride (100 ml) and washed successively with water (30 ml) and brine (30 ml). The organic layer was dried over $MgSO_4$ and was

evaporated *in vacuo*. The resulting viscous oil, was used without further purification. The crude product was refluxed in 6 N HCl for 24 h, the reaction allowed to cool, and phthalic acid was removed by filtration. The filtrate was concentrated *in vacuo* and was chromatographed over 2.5 x 10 cm of DOWEX 50W x 8 (NH_4^+ form). The column was washed with water (300 ml), 0.2 M ammonium hydroxide (120 ml) and then eluted with 2 M ammonium hydroxide and fractions (10 ml) containing the product as judged by TLC (silica, ethylacetate/hexanes (1:3), R_f 0.05) were pooled and taken to dryness. The solid was recrystallised from hot water-ethanol. Yield, 0.31 g.

Melting point 251-254°C (literature value 255-257°C). ESMS: exact mass calculated for $C_6H_{12}N_2O_2$, 144.17; found, 144.32. $[\alpha]_D$ (1.33% in water) = 0.003 ± 0.002. ^{1}H NMR (250 MHz, D_2O) δ 5.56 (m, 2H, CHγ, CHδ), 3.40 (d, 2H, J = 6.5 Hz, $CH_2\varepsilon$), 3.28 (t, 1H, J = 6.0 Hz, CHα), 2.31 (dd, 2H, J = 6.0 Hz, 6.5 Hz, $CH_2\beta$).

3.4 Treatment of *r*lucD with proteases

The susceptibility of *r*lucD to proteolytic degradation was investigated both in the absence as well as in the presence of cofactors and analogs (FAD, ADP, $NADP^+$, NADPH) and substrate, L-lysine. The effect of endopeptidases (TPCK-trypsin, TLCK-chymotrypsin, and thermolysin) and exopeptidases (carboxypeptidases A, B, and Y) on both the structural integrity as well as catalytic competency of *r*lucD was investigated by monitoring changes in the SDS-PAGE profile and lysine:N^6-hydroxylase activity respectively.

3.4.1 Reaction with endopeptidases

Preliminary experiments, performed with TPCK-trypsin, pertained to establishing conditions optimal for monitoring the effect of proteases on both the structural integrity as well as the catalytic function of *r*lucD. Initially, the effect of temperature on both the inherent stability of *r*lucD as well as its susceptibility to proteolytic degradation was

investigated. These studies revealed that : (i) *r*IucD undergoes irreversible inactivation when exposed to 51°C for 2 minutes, presumably due to thermal denaturation; (ii) exposure of the protein at 45°C for 5 minutes has no such adverse effects as indicated by the complete retention of its monooxygenase activity when assayed at 37°C under conditions normally employed; (iii) maintenance of the protein at 37°C is accompanied by a steady decline in its monooxygenase activity, with approximately 30% loss of original activity being noted after 100 minutes of incubation; and (iv) *r*IucD preparations are relatively stable at 25°C over a period of 3 hours.

The next phase of these studies pertained to experiments to identify the concentration of protease that would effect degradation of *r*IucD at a rate suitable for monitoring the process by both SDS-PAGE as well as by an assessment of its monooxygenase activity. These studies performed with TPCK-trypsin at 25°C showed that : (i) at a substrate:protease ratio of 100:1, the rate of proteolysis was slow, with 80% of intact *r*IucD still remaining after 60 minutes of reaction; (ii) increasing the protease concentration to a substrate:enzyme ratio of 20:1, led to a relatively greater extent of proteolysis with approximately 70% of *r*IucD degraded after 60 minutes of incubation; and (iii) at a substrate:protease ratio of 2:1, the rate of proteolysis was rapid with less than 10% of monooxygenase activity being noted after 12 minutes of incubation.

Finally, since *r*IucD's native conformation depends on its maintenance in media of ionic strength ≥ 0.25 (46), experiments were also performed at various salt (NaCl or potassium phosphate) concentrations. These studies revealed that susceptibility of *r*IucD to proteolysis declined progressively with increases in the ionic strength of the reaction medium. However, this phenomenon was not unique to *r*IucD, since similar studies with

casein (or azocasein) as substrate also showed progressive loss in the catalytic efficiency of TPCK-trypsin in media of ionic strength > 0.2.

As a result of the above mentioned studies, the following protocol was employed. *r*lucD (14 μM) in potassium phosphate (100 mM, pH 7.0) was treated with TPCK-trypsin (7 μM) and the reaction allowed to proceed at 25°C. The concentration of the cofactors, analog(s), or substrate, when included in the reaction was: FAD (0.2-1.0 mM), ADP (1 mM), NADPH (1 mM), $NADP^+$ (1 mM) and L-lysine (5 mM). At desired time intervals, aliquots were removed and treated with SBTI (2-fold molar excess over that of TPCK-trypsin) to stop further proteolysis. These samples were used for SDS-PAGE analysis and for the measurement of lysine:N^6-hydroxylase activity.

The conditions used to study the action of TLCK-chymotrypsin on *r*lucD were similar to those employed in the case of TPCK-trypsin except for the use of PMSF, instead of SBTI, to stop further proteolysis. In the case of thermolysin, *r*lucD (12 μM) in PIPES buffer (100 mM, pH 7.5) containing $CaCl_2$ (10 mM) was treated with the protease (6 μM). Aliquots drawn at desired intervals were treated with EDTA (10 mM) to stop further proteolysis and used for SDS-PAGE analysis and assessment of N^6-hydroxylase activity.

3.4.2 Reaction with exopeptidases

The experimental conditions for the treatment either with CPDA or with both CPDA and CPDB were: *r*lucD (10 μM) in potassium phosphate (100 mM, pH 7.0-8.0), exopeptidase(s) (3 μM of CPDA or 3 μM of each CPDA and CPDB, when used in combination) and temperature 25°C or 37°C. Aliquots drawn at desired intervals were used for SDS-PAGE analysis and for measurement of lysine:N^6-hydroxylase activity.

In experiments with CPDY, a typical reaction mixture, in a final volume of 1 mL comprised: potassium phosphate (100 mM, pH 6.0), *r*IucD (10 μM) and CPDY (0.3 μM). The reaction was allowed to proceed at 37°C. Aliquots drawn at desired intervals were either diluted (1:1000) with phosphate buffer (pH 7.0) or with Tris-glycine buffer (200 mM, pH 8.3). The former sample was used for the determination of lysine:N^6-hydroxylase activity and the latter for SDS-PAGE analysis. The final concentration of the cofactor or the substrate, when included, was as follows: FAD (1 mM), ADP (1 mM), $NADP^+$ (1 mM) and L-lysine (5 mM).

In some experiments, the C-peptide (the synthetic decapeptide with amino acid sequence identical with that of the segment comprising residues 416-425 of *r*IucD, except for the D-configuration of its C-terminal residue) was included in the reaction mixture over a concentration range of 0.1-0.5 mM.

3.4.3 Amino acid analyses

For quantitative estimation of the amino acids released by action of exopeptidases, the procedure was similar to that documented previously (82). Aliquots drawn at desired intervals were treated with a slurry of Dowex 50-X16 (H^+ form resin). The resin was washed extensively with water and the amino acids were recovered by elution with 6N HCl. After removal of HCl, the sample was analysed for amino acids by ion exchange chromatography (83).

3.4.4 Influence of FAD and ADP on the catalytic activity of endopeptidases

The measurement of the proteolytic activity of endopeptidases (TPCK-trypsin, TLCK-chymotrypsin, and thermolysin) was performed using azocasein as the substrate (84). A typical reaction, in a final volume of 3 mL, consisted of azocasein (1% w/v), potassium phosphate or PIPES (100 mM, pH 7.5) and endopeptidase (150 μg). Following incubation at

25°C for 30 minutes, the reaction was terminated by the addition of an equal volume of TCA (10%). After an hour of standing at room temperature, the absorbance at 336 nm of the supernatant was recorded. The principle of the method is based on the conversion of the protein to TCA soluble oligopeptides due to degradation by proteases. FAD and ADP, when included in the assay were used at a final concentration of 1 mM.

3.4.5 Effect of ADP and C-peptide on the catalytic function of CPDY

The enzymatic activity of CPDY was assessed using furyl acryloyl-L-Phe-L-Ala (FA-Phe-Ala) as substrate (85). Typically, the reaction mixture of 1 mL in volume, consisted of: potassium phosphate (100 mM, pH 6.0), FA-Phe-Ala (0.5-1.0 mM) and CPDY (10 µg). The assay, initiated by the addition of CPDY, was followed by monitoring the decrease in absorbance at 340 nm. The concentration of ADP, when included, was 1 mM while that of the C-peptide was varied over the range of 0.06-0.5 mM.

3.5 Analytical Methods

3.5.1 Determination of the homogeneity and molecular weight of the protein preparations

SDS-PAGE analyses of *r*IucD and its variants at various stages of their purification were performed using 10% polyacrylamide gels according to the procedure of Laemmli (86).

Whole cell lysates were also examined for the presence of the *iuc*D gene product and these were prepared by suspension of cells, collected by centrifugation after 24 hours of growth, in SDS-PAGE sample buffer and boiled for 3 minutes.

3.5.2 Determination of protein concentration

3.5.2.1 Spectrophotometric method

The absorbance of lysine:N^6-hydroxylase was measured at 280 nm and the concentration of lysine:N^6-hydroxylase, or its muteins, was estimated using an ε_M of 62,000 M^{-1} cm^{-1} (59).

3.5.2.2 Bradford assay

In some cases, protein concentration was determined by the Coomassie blue binding technique reported by Bradford (87). The Coomassie blue reagent was purchased from BioRad laboratories.

In a typical procedure, an aliquot (100 µL) of the protein was treated with 5 mL of the above reagent. After thorough mixing, the absorbance at 595 nm was recorded. A reagent blank using buffer instead of protein solution served as a control. The concentration of the protein was estimated by reference to a calibration curve constructed using a solution of bovine serum albumin (over the range 0-1.0 mg/mL).

3.5.3 Determination of DNA concentration

The concentration of DNA, either single or double stranded, was determined using its absorbance at 260 nm. An absorbance of 1.0 at 260 nm corresponds to 50 ng/µL and 33 ng/µL for double stranded and single stranded DNA, respectively (88).

3.5.4 Determination of lysine:N^6-hydroxylase activity

The protocol employed for the measurement of lysine:N^6-hydroxylase activity was similar to that reported previously (40). A typical assay, in a final volume of 5 mL, consisted of: potassium phosphate (100 mM, pH 7.2), L-lysine (1 mM), FAD (40 µM), $NADP^+$ (160 µM), G-6-P (800 µM), G-6-P dehydrogenase (1.25 units), and *rlucD* (83.3 nM). Following incubation at 37°C for 15 minutes, the reaction was terminated by the addition of a slurry of Dowex 50W-X8 (200-400 mesh, H^+ form) resin in distilled water. The entire mixture was

transferred to a 1.4 x 25-cm glass column and washed with 0.2N HCl (40 mL) prior to elution with 6N HCl (25 mL). The effluent was taken to dryness and the residue was dissolved in water and used for the determination of N^6-hydroxylysine by the iodine oxidation procedure (89).

3.5.5 Determination of NADPH oxidation

The oxidation of NADPH was followed by the decrease in absorbance at 340 nm. A typical assay mixture, in a 1 mL volume, consisted of potassium phosphate (200 mM, pH 7.0), FAD (40 μM), NADPH (200 μM), L-lysine (1 mM), and *r*lucD (2-3 μM). A baseline was established by adding FAD and NADPH to the potassium phosphate and recording the absorbance for 30 seconds. At this point *r*lucD, or its muteins, was added, the solution mixed and the decrease in A_{340} monitored for 1 minute. L-Lysine was then added to the assay, the solution mixed and the decrease in A_{340} monitored for a further 2 minutes. The initial decrease in A_{340} in the absence of L-lysine reflects the NADPH oxidation that is not coupled to the N-hydroxylation process.

3.5.6 Determination of kinetic parameters

The effect of Cys→Ala replacement(s) in *r*lucD on its K_M values for FAD and L-lysine was investigated as follows. In the case of K_M determination for FAD, the concentrations of L-lysine (1 mM) and NADPH (200 μM) were maintained constant while that of the flavin cofactor was varied over the range of 0-50 μM. For the determination of K_M for L-lysine, the concentration of FAD (30 μM for all except C31A/C51A *r*lucD which was 60 μM) and NADPH (200 μM) was held constant and that lysine was varied over the range of 0-10 mM. Identical assay mixtures except for the increasing concentrations of FAD (or L-lysine) were employed and the initial rate of NADPH oxidation was recorded by

monitoring the decrease in absorbance at 340 nm. Appropriate correction was made for the NADPH oxidation that occurs in the absence of the hydroxylatable substrate. These experiments were repeated twice. Assessment of K_M was achieved using GraFit 3.0 by the Marquart-Levenberg method for non-linear regression (90).

Since the rate of N-hydroxylation of L-lysine is inhibited at high concentrations of FAD (> 80 mM) and NADPH (≥ 300 mM), conditions chosen in the experiments designed to assess the K_M value for FAD were found to be optimal for the determination of k_{cat} of the protein. The V_{max} obtained from the double reciprocal plot provided the basis for the estimation of k_{cat}.

3.5.7 Determination of H_2O_2 production

The procedure described by Hildebrandt *et al.* (91) was used for the quantitative determination of H_2O_2 production by *rl*ucD. In a typical experiment, the assay mixture, in a final volume of 5 mL, consisted of: potassium phosphate (100 mM, pH 7.0), FAD (40 μM), $NADP^+$ (80 μM), G-6-P (1 mM), G-6-P dehydrogenase (1.25 units) and *rl*ucD (83.3 nM). The reaction was allowed to proceed at 37°C for 15 minutes. At desired intervals, aliquots (1.5 mL) were removed and the reaction stopped by the addition of an equal volume of TCA (3% w/v). The mixture was centrifuged (6000 x g) for 5 minutes. The clear supernatant was treated with ferrous ammonium sulphate (0.5 mL, 10 mM) followed by potassium thiocyanate (0.2 mL, 2.5 M). After 10 minutes at room temperature, the absorbance at 480 nm was recorded. A calibration curve constructed using authentic H_2O_2 (0-100 μM) provided the basis for quantitation of the amount present in the samples.

In experiments designed for the determination of H_2O_2 under conditions of lysine:N^6-hydroxylation, assay mixtures also included L-lysine (1 mM). After 15 minutes of

Figure 6: **Standard curve used for the quantitative determination of H_2O_2**

Aliquots of H_2O_2 (concentrations as shown) were analysed by Hildebrandt's procedure (91) to construct the reference curve.

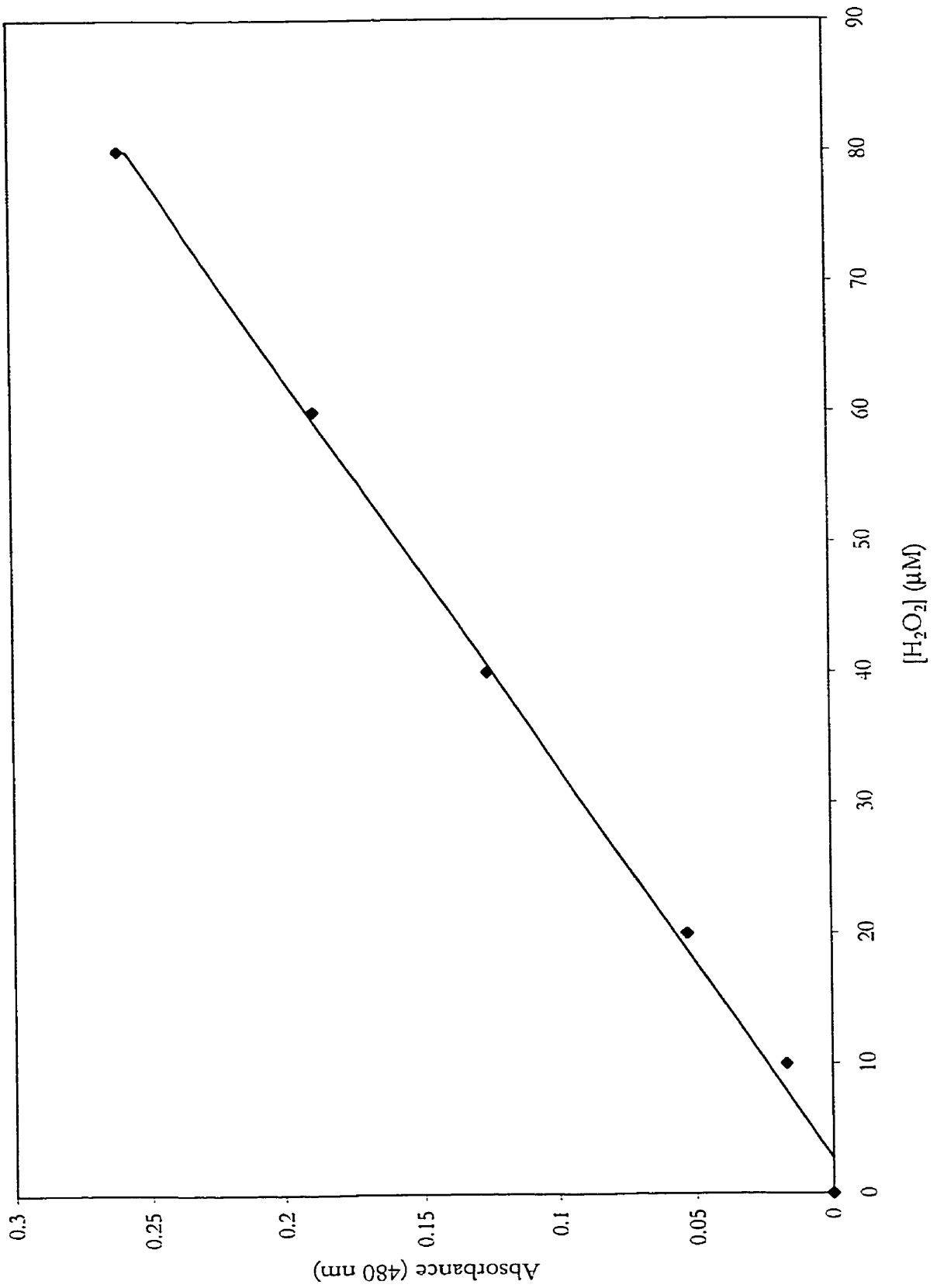
Absorbance (480 nm)
0.3
0.25
0.2
0.15
0.1
0.05
0
0
10
20
30
40
50
60
70
80
90
[H2O2] (µM)

incubation, a 3.5 mL aliquot was used for the determination of N^{ϵ}-hydroxylysine and the remaining aliquot for H_2O_2 determination.

3.5.8 Determination of cysteine residues (92)

The number of thiol groups accessible to modification in the native conformation of *r*lucD, or its variants, was assessed by treatment with DTNB. In a typical experiment, final volume of 1 mL, the procedure adopted was as follows: to a solution (900 µL) of DTNB (500 µM) in potassium phosphate (200 mM, pH 8.0), an aliquot (100 µL) of *r*lucD was introduced and the increase in absorbance at 412 nm was recorded until such change was negligible. The final concentration of *r*lucD in these reactions was in the range of 3-5 µM. Appropriate corrections for dilution and contributions due to spontaneous hydrolysis were achieved by the use of controls which were identical to the reaction samples but for the omission of *r*lucD. The quantitation of the number of thiol groups per mole of *r*lucD was achieved using an ε_M value of 14,150 $M^{-1}cm^{-1}$ for 2-nitro-5-thiocyanobenzoate anion (93).

The same reaction was performed in the presence of guanidine hydrochloride (4 M), conditions that effect the denaturation of the protein, providing an estimate of the total number of cysteine residues in *r*lucD.

3.5.9 Reaction of *r*lucD with DPIP

The ability of *r*lucD muteins to form covalent adducts with DPIP was assessed by the procedure described previously (58). In a typical experiment, the initial absorbance of a solution (800 µL) of DPIP (100 µM) in 200 mM potassium phosphate, pH 7.0 was recorded prior to the introduction of an aliquot (200 µL) of the desired *r*lucD mutein preparation to achieve a final concentration of 10 µM with respect to the protein. Following thorough mixing, the reaction was monitored until there was no further decrease in the absorbance at

600 nm, a process which required 6-8 min. The magnitude of the decrease in absorbance at 600 nm was recorded. Since the participation of each cysteine residue in the oxidative addition process results in a decrease in absorbance at 600 nm, the magnitude of diminution in absorbance will be proportional to the number of thiol functions involved in the reaction with DPIP. Hence, the number of cysteine residues involved in conjugation was established from the total decrease in absorbance at 600 nm using an operational ε_M value of 1×10^4 $M^{-1}cm^{-1}$ for the dye (60-62).

In some instances, the reaction mixture was subsequently subjected to chromatography on a 10 x 1 cm column of Biogel P2 with 200 mM potassium phosphate, pH 7.0 serving as equilibration and elution medium. The absorbance of the recovered protein at 280 nm and 654 nm was recorded. In these studies, parent *r*lucD preparation served as control. This data served to establish the stoichiometry of the process.

3.5.10 FAD and DPIP reductase activity

The ability of both unmodified as well as covalent DPIP conjugates of *r*lucD and its muteins to catalyse the FAD-dependent electron transfer process between NADPH and the exogenous dye was investigated. The procedure was similar to that reported previously (58). Thus, protein samples incubated with DPIP for 1 minute prior to the introduction of NADPH followed by FAD were taken to approximate the situation that occurs with the unmodified protein preparations, while those preincubated with the dye for 15 minutes were regarded to mimic the phenomenon that prevails in the case of covalent DPIP adducts of the proteins.

Typically, the reaction mixture in a final volume of 1 mL, consisted of DPIP (100 μM) and *r*lucD or its mutein (2.5 μM) in 200 mM potassium phosphate, pH 7.0. After either 1 or 15 minutes of incubation, an aliquot of NADPH solution was introduced to achieve a

final concentration of 200 μM with respect to the cofactor. The decrease in absorbance at 600 nm was monitored for 40 s. This was followed by the addition of an aliquot of FAD solution to achieve a final concentration of 40 μM and the decrease in the absorbance was again recorded over a period of 60 s. The initial process represents DPIP reductase activity in the absence of FAD while the latter reflects the same phenomenon in the presence of the flavin cofactor.

It is pertinent to note that the term "diaphorase" has been commonly used to describe the electron transfer reaction between NAD(P)H and an artificial electron acceptor in the presence of flavin cofactor (94,95). In this study, the phenomenon is referred to as "DPIP reductase" activity. Such a definition would allow for a clear distinction between the processes that occur in the absence and in the presence of the flavin cofactor.

3.5.11. Purification of anti-*rlucD* antibody from rabbit serum

Polyclonal anti-*rlucD* (developed in rabbits) was purchased from Alpha Diagnostic International. This was purified with the aid of MAbTrap™ GII kit (Pharmacia). The procedure is given below.

The kit (stored at 4°C) was allowed to equilibrate to room temperature over a period of 30 minutes. The HiTrap Protein G column was washed with 5 mL of water (MilliQ filtered) prior to its equilibration with buffer EQ (3 mL). Rabbit serum containing anti-*rlucD* was filtered (Gelman filter, 0.45 μm) and diluted with an equal volume of buffer EQ. An aliquot (2 mL) of this material was applied to the HiTrap Protein G column. The gel was washed with buffer EQ (7 mL) and was subsequently eluted with buffer EL (5 mL), the effluent collected in 1 mL fractions in tubes containing buffer NE (75 μL) to bring the solution to pH 7.0. The concentration of the protein was determined both by Bradford assay as well as absorbance at 280 nm. Protein rich fractions were pooled and desalted by

chromatography on a 15 x 1 cm column of Sephadex G-15 (50 mM potassium phosphate, pH 7.0 containing 150 mM NaCl serving as equilibration and elution medium). The fraction containing protein was stored at 4°C.

3.5.12 Western blot analysis

Protein samples (25 µg), after separation by SDS-PAGE (10% gel), were transferred to nitrocellulose over 2 hours at 4°C (100 V constant voltage) followed by two brief washes in Tris-buffered saline (TBS; 20 mM Tris, 500 mM NaCl, pH 7.5). Non-specific binding of the antibody was inhibited by blocking the membrane with 5% skim milk powder (w/v) in TBS overnight at 4°C. The membrane was then rinsed twice with TTBS (TBS containing 0.05% Tween-20) for 5 minutes at room temperature prior to incubation with purified polyclonal rabbit anti-*r*IucD (1:2000 dilution in TTBS) for 2 hours at room temperature. The membrane was rinsed twice with TTBS for 10 minutes at room temperature prior to incubation with goat anti-rabbit alkaline phosphatase conjugated secondary antibody (1:3030 dilution in TTBS) for 2 hours at room temperature. The membrane was subsequently washed twice for 5 minutes in TTBS and once for 5 minutes in TBS at room temperature prior to detection by incubation with nitroblue tetrazolium and bromochloroindolyl phosphate (96).

3.5.13 CD

CD spectra were recorded over the range 185-250 nm on a Jasco J-700 Spectropolarimeter set at 20 mdeg sensitivity, 0.2 nm resolution, 4 unit accumulation, 8 s response and a scanning speed of 200 nm/min. *r*IucD concentration was 5 µM in potassium phosphate (200 mM, pH 7.0). Measurements were made in a 300 µL cylindrical quartz cell with a 1 mm pathlength. Concentrations of ligands when used were: FAD (200 µM) and L-lysine (5 mM).

3.5.14 DSC

Differential scanning calorimetric studies were performed using a Nano DSC from Calorimetry Sciences Corp., Provo, UT. *r*lucD concentration: 1 mg/ml in potassium phosphate (200 mM, pH 7.0) containing DTT (1 mM). Concentrations of ligands when present: FAD (0.5 mM); ADP (1 mM); L-lysine (5 mM). heating rate: 1 deg/min.

4.0 Results

4.1 Physico-chemical characterisation of *r*lucD

Isolation and purification of the recombinant form of lucD was achieved by employing procedures that have been previously documented (46,47,59). The final step in the above protocol involves chromatography on Orange A Dyematrex with the recovery of protein being achieved by elution with a medium containing high concentrations of NaCl ($\geq$ 500 mM). As reported earlier (46) *r*lucD isolated under such conditions was recovered as an apoprotein in its tetrameric state and required NADPH and FAD for its catalytic function. Since high concentrations of Cl^- ions have been noted to exert a chaotropic effect (58), protein preparations, isolated in the current investigations, were routinely rendered free of Cl^- ions by ultrafiltration with repeated supplementation with 200 mM potassium phosphate, pH 7.0. This procedure also allowed for considerable (approximately 10-15 fold) increase in protein concentration. Since changes in operational manipulations can have profound influence on the properties of proteins and other biologically active materials, especially allosteric enzymes which are known to become desensitised by the mildest possible treatment (97,98), physico-chemical properties of *r*lucD were assessed subsequent to its transfer to a chloride free buffer medium as mentioned above.

4.1.1 Stability of *r*lucD

Superdex 200 chromatography of rlucD immediately after protein isolation from Orange A Dyematrex revealed the protein to exist as a tetramer, with a molecular weight $\approx$200 kDa, an observation in agreement with that previously recorded (47). Furthermore, the tetrameric organisation of *r*lucD did not appear to involve inter-subunit disulphide bridges since the protein, upon SDS-PAGE under non-reducing conditions, migrated as a single

component of molecular weight ≈50 kDa, corresponding to that of the monomer. Storage of *r*IucD, either at 4°C or -80°C, under conditions that minimise its denaturation (potassium phosphate, pH 7.0, ionic strength ~0.25) has been found to be accompanied by a progressive loss in its monooxygenase activity. This phenomenon could be reversed with complete restoration of monooxygenase function by treatment with thiol reagents such as DTT (≥10 mM), indicating participation of the protein's cysteine residues in the formation of disulphide bridges during its storage. In order to assess whether these disulphide bridges occurred within the tetramer (intra-tetramer) or between tetramers (inter-tetramer) of *r*IucD, the molecular weight of the protein was monitored by chromatography on Superdex 200 matrix at various intervals subsequent to its isolation. These studies have revealed that *r*IucD, immediately after isolation, is expected to exist predominantly as a tetramer (Figure 7A). During storage, this form of the protein disappears with the concomitant appearance of species with molecular weights > 200 kDa (Figure 7B). Treatment of such protein preparations with DTT results in the restoration of the initial tetrameric state (Figures 7C and 7D), indicating a rupture of inter-tetrameric disulphide bridges by the thiol reagent. As noted above, DTT treatment is also accompanied by restoration of the monooxygenase function of the protein. However, it is not possible to attribute the regeneration of enzymatic activity solely to the rupture of inter-tetramer disulphide bridges, since similar linkages occurring either within or between the monomeric subunits contributing to the tetrameric structure of the protein are also prone to reduction by the thiol reagents.

4.1.2 Studies with substrate analogs and other compounds

*r*IucD has been shown to be stringently specific, with only L-lysine and (S) 2-aminoethyl-L-cysteine serving as hydroxylatable substrates (47,99). Among the various lysine analogs studied, L-α-N-methyl-lysine was found to be a poor substrate (approximately 20%

Figure 7: **Chromatography of *r*lucD on Superdex 200**

The conversion of the tetrameric form of *r*lucD to polytetrameric species and the reversal of this process by DTT was monitored by chromatography of the samples on a 10 mm x 30 cm Superdex 200 column with 100 mM potassium phosphate, pH 7.0 serving both as equilibration and elution medium. Prior to chromatography of *r*lucD samples, calibration was achieved by the determination of the retention times of molecular weight standards as follows: Cytochrome c (12.4 kDa), 17.6 min; carbonic anhydrase (30 kDa), 16.5 min; albumin (67 kDa), 14.1 min; alcohol dehydrogenase (128 kDa), 12.8 min; and β-amylase (200 kDa), 12.2 min. Under these conditions, freshly prepared *r*lucD was found to have a retention time of 12.4 min.

Experimental conditions: protein concentration as shown; eluant, 100 mM potassium phosphate, pH 7.0; flow rate, 1 mL/min; chart speed, 0.4 cm/min.

A. *r*lucD immediately after isolation from chromatography on Orange A Dye matrix (46); 50 µL (8 µg) of sample was injected
B. *r*lucD sample from storage at -80°C, allowed to thaw at 4°C for 24 hours (free of NaCl and DTT); 25 µL (34 µg) of sample was injected
C. *r*lucD, same as in B but for treatment with DTT (10 mM) for 75 minutes; 25 µL of sample was injected
D. *r*lucD, same as in B but for treatment with DTT (50 mM) for 180 minutes; 25 µL of sample was injected.

Species emerging at 12.4 min represents the *r*lucD tetramer; species emerging at times <12.4 min reflect the polytetrameric form(s) of *r*lucD; and the species emerging at times >12.4 min represent buffer ions and/or DTT.

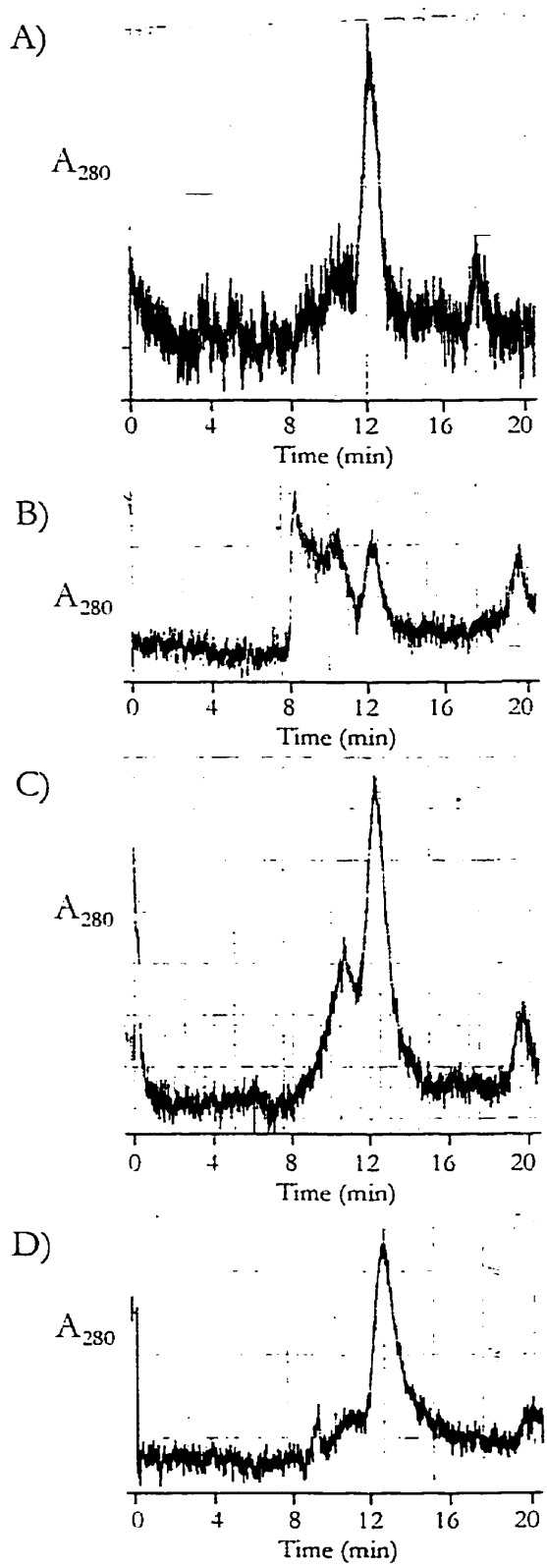
A)
A_{280}
0
4
8
12
16
20
Time (min)
B)
A_{280}
0
4
8
12
16
20
Time (min)
C)
A_{280}
0
4
8
12
16
20
Time (min)
D)
A_{280}
0
4
8
12
16
20
Time (min)

as effective as L-lysine) while *trans*-4,5-dehydro-L-lysine was devoid of this function. L-norleucine and L-methionine were found to inhibit lysine:N^6-hydroxylation mediated by *r*lucD (99). In the current investigations, the ability of hitherto untested lysine analogs to serve as either substrates or inhibitors of *r*lucD was explored. The compounds included were: L-β-lysine, DL-*cis*-4,5-dehydrolysine, L-methionine, DL-trifluoromethionine, DL-S-methylmethionine, DL-methionine phosphinate, DL-methionine phosphonate, L-methionine sulfoxide, L-norleucine, dimedone, and *cis*-Δ-4-tetrahydrophthalimide. Structures are shown in Figure 8. The last two compounds, although not substrate analogs were included to determine if a protein-sulfenic acid intermediate played a role in the enzyme's catalytic function by red-ox regulation (100). The ability of these two compounds to trap sulfenic acid(s) has been documented (101,102).

L-β-Lysine failed to serve either as a substrate or as an inhibitor of *r*lucD. On the other hand, *cis*-4,5-dehydrolysine was found to be a substrate, although only 20% as effective as L-lysine. As reported earlier (99), both L-norleucine and L-methionine served as inhibitors of *r*lucD's monooxygenase activity. Further studies indicated L-norleucine to function as a competitive inhibitor (Figure 9) with a K_i value of approximately 340 μM. None of the other methionine analogs exhibited inhibitory action on *r*lucD's monooxygenase function. While *cis*-Δ-4-tetrahydrophthalimide failed to inhibit rlucD, dimedone appeared to exert an adverse effect. Total inhibition of lysine:N^6-hydroxylase activity was noted by inclusion of dimedone (1mM) in the assay. Further investigation of this phenomenon revealed dimedone to have no effect when *r*lucD's monooxygenase activity was assessed by monitoring oxidation of NADPH coupled to N^6-hydroxylation of lysine. Furthermore, dimedone was found to interfere in the quantitative determination of both NH_2OH and N^6-hydroxylysine.

Figure 8: **Structures of L-lysine analogs and other compounds**

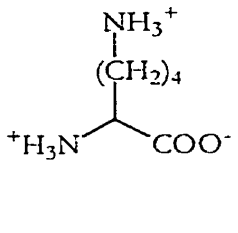

L-lysine

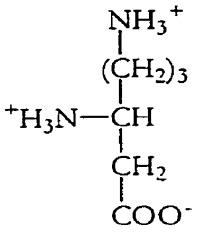

β-lysine

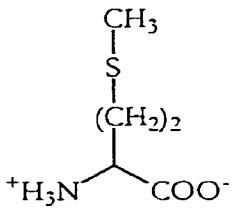

L-methionine

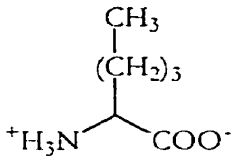

L-norleucine

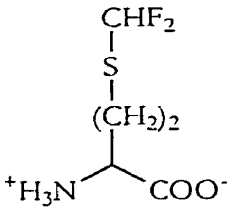

DL-difluoromethionine

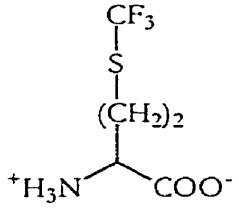

DL-trifluoromethionine

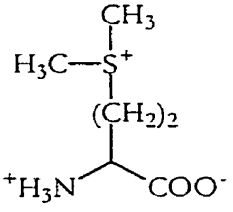

S-methylmethionine

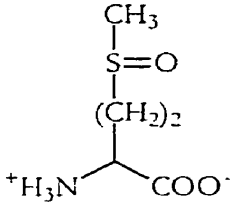

L-methionine sulfoxide

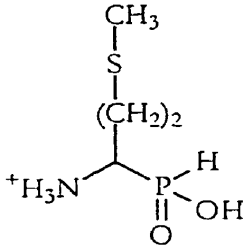

DL-methionine phosphinate

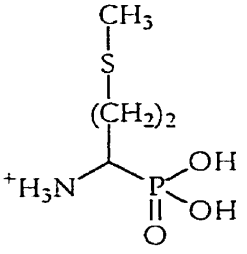

DL-methionine phosphonate

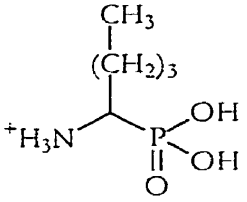

DL-norleucine phosphonate

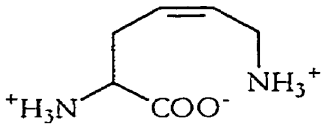

cis-4,5-dehydrolysine

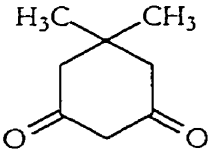

5,5-dimethyl-1,3-cyclohexanedione
(dimedone)

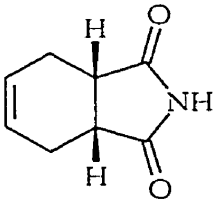

cis-1,2,3,6-tetrahydrophthalimide

Figure 9: **Influence of L-norleucine on *Aluc*D mediated N^6-hydroxylation of L-lysine. Double reciprocal plot of the data.**

◆-◆ no L-norleucine

■-■ 0.2 mM L-norleucine

●-● 1.0 mM L-norleucine

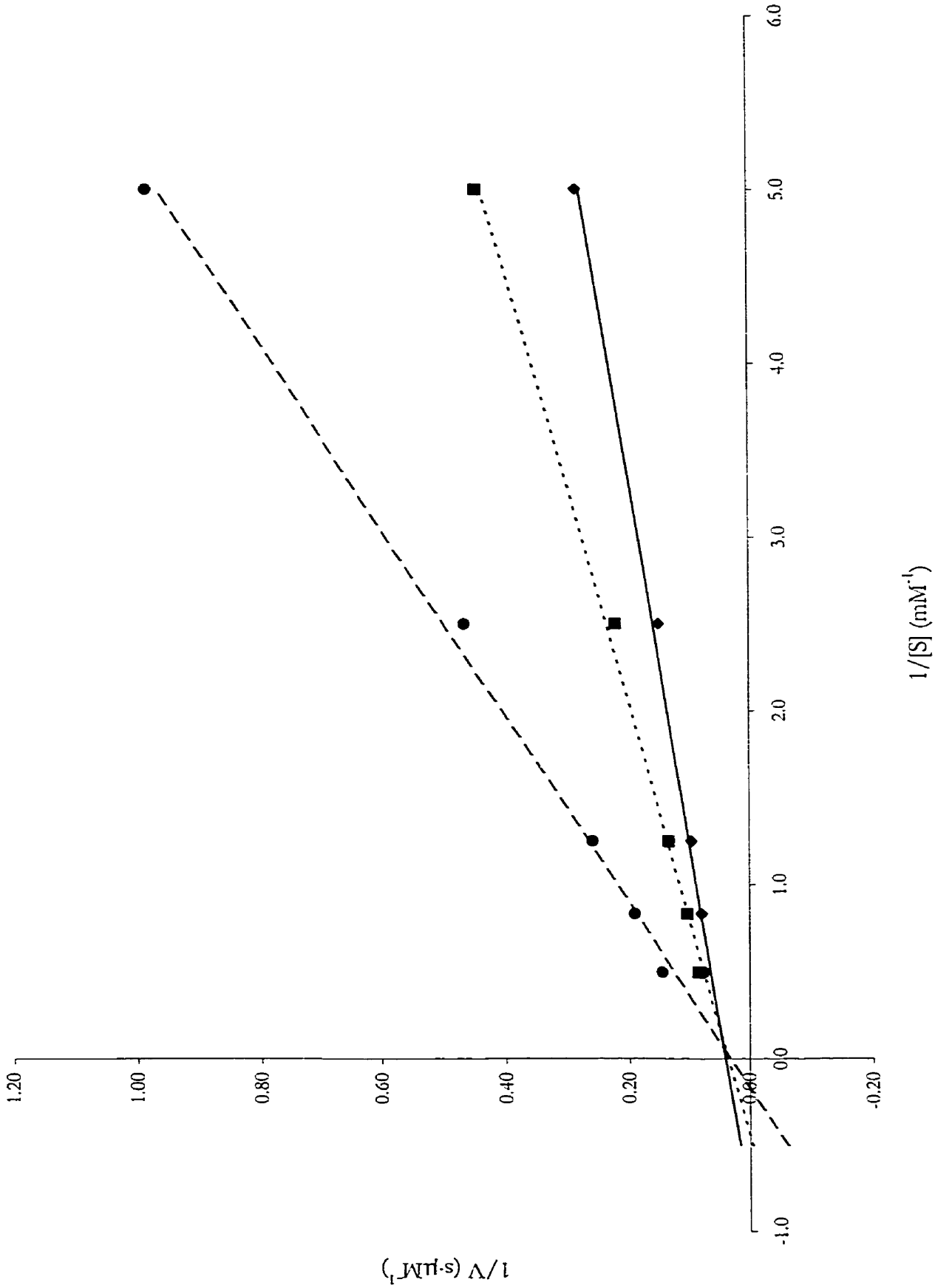
1/V (s·μM⁻¹)
1.20
1.00
0.80
0.60
0.40
0.20
0.00
-0.20
-1.0
0.0
1.0
2.0
3.0
4.0
5.0
6.0
1/[S] (mM⁻¹)

Table 4: **Influence of various L-lysine analogs and other compounds on the monooxygenase activity of *r*IucD**

Effector	Lysine:N^6-hydroxylase Activity[a] (%)	
	+L-lysine	-L-Lysine
None	100	0
β-lysine	100	0
cis-4,5-dehydrolysine	102	21
L-norleucine	52 (18)	0
L-methionine[b]	56 (16)	0
DL-trifluoromethionine[b]	(78)	0
L-methionine sulfoxide	97	0
DL-norleucine phosphonate	108	0
DL-methionine phosphonate	96	0
DL-methionine phosphinate	98	0
DL-S-methylmethionine	100	0
Difluoromethionine	100	0
cis-Δ-4-tetrahydrophthalate	100	0
dimedone[c]	0	0

[a] Typical assay, in a final volume of 5 mL, consisted of: L-lysine (1 mM), potassium phosphate (100 mM, pH 7.0), FAD (30μM), DTT (2 mM), $NADP^+$ (80 μM), G-6-P (2.5 mM), G-6-P dehydrogenase (1.25 units) and *r*IucD (100 nM). The incubation period was 15 minutes at 37°C and the amount of N^6-hydroxylysine was determined as described in Methods. The compounds were included at a final concentration of 1 mM. In instances where *r*IucD's activity was also assessed by monitoring NADPH oxidation, G-6-P, G-6-P dehydrogenase and $NADP^+$ were omitted and NADPH (200 μM) was included.

[b] Values obtained at 5 mM concentration of effector in the assay shown in parenthesis.

[c] Loss of activity due to dimedone forming an adduct with N^6-hydroxylysine and thus interfering in its quantitative determination (see text).

The ability of carbonyl compounds to interfere in the quantitative determination of hydroxylamine and its derivatives by the iodine oxidation procedure has been documented (89). The results are summarised in Table 4.

4.1.3 Influence of L-norleucine and L-methionine on NADPH oxidation in the absence of L-lysine

Since L-norleucine and L-methionine inhibit *r*lucD mediated lysine:N^{ζ}-hydroxylation their influence on the protein's inherent ability to promote FAD-dependent NADPH oxidation was examined. As shown in Table 5 both L-norleucine and L-methionine inhibit NADPH oxidation that occurs in the absence of L-lysine.

Finally, the influence of L-norleucine on the interaction between *r*lucD and its flavin cofactor was investigated. The dissociation constant, K_D, of the *r*lucD•FAD complex was determined both in the absence and in the presence of L-lysine (5 mM) or L-norleucine (5 mM). The *r*lucD•FAD complex has been shown to be characterised by a K_D value ≈16 μM (101) and this value is only marginally affected by the presence of L-lysine (K_D ≈17.8 μM). In contrast, the K_D value for the complex in the presence of L-norleucine is approximately 4.6 μM, indicating that the analog promoted a relatively stronger interaction between *r*lucD and its flavin cofactor. This was further confirmed by the following observation. Chromatography of a mixture of *r*lucD (10 μM) and FAD (200 μM) on a 20 x 1 cm column of BioGel P4 (200-400 mesh) (equilibration and elution buffer was 200 mM potassium phosphate, pH 7.0) resulted in a clear separation of the two components with the protein emerging free of the flavin cofactor. When a similar experiment was performed in the presence of L-norleucine (in both the equilibration and elution buffers) the protein recovered was found to be associated with the flavin cofactor in the amount corresponding

Table 5: **Influence of L-norleucine and L-methionine on *rlucD* mediated NADPH oxidation in the absence of L-lysine**

Compound	Activity (%)
None	100
L-norleucine	
1 mM	69
5 mM	62
L-methionine	
1 mM	56
5 mM	47

A typical assay in a final volume of 1 mL comprised: NADPH (200 µM), FAD (30 µM), DTT (2 mM), *rlucD* (2 µM), and potassium phosphate (100 mM, pH 7.0). The reaction was monitored by recording the decrease in absorbance at 340 nm. The compound(s) when included are used at the final concentrations indicated.

to approximately 0.5 mole per mole of *r*lucD. Thus L-norleucine would appear to enhance the protein's affinity for the flavin cofactor.

4.2 Studies with S-carboxymethyl-*r*lucD

Treatment of *r*lucD with thiol modifying agents such as DTNB or ICH_2COO^- has been found to be accompanied by a loss of its monooxygenase function. In sharp contrast, replacement of its Cys51 and Cys158 residues, identified as the targets of alkylation by ICH_2COO^-, has no such adverse effect (59). These apparently incongruous findings prompted further studies so as to establish the basis for the loss of *r*lucD's ability to effect N^6-hydroxylation of L-lysine upon chemical modification of its thiol functions. Consequently the protein was converted to its S-carboxymethyl derivative by alkylation with ICH_2COO^- (58).

Initial efforts pertained to chromatography of the S-carboxymethyl-*r*lucD on Superdex 200. This study revealed S-carboxymethyl-*r*lucD to occur as a tetramer similar to the parent protein. Furthermore, the DSC profile of S-carboxymethyl-*r*lucD would appear to be very similar to that of the parent protein (Figure 10). The above observations demonstrate that chemical modification of *r*lucD is not accompanied by major aberrations in its structural organisation.

Furthermore, its affinity for the flavin cofactor was not adversely affected as indicated by its ability to mediate the reduction of exogenous electron acceptors, such as DPIP. FAD has been shown to be an obligatory participant in the electron transfer processes catalysed by *r*lucD and its S-carboxymethyl derivative (58). *r*lucD has been noted to rapidly lose its ability to accommodate FAD in the electron transfer processes in the presence of DPIP. This outcome has been linked to the covalent modification of the

Figure 10: **DSC profiles for *r*IucD and S-carboxymethyl *r*IucD**

*r*IucD and S-carboxymethyl-*r*IucD (≈1 mg/mL) in potassium phosphate (200 mM, pH 7.0) containing DTT (1 mM) was heated at a rate of 1 K/min.

——— *r*IucD ; - - - - - S-carboxymethyl *r*IucD

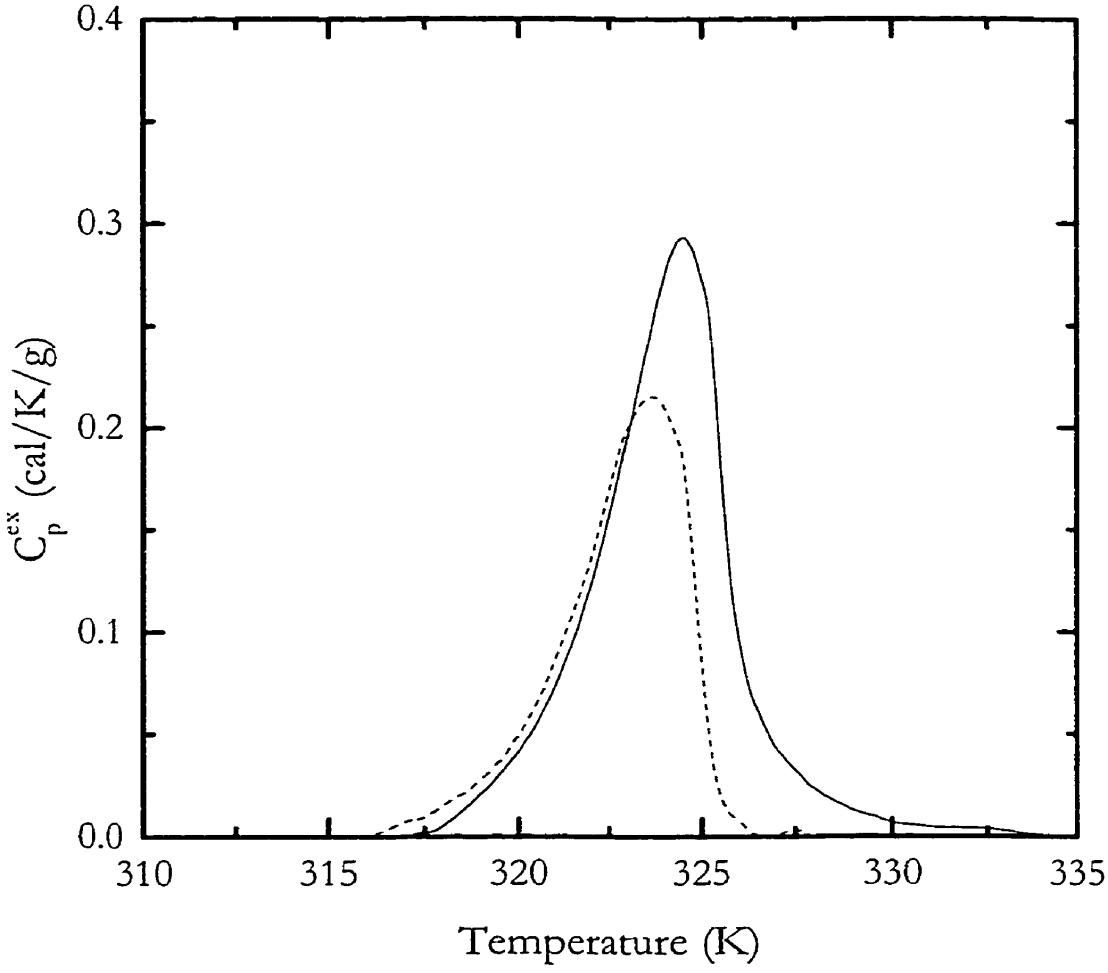
0.4
0.3
0.2
0.1
0.0
C_p^{ex} (cal/K/g)
310
315
320
325
330
335
Temperature (K)

protein's thiol functions by DPIP, resulting in a loss of its catalytic activity. In contrast, S-carboxymethyl-*r*IucD, by virtue of its inability to undergo covalent interaction with DPIP, has been found to accommodate FAD in its diaphorase function (58). These reactions are illustrated in Schemes 4 and 5. When cytochrome c, which cannot enter into such covalent interaction, was used as an electron acceptor, both rIucD and its S-carboxymethyl derivative were found to be as effective in diaphorase activity. These results are shown in Figure 11.

4.3 Physico-chemical characterisation of *r*IucD muteins

4.3.1 Isolation and purification

The individual replacement of Cys31, Cys146 and Cys166 of *r*IucD with alanine was achieved by effecting appropriate site directed mutagenesis of *iucD* present in pAT5 (see procedures outlined on pp. 34-35). pAT5 harbouring the *iucD* gene variant encoding for C31A-*r*IucD served as a template for the production of the protein with both Cys31 and Cys51 substituted with alanine. The incorporation of the desired mutation(s) was confirmed by the determination of the nucleotide sequence of *iucD* and this approach also served as a means to verify the absence of other mutations in the gene.

The plasmid preparations containing the *iucD* or its variants were used to transform *E. coli* DH5α (or in some instances *E. coli* BL21(DE3)) and the cultures (1.5L) were used for the production of *r*IucD or its mutein(s). Cultures expressing catalytically functional IucD have been noted to accumulate N^6-hydroxylysine in the medium and this feature provided a preliminary diagnostic means of assessing the effect of mutation(s) in *iucD*. After 16-24 hours of growth, the cells were collected by centrifugation (6000 x g) for 15 minutes. The supernatant, prior to being discarded, was tested for the presence of N^6-hydroxylysine by the iodine oxidation procedure (89). Such an analysis revealed that cultures expressing C31A-, C146A-, C166A-, and C31A/C51A-*r*IucD to be capable of producing N^6-hydroxylysine,

Scheme 4: **Mechanism for NADPH-dependent reduction of exogenous DPIP by covalent *Ac*ucD-DPIP complex** (103)

DPIP reductase activity that occurs in the absence of FAD (p. 50).

1. First oxidative addition.
2. Electron transfer to free DPIP.
3. Second oxidative addition.
4. Inability to bind FAD.

DPIP = 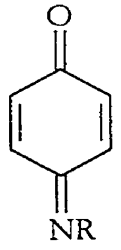

R = 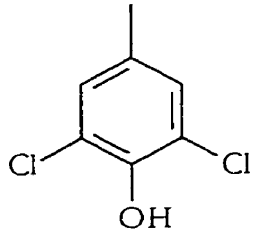

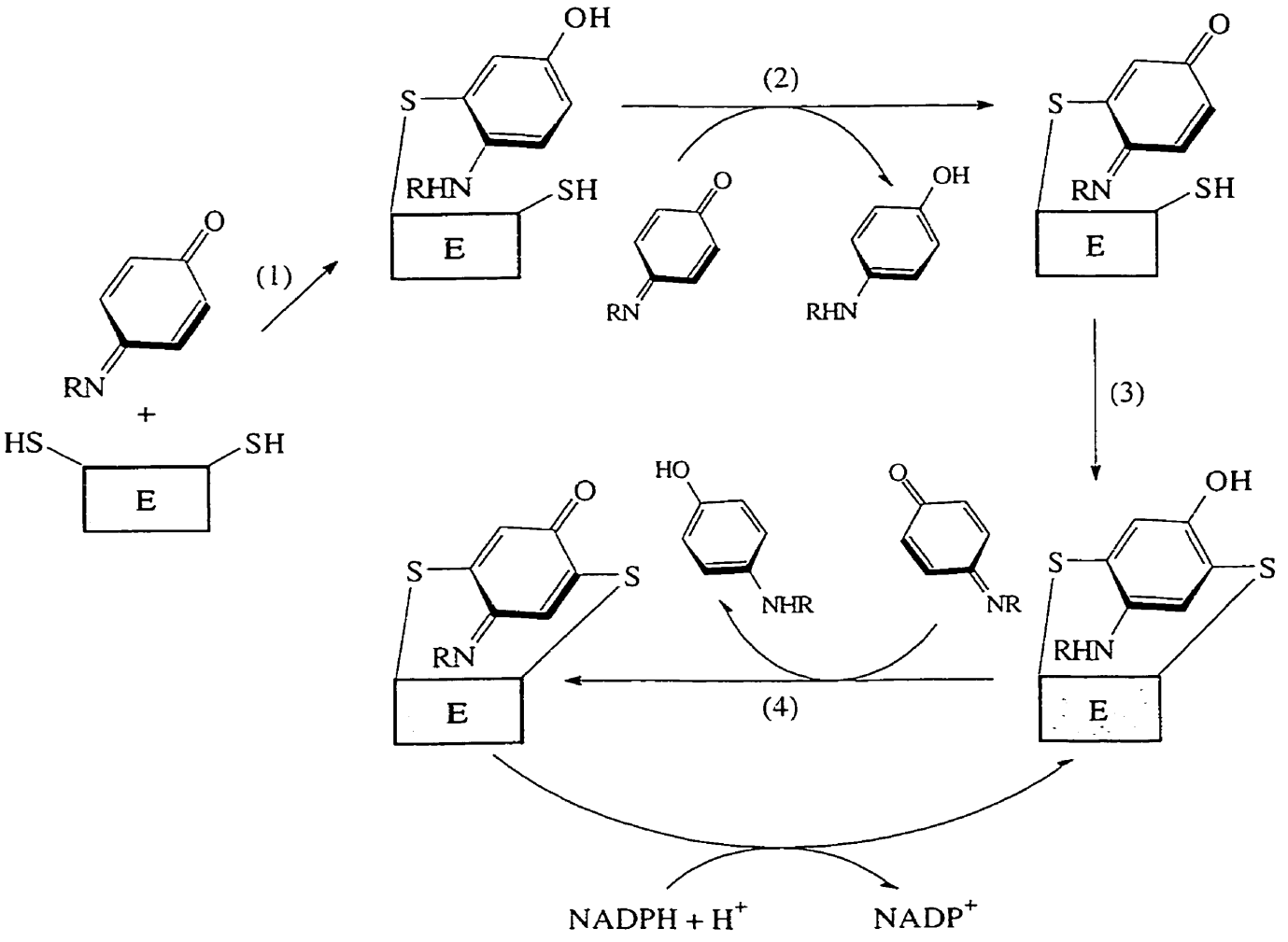
(1)
(2)
(3)
(4)
RN
HS
SH
E
RHN
OH
O
S
NHR
NR
HO
NADPH + H+
NADP+

Scheme 5: **Mechanism for NADPH-dependent reduction of exogenous DPIP by noncovalent complex of *Ruc*D and DPIP** (103)

Diaphorase activity (p. 50).

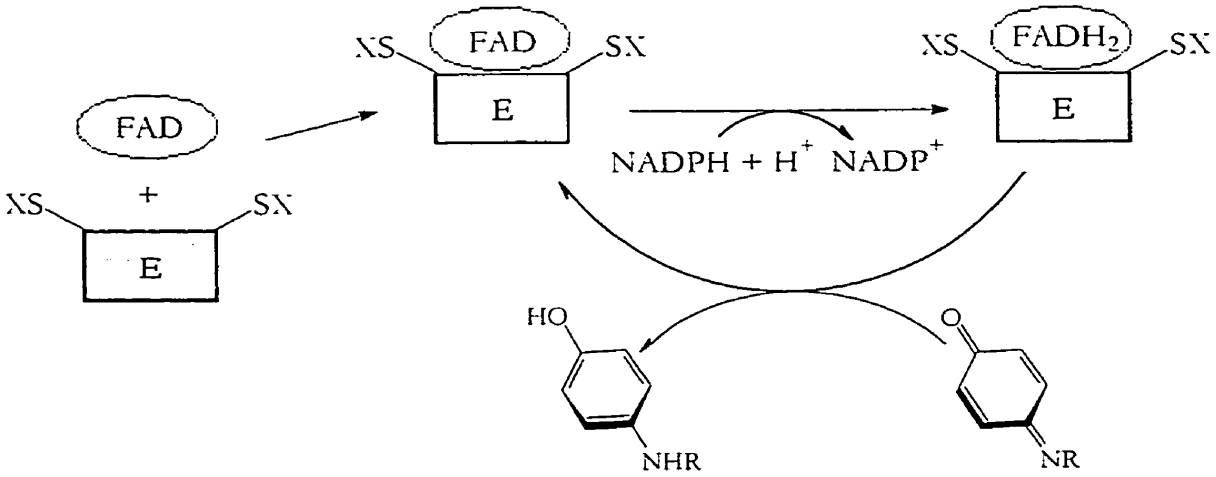
FAD
XS
SX
E
+
XS
SX
E
XS
FAD
SX
E
NADPH + H+ NADP+
XS
FADH2
SX
E
HO
NHR
O
NR

Figure 11: **Cytochrome c reduction catalysed by *r*IucD and its S-carboxymethyl derivative**

A typical reaction mixture in a final volume of 1 mL consisted of: potassium phosphate (100 mM, pH 7.0), NADPH (200 μM), FAD (40 μM), Cyt c (100 μM) and *r*IucD or its S-carboxymethyl derivative (0.9 μM). The reaction was monitored by following the increase in absorbance at 550 nm.

1. *r*IucD
2. S-carboxymethyl *r*IucD
3. 2. + L-lysine (1 mM)
4. 1. + L-lysine (1 mM) or SOD (10 μg)
5. Blank (no enzyme)

These observations suggest that modification of *r*IucD's cysteine residues by ICH_2COO^- does not affect its binding of cofactors, NADPH and FAD. Hence, the loss of monooxygenase activity may arise due to constraints imposed on the binding of the substrate.

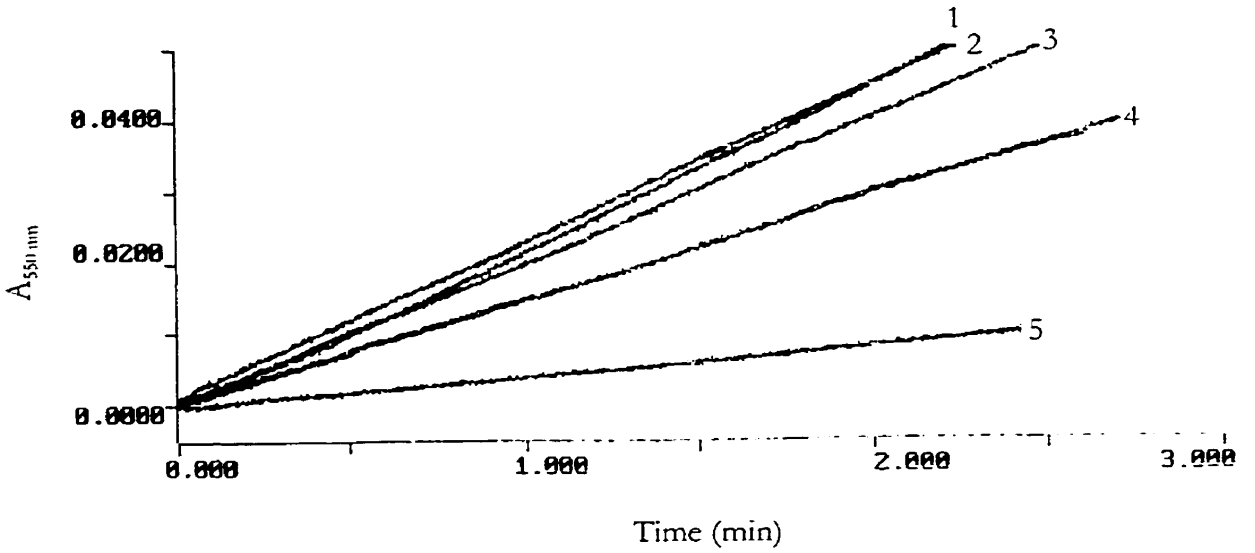
1
2
3
4
5
0.0400
0.0200
0.0000
$A_{550\,nm}$
0.000
1.000
2.000
3.000
Time (min)

indicating that the protein's monooxygenase activity was not adversely affected by the above amino acid replacements.

The isolation and purification of *r*IucD or its muteins was accomplished by the procedures described earlier (pp. 36-37). Following recovery from Orange A Dyematrex, the protein was rendered free of Cl^- ions by membrane filtration (Amicon Centriprep) followed by dialysis against potassium phosphate (200 mM, pH 7.0). As noted earlier, this procedure also served as a means for obtaining concentrated protein preparations.

SDS-PAGE analysis of the *r*IucD variants is shown in Figure 12.

4.3.2 Cysteine content of *r*IucD muteins

As noted earlier, the analysis of the nucleotide sequence of *iucD* variants encoding for the *r*IucD muteins served to confirm the incorporation of the desired exchange of the nucleotides in the gene. However, in order to unequivocally demonstrate the replacement of cysteine residue(s) with alanine(s), the determination of the total number of such residues present in the various *r*IucD muteins was undertaken. This was accomplished by the reaction of the protein with DTNB (500 μM) in potassium phosphate (200 mM, pH 8.0) containing guanidine hydrochloride (4.0 M). The increase in absorbance at 412 nm was recorded and the number of cysteine residues present in the protein was estimated using an ε_M value of 14150 $M^{-1}cm^{-1}$ for the 2-nitro-5-thiocyanobenzoate (93). Since *r*IucD contains five cysteine residues, its variants with single cysteine replacements should be characterised by the presence of one less thiol function. As shown in Table 6, C31A-, C146A-, and C166A-*r*IucD preparations show the presence of approximately 4 moles of cysteine residues per mole of protein and in the case of C31A/C51A-*r*IucD the observed value is 3 moles of cysteines per mole of protein. Thus, the data recorded in Table 6 would appear to be in conformity with those expected on the basis of Cys→Ala replacements in *r*IucD.

Figure 12: **SDS-PAGE analysis of *r*lucD and its muteins**

From left → right

Lane 1, molecular weight standards: phosphorylase b (97.4 kDa), serum albumin (66.2 kDa), ovalbumin (45 kDa), carbonic anhydrase (31 kDa), trypsin inhibitor (21.5 kDa), and lysozyme (14.4 kDa); lane 2, *r*lucD; lane 3, C31A-*r*lucD; lane 4, C51A-*r*lucD; lane 5, C146A-*r*lucD; lane 6, C158A-*r*lucD; lane 7, C166A-*r*lucD; lane 8, C31A/C51A-*r*lucD; and lane 9, C51A/C158A-*r*lucD. (200 pmoles of each protein)

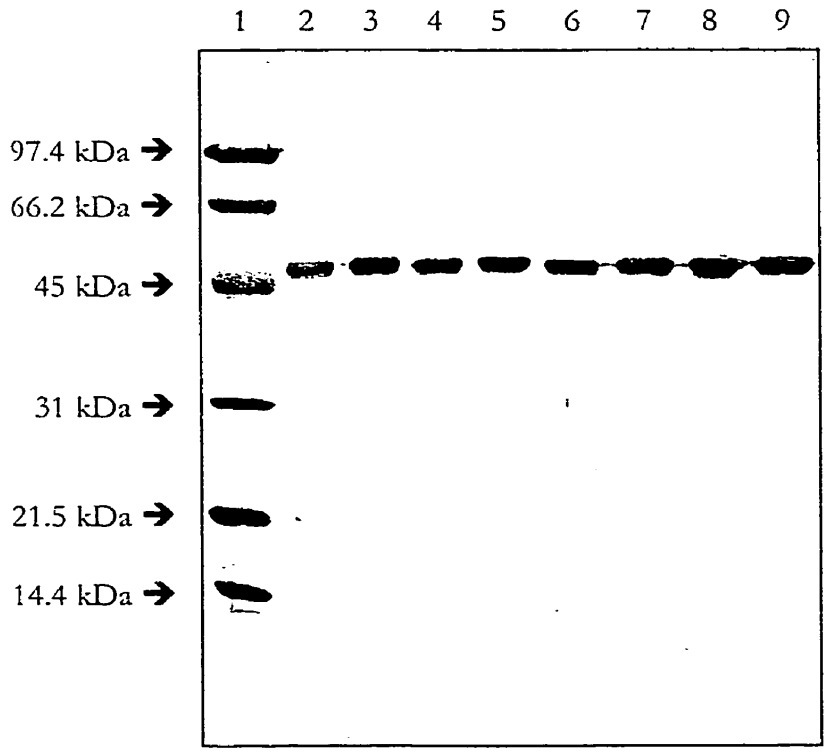
1 2 3 4 5 6 7 8 9
97.4 kDa
66.2 kDa
45 kDa
31 kDa
21.5 kDa
14.4 kDa

Table 6: **Total number of cysteine residues in *r*lucD and its muteins**

Protein	Number of Cysteine Residues[a]
*r*lucD	4.85 (5)
C31A-*r*lucD	3.95 (4)
C146A-*r*lucD	3.93 (4)
C166A-*r*lucD	4.04 (4)
C31A/C51A-*r*lucD	2.93 (3)
C51A-C166A-*r*lucD	2.77 (3)

[a] The protein (2-5 μM) was treated with DTNB (500 μM) in potassium phosphate (200 mM, pH 8.0) containing guanidine hydrochloride (4 M). ΔA_{412} was used to calculate the number of cysteine residues (see text). The values in parentheses indicate the probable number of cysteine residues per mole of protein.

The values shown represent the average of determinations done in duplicate.

4.3.3 Reactivity of cysteine residues in the native conformation of the protein

Similar reaction of the protein with DTNB under identical conditions except for the omission of guanidine hydrochloride provided an estimate of the thiol function(s) accessible to modification in the native conformation of the protein. For the sake of clarity in presentation as well as for the purpose of comparison, the results of similar studies recorded earlier (59) with *r*lucD, C51A-*r*lucD, C158A-*r*lucD, and C51A/C158A-*r*lucD are presented in Figure 13.

In the current investigations, C31A-*r*lucD behaves similarly to *r*lucD by showing the presence of three thiol functions capable of undergoing modification with DTNB, the reaction with two thiols being "fast" and that of the third being "slow". And the situation in the case of C31A/C51A-*r*lucD is similar to that of C51A-*r*lucD in that it has one "fast " and one "slow" reacting thiol function, indicating that Cys31 does not contribute to the second "fast" reacting thiol group in *r*lucD. In the case of C166A-*r*lucD, which still has Cys158 (the residue shown to be the "slow" reacting thiol function in *r*lucD) intact, DTNB titration indicates the presence of two "fast" reacting cysteine residues. Finally, the replacement of Cys146 with alanine results in profound conformational changes in *r*lucD, rendering all of its cysteine residues accessible to modification by DTNB. Of the four cysteine residues present in the protein, three are "fast" in their reaction with DTNB, while the fourth is "slow" to undergo such modification. All of these results are shown in Figure 14 and summarised in Table 7.

4.3.4 Thermal stability

The effect of Cys→Ala replacements on the structural integrity of *r*lucD was assessed by monitoring the change in its thermal stability. Accordingly, DSC profiles of *r*lucD and its variants (developed in the current study as well as those obtained earlier) were

Figure 13: **Accessibility of cysteine residues of *r*lucD and its muteins to modification by DTNB**
Redrawn based on data from Marrone, L. and Viswanatha, T. (1997) *Biochim Biophys Acta* **1343**, 263-277.

The desired protein preparation in 1 mL of potassium phosphate (200 mM, pH 8.0) was treated with an aliquot (100 µL) of DTNB (5 mM) and the progress of the reaction was monitored at 412 nm. After correction for the spontaneous hydrolysis of the reagent, ΔA values at 412 nm at various intervals of the reaction were used to determine the number of thiol group(s) modified per monomer of the protein.

○-○ *r*lucD
■-■ C51A-*r*lucD
●-● C158A-*r*lucD
□-□ C51A/C158A-*r*lucD

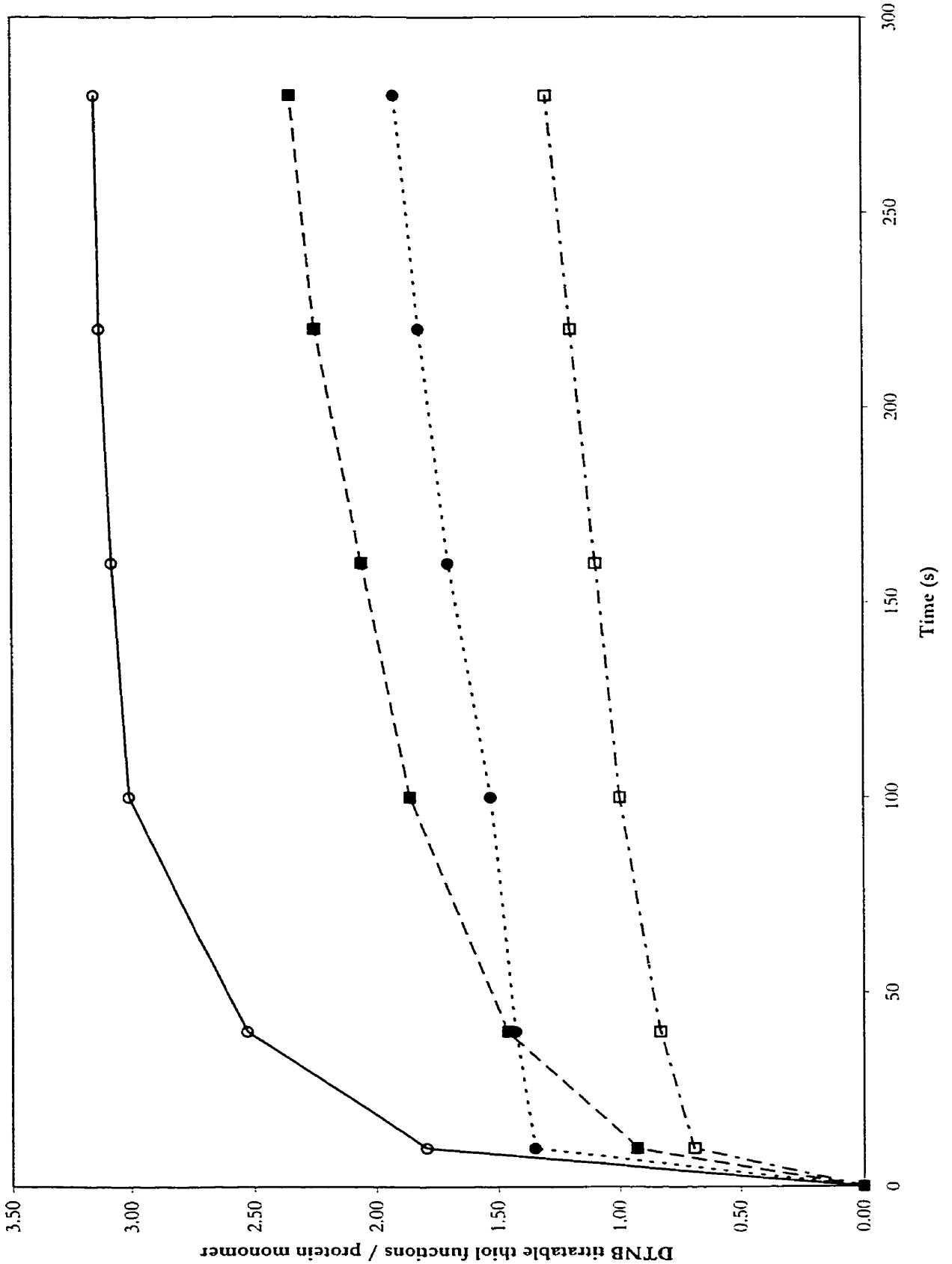
DTNB titratable thiol functions / protein monomer
3.50
3.00
2.50
2.00
1.50
1.00
0.50
0.00
0
50
100
150
200
250
300
Time (s)

Figure 14: **Accessibility of cysteine residues of *r*lucD muteins to modification by DTNB**

The protein (2-5 μM) in potassium phosphate (200 mM, pH 8.0) was treated with DTNB (500 μM). The increase in absorbance at 412 nm was recorded. The number of cysteine residues modified was calculated using an ε_M value of 14150 $M^{-1}cm^{-1}$.

○-○ C31A-*r*lucD

■-■ C146A-*r*lucD

●-● C166A-*r*lucD

□-□ C31A/C51A-*r*lucD

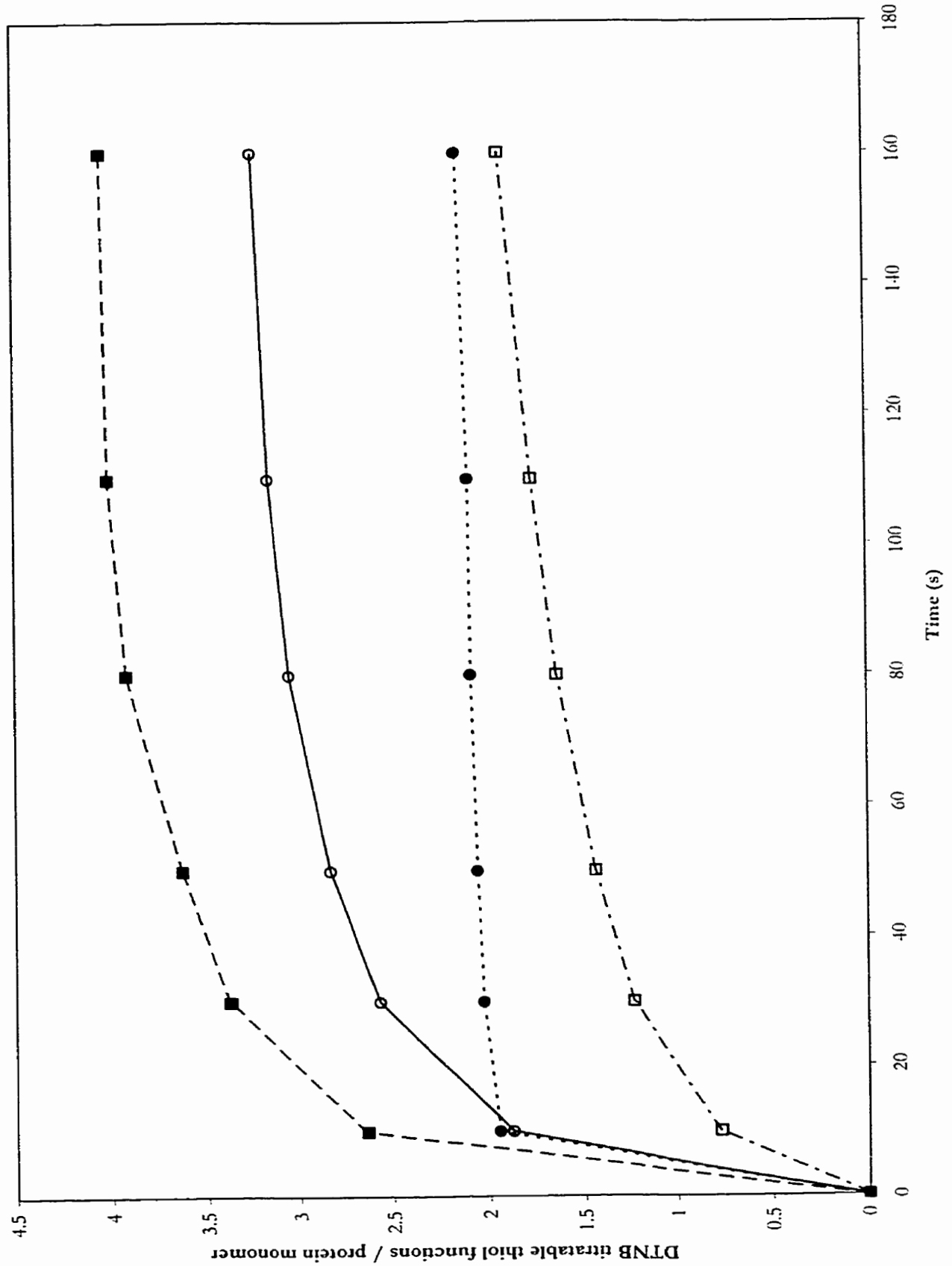
DTNB titratable thiol functions / protein monomer
4.5
4
3.5
3
2.5
2
1.5
1
0.5
0
0
20
40
60
80
100
120
140
160
180
Time (s)

Table 7: **Number of cysteine residues susceptible to modification by DTNB in the native conformation of *r*lucD and its muteins**

Protein	Number of Cysteine Residues Accessible to Modification in the Native State [a]	
	Fast	Slow
*r*lucD	2	1
C31A-*r*lucD	2	1
C51A-*r*lucD	1	1
C146A-*r*lucD	3	1
C158A-*r*lucD	2	—
C166A-*r*lucD	2	—
C31A/C51A-*r*lucD	1	1
C51A/C158A-*r*lucD	1	—
C51A/C166A-*r*lucD	1	—

[a] Estimated from Figures 13 and 14.
The experimental conditions are those described in the legends to Figures 13 & 14. Fast, reaction time ≤ 20 sec; slow, reaction time ≥ 150 sec.

recorded and these are shown in Figures 15 A-H. As shown in Figure 15A, *r*IucD is characterised by a T_M value of 324.5 K. Although, at first glance, the DSC profiles of *r*IucD and its muteins appeared to be similar, single cysteine replacements other than that of Cys51 resulted in a lowering of the T_M value with such decrease being maximum (2.4 K) in the case of C166A-*r*IucD (Table 8). In the case of C146A-*r*IucD and C166A-*r*IucD, the transition from the native to the denatured state is not smooth as indicated by the tailing in their DSC profiles. This feature may indicate the presence of region(s) that are relatively more prone to thermal denaturation than other areas in the protein as a consequence of the replacement of the cysteine residue. It is pertinent to note that the yield of the protein in cultures expressing C146A-*r*IucD, C158A-*r*IucD and C166A-*r*IucD is low relative to that in the one producing unmodified *r*IucD, although growth conditions were identical in all instances. This finding may be a reflection of these *r*IucD muteins being more susceptible to denaturation under growth conditions (37°C, 24 hours and vigorous shaking) than the parent protein. In the case of C51A-*r*IucD, the amino acid replacement results in an increase in the T_M (325.5 K) compared to the value of 324.5 K for unmodified *r*IucD. This enhanced thermal stability is also reflected in the protein being more stable and exhibiting approximately 40% increase in specific activity (with respect to monooxygenase function) when compared to the parent protein. Introduction of a second cysteine replacement in C51A-*r*IucD results in a lowering of the T_M value.

4.3.5 Reaction with DPIP

In addition to its being capable of serving as a terminal electron acceptor, DPIP can also function as a thiol modifying agent by virtue of its ability to participate in oxidative addition reaction(s) with mercaptans (60-62). Hence, the preparations of *r*IucD and its variants have to be rendered free of extraneous thiols (primarily DTT) prior to their use in

Figure 15 A-D: **DSC profiles of *r*IucD, C31A-, C51A-, and C146A-*r*IucD**

*r*IucD, C31A-, C51A-, and C146A-*r*IucD (≈1 mg/mL) in potassium phosphate (200 mM, pH 7.0) containing DTT (1 mM) was heated at a rate of 1 K/min.

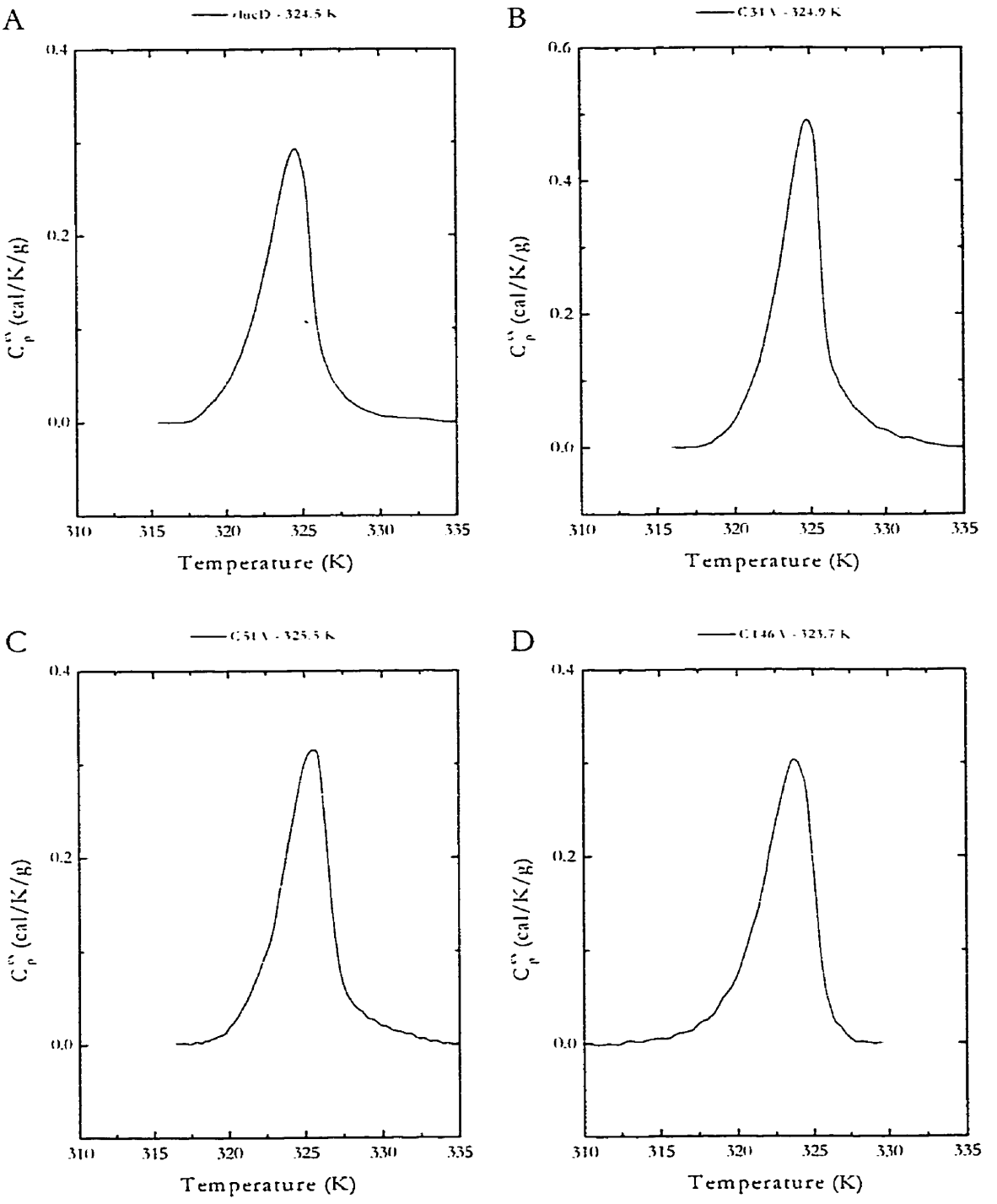
A
B
C
D
Temperature (K)
Temperature (K)
Temperature (K)
Temperature (K)

Figure 15 E-H: **DSC profiles of C158A-, C166A-, C31A/C51A-, and C51A/C158A-*r*lucD**

C158A-, C166A-, C31A/C51A-, and C51A/C158A-*r*lucD (≈1 mg/mL) in potassium phosphate (200 mM, pH 7.0) containing DTT (1 mM) was heated at a rate of 1 K/min.

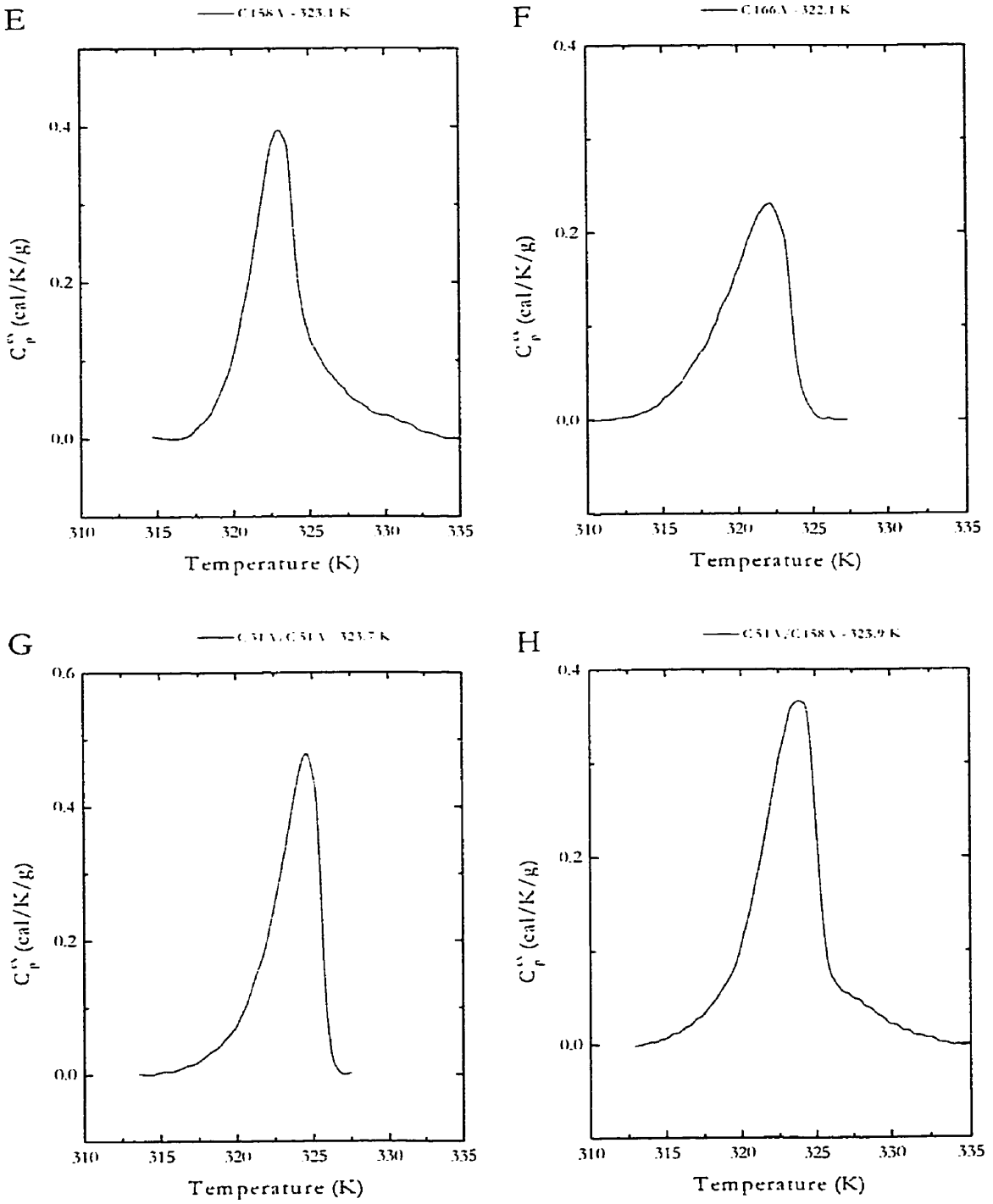
E
C158A - 323.1 K
0.4
0.2
0.0
C_p'' (cal/K/g)
310
315
320
325
330
335
Temperature (K)
F
C166A - 322.1 K
0.4
0.2
0.0
C_p'' (cal/K/g)
310
315
320
325
330
335
Temperature (K)
G
C51A/C51A - 323.7 K
0.6
0.4
0.2
0.0
C_p'' (cal/K/g)
310
315
320
325
330
335
Temperature (K)
H
C51A/C158A - 323.9 K
0.4
0.2
0.0
C_p'' (cal/K/g)
310
315
320
325
330
335
Temperature (K)

Table 8: **Summary of T_M values for *r*lucD and its muteins**

Protein	T_M (K)	ΔT_M (K)
*r*lucD	324.5	—
C31A-*r*lucD	324.9	+0.4
C51A-*r*lucD	325.5	+1.0
C146A-*r*lucD	323.7	-0.8
C158A-*r*lucD	323.1	-1.4
C166A-*r*lucD	322.1	-2.4
C31A/C51A-*r*lucD	323.7	-0.8
C51A/C158A-*r*lucD	323.9	-0.6

Values taken from Figure 15 A-H.

experiments with DPIP. This was accomplished by chromatography of the protein preparations on a 20 x 1 cm BioGel P4 (200-400 mesh) column with potassium phosphate (200 mM, pH 7.0) serving both as equilibration and elution medium.

In these investigations, attention was focused on the following two aspects: (i) the assessment of the number of cysteine residues of the protein involved in the oxidative addition reaction with DPIP; and (ii) the ability of the covalent DPIP conjugate of the protein to bind FAD, the cofactor essential for its catalytic function(s).

The first of these objectives was achieved by recording the decrease in absorbance at 600 nm for 10 minutes after initiating the reaction between the desired protein preparation and DPIP (see pp. 48-49 for details). Oxidative addition of thiol(s) (Scheme 4) would lead to conversion of the quininoid structure of DPIP to its leuco form as indicated by the diminution in absorbance at 600 nm. The magnitude of the decrease is proportional to the number of cysteine residue(s) participating in the oxidative addition process. The data presented in Table 9 show the number of cysteine residues of *r*lucD or its muteins involved in the conjugation reaction with DPIP. In the case of *r*lucD and C158A-*r*lucD, two cysteine residues would appear to be involved in conjugation with the dye and these results are in agreement with those recorded previously (59). C31A-*r*lucD mimicked *r*lucD and C158A-*r*lucD in that its interaction with DPIP also involved two thiol functions. As noted before (59), the interaction of DPIP with C51A-*r*lucD involved just one cysteine residue and the same situation prevailed for C31A/C51A-*r*lucD. These observations suggest that Cys51 in *r*lucD contributes to one of the two thiol groups participating in the oxidative addition reaction with DPIP, and a cysteine residue other than Cys31 in *r*lucD provides the second thiol group for conjugation with the dye. In the case of C166A-*r*lucD, approximately two thiol functions were involved in the conjugation process with DPIP. Finally, replacement of

Table 9: **Number of cysteine residues involved in the oxidative addition reaction with DPIP**

Protein	Number of Cysteine Residues Involved in Conjugation[a]	Number of DPIP molecules Involved in Conjugation
*r*IucD	1.94 (2)	1
C31A-*r*IucD	2.13 (2)	1
C51A-*r*IucD	1.24 (1)	1
C146A-*r*IucD	3.00 (3)	2
C158A-*r*IucD	1.98 (2)	1
C166A-*r*IucD	1.79 (2)	1
C31A/C51A-*r*IucD	1.00 (1)	1
C51A/C158A-*r*IucD	0.89 (1)	1
C51A/C166A-*r*IucD	0.85 (1)	1

[a] After initiating the reaction between the protein and DPIP, the decrease in A_{600} was recorded until there was no further change and this was reached after 6-8 minutes. Since each oxidative addition of a thiol group to DPIP results in the diminution in the absorbance at 600 nm, the magnitude of the decrease is proportional to the number of cysteine residues involved in the conjugation with the dye. The number was calculated from the decrease in absorbance using an ε_M value of 1×10^{-4} $M^{-1}cm^{-1}$.

The values in parentheses represent probable numbers of cysteine residues involved in conjugation with DPIP.

Cys146 of *r*lucD with alanine resulted in rendering three of its cysteine residues amenable to interaction with the dye.

The second aspect of this study concerned the ability of DPIP-protein conjugates to accommodate the flavin cofactor (FAD) in their catalytic function. To this end, two identical assay mixtures were prepared, both containing the desired protein (*r*lucD or its mutein) and DPIP. The reaction between the dye and the protein was allowed to proceed for 1 minute, in the first mixture, and 15 minutes in the second mixture. The first sample served to approximate conditions at the initiation of the reaction, while the second sample represented the situation that prevails subsequent to the protein's conjugation with DPIP. The ability of each of these samples to promote NADPH-dependent reduction of the exogenous dye was recorded both in the absence as well as in the presence of FAD (see pp. 49-50 for details). These are designated A (absence of FAD) and B (presence of FAD) in Figure 16. The observations recorded in the presence of FAD (section B, Figure 16) reflect the ability of the DPIP-protein conjugate to accommodate FAD in the catalytic mechanism. The results obtained are shown in Figure 16 and would appear to fall into three categories: (i) proteins which are unable to interact with the flavin cofactor subsequent to their covalent conjugation with DPIP. In these cases, the enhancement in the role of electron transfer process due to the presence of FAD can be observed in the protein sample pre-treated with DPIP for 1 minute, but not after 15 minutes of such treatment. Thus, the protein appears to lose its ability to bind FAD subsequent to its covalent modification by DPIP (58). This type of phenomenon was observed in the case of *r*lucD, C31A-*r*lucD, C158A-*r*lucD and C166A-*r*lucD (Figure 16a); (ii) *r*lucD muteins capable of accommodating FAD despite their covalent conjugation with DPIP. With these proteins, the ability of FAD to promote the electron transfer process is not affected by their prior incubation with the dye. C51A-*r*lucD,

Figure 16: **Ability of *r*lucD-DPIP conjugates to promote FAD-dependent reduction of exogenous dye**

In a typical experiment, two samples of *r*lucD (3 μM) in potassium phosphate (200 mM, pH 7.0) were prepared. Reaction with DPIP (100 μM) was allowed to proceed for 1 minute (●-●) in one and for 15 minutes (O-O) in the other. With NADPH serving as the electron donor, the ability of each of these samples to promote reduction of the exogenous dye both in the absence (A) and the presence (B) of FAD was examined.

a) observations noted in the case of *r*lucD, C31A-, C158A-, and C166A-*r*lucD preparations
b) observations recorded with C51A-, C51A/C158A-, and C31A/C51A-*r*lucD
c) C146A-*r*lucD

Data shown are typical of results obtained in experiments performed in triplicate.

a)

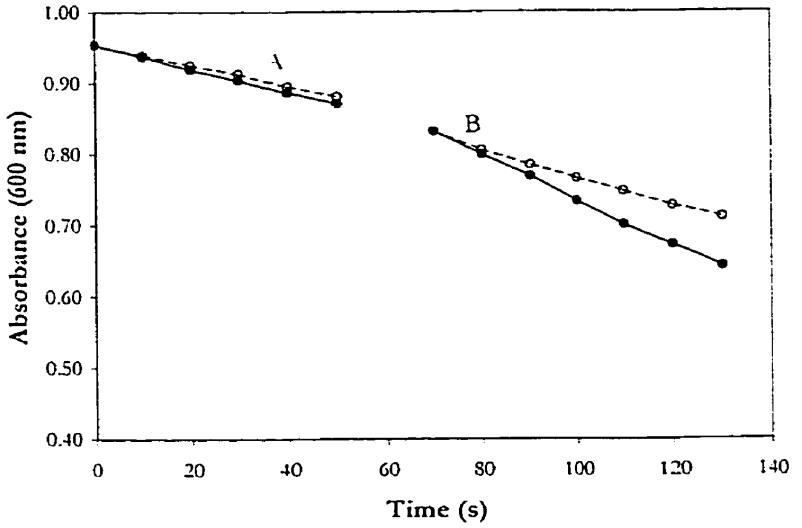
1.00
0.90
0.80
0.70
0.60
0.50
0.40
Absorbance (600 nm)
A
B
0
20
40
60
80
100
120
140
Time (s)

b)

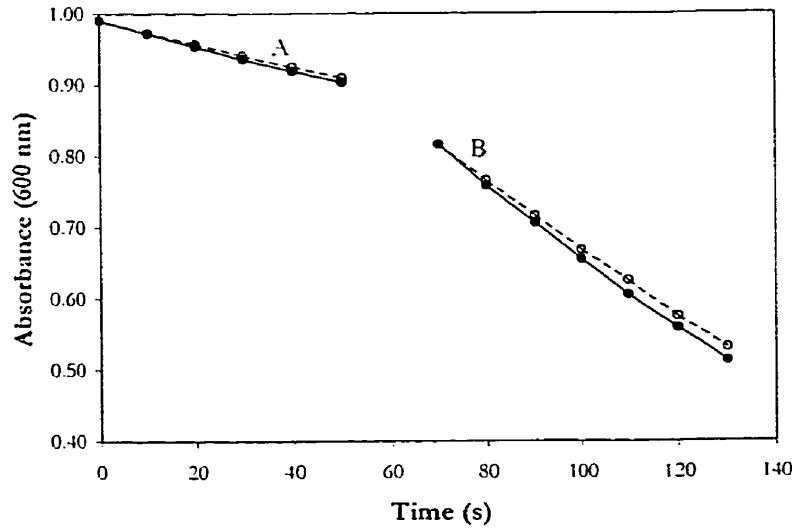
1.00
0.90
0.80
0.70
0.60
0.50
0.40
Absorbance (600 nm)
A
B
0
20
40
60
80
100
120
140
Time (s)

c)

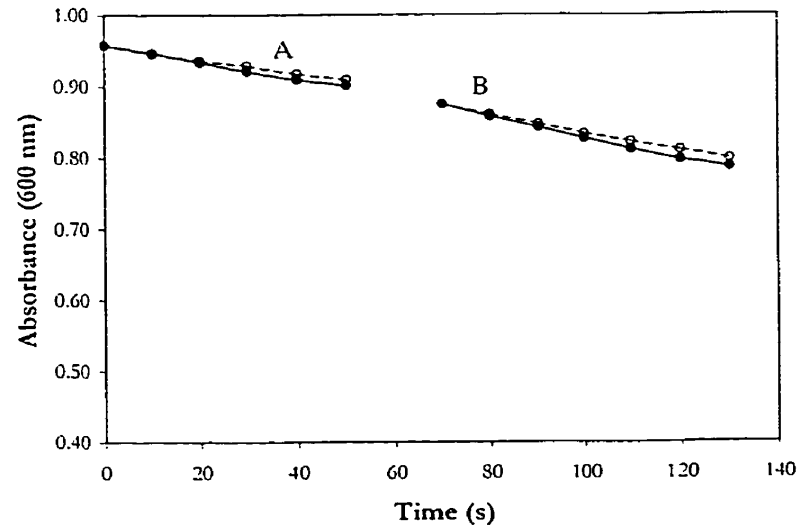
1.00
0.90
0.80
0.70
0.60
0.50
0.40
Absorbance (600 nm)
A
B
0
20
40
60
80
100
120
140
Time (s)

C31A/C51A-*r*lucD and C51A/C158A-*r*lucD exhibited this phenomenon (Figure 16b); and finally (iii) a case where FAD had no effect on the electron transfer process regardless of the period of the protein's prior exposure to the dye. This situation was observed in the case of C146A-*r*lucD. The reaction of this protein with DPIP would appear to be extremely rapid such as to instantaneously abolish its ability to interact with FAD (Figure 16c).

4.3.6 Kinetic parameters

The effect of Cys→Ala replacements in *r*lucD on the K_M values and the catalytic efficiency, k_{cat}, were examined using its substrate, L-lysine, and FAD, one of its cofactors.

The dissociation constant, K_D, for the *r*lucD•FAD complex has been shown to be approximately 16 μM (cited on p. 60). In the current investigations, attention was focused towards K_M rather than K_D based on the following considerations. K_D is a dissociation constant of the enzyme•FAD complex and in view of the absence of the other obligatory participants (NADPH, the other cofactor, and the substrate L-lysine) in the catalytic mechanism of the protein, its significance is difficult to fathom. In contrast, the K_M' value, which is a composite of dissociation constants of the complexes of the enzyme with various forms of the flavin cofactor (FAD, $FADH_2$, FADOOH, and FADOH) that occur in the catalytic cycle of the protein, would appear to be an appropriate parameter to consider.

The rate of L-lysine-dependent oxidation of NADPH was monitored over a range of concentration (0-50 μM) of FAD with the concentrations of NADPH (200 μM) and L-lysine (1 mM) maintained constant (see pp. 45-46 for details). Appropriate correction was made for the process of NADPH oxidation in the absence of L-lysine. The data provided the basis for the evaluation of the K_M values for FAD. The K_M values for FAD observed in the case of *r*lucD and its muteins are given in Table 10.

Table 10: **Kinetic parameters of *r*lucD and its muteins**

Protein	K_M (μM)		kcat [a] (sec^{-1})
	FAD	L-lysine	
*r*lucD	3.29 ± 0.10	390 ± 68	0.405 ± 0.01
C31A-*r*lucD	2.46 ± 0.05	466 ± 26	0.351 ± 0.06
C51A-*r*lucD	1.57 ± 0.02	nd	0.479 ± 0.01
C146A-*r*lucD	1.94 ± 0.29	423.5 ± 67	0.243 ± 0.05
C158A-*r*lucD	nd	nd	nd
C166A-*r*lucD	2.19 ± 0.10	420 ± 36	0.305 ± 0.01
C31A/C51A-*r*lucD	5.59 ± 0.05	389 ± 24	0.614 ± 0.02
C51A/C158A-*r*lucD	2.13 ± 0.21	nd	0.543 ± 0.01

A typical assay mixture, in a 1 mL volume, consisted of *r*lucD (2 μM) in potassium phosphate (200 mM, pH 7.0), with DTT (1 mM). The concentrations of NADPH (200 μM) and L-lysine (1 mM) were maintained constant while that of the flavin cofactor was varied over the range of 0-50 μM in experiments designed to determine K_M of the flavin cofactor.

For the determination of the K_M for L-lysine, the concentrations of NADPH (200 mM) and FAD (30 μM for all except C31A/C51A *r*lucD which was 60 μM) were held constant while the L-lysine concentration was varied over 0-10 mM.

[a] Since high concentrations of FAD (≥ 80 μM), NADPH (≥ 200 μM) and L-lysine (2 mM) inhibit L-lysine monooxygenase activity, k_{cat} values were estimated from data recorded in the experiments designed to determine the K_M value for FAD.

An examination of the data indicates that single Cys→Ala replacement in *r*lucD led to a slight lowering of K_M for FAD, with the maximum of such decrease noted in the case of C51A-*r*lucD (K_M value of ≈1.6 μM compared to a value of ≈3.3 μM for unmodified *r*lucD). A two-fold increase in the K_M was noted in the case of C31A/C51A-*r*lucD.

For the determination of K_M values for L-lysine, its concentration was varied over the range of 0-10 mM while maintaining concentration of NADPH (200 μM) constant and that of FAD at 10 x K_M for *r*lucD and its muteins (30-60 μM). The initial rate of NADPH oxidation at each concentration of L-lysine was recorded and corrected for the spontaneous process occurring in the absence of substrate. Plots of velocity versus substrate concentration of the data and analysis using the program GraFit provided the basis for the assessment of the K_M values. The results are presented in Table 10.

An examination of the data indicated that single Cys→Ala replacement in *r*lucD to have no significant effect on its K_M value for L-lysine. In the case of proteins with two Cys→Ala substitutions, modest increases (less than two-fold) in the K_M values was noted. Finally, the k_{cat} values were calculated from the data in the studies for the determination of K_M for FAD. The results are shown in Table 10.

As noted before, *r*lucD and its muteins catalyse NADPH oxidation in the absence of hydroxylatable substrate, resulting in the production of H_2O_2. The extent of such a process occurring under conditions of hydroxylation of L-lysine was assessed by quantitative estimation of H_2O_2 produced during the period. Thus, a typical assay in a volume of 5 mL contained: potassium phosphate (200 mM, pH 7.0), FAD (40 μM), L-lysine (1 mM), NADP+ (160 μM), G-6-P (800 μM) and G-6-P dehydrogenase (1.25 units). After incubation at 37°C for 15 minutes, an aliquot (1.5 mL) was used for H_2O_2 determination and

Table 11: **Production of N^6-hydroxylysine and H_2O_2 by *r*IucD and its muteins**

Protein	N^6-hydroxylysine (nmoles)	H_2O_2 (nmoles)	Total NADPH Consumed (nmoles)
*r*IucD	359	137	496
C31A-*r*IucD	462	143	603
C51A-*r*IucD	453	148	603
C146A-*r*IucD	173	144	317
C158A-*r*IucD	350	138	488
C166A-*r*IucD	399	142	541
C31A/C51A-*r*IucD	379	153	530
C51A/C158A-*r*IucD	499	160	559

Assay mixture, 5 mL volume, was incubated at 37°C for 15 min. An aliquot (1.5 mL) was used for H_2O_2 estimation (91) and the remainder for determination of N^6-hydroxylysine (89).

[a] the values shown represent the amount (converted to the nearest whole number) in the initial volume (5 mL) of the assay.

the remainder (3.5 mL) used for the determination of N^6-hydroxylysine. The results obtained are shown in Table 11. In the case of *r*IucD, H_2O_2 production during conditions of hydroxylation of the substrate constitutes approximately 22% of the NADPH consumed during the period. Whether this is a reflection of the degree of uncoupling between the processes of NADPH oxidation and lysine:N^6-hydroxylation will be addressed later. The effects of Cys→Ala replacement in *r*IucD were as follows. Single Cys→Ala substitution in *r*IucD was found to have no significant effect on the extent of H_2O_2 produced under hydroxylating conditions. A slight enhancement in the amount of H_2O_2 produced was noted when two cysteine residues were replaced with alanine. Except for Cys146→Ala substitution, single cysteine replacements in *r*IucD had no appreciable effect on its monooxygenase activity. The Cys146→Ala change in *r*IucD was accompanied by approximately 40% decrease in its N-hydroxylase activity. Replacement of Cys31 and Cys51 with alanine resulted in an approximately 30% increase in *r*IucD's monooxygenase activity and this is also observed in the case of C51A/C158A-*r*IucD.

4.4 Interaction of *r*IucD with its ligands

The conformational changes in *r*IucD accompanying its interaction with its ligands were assessed by examining the CD spectra, DSC profiles of the protein, and its susceptibility to degradation by proteases. Neither the CD spectra nor the DSC profile of *r*IucD was significantly affected in the presence of its cofactors or substrate (Figures 17 & 18). However, its susceptibility to the action of proteases was found to be influenced by the presence of some of its ligands, the details are given below.

Figure 17: **CD spectra of *r*lucD**

*r*lucD (5 μM) in potassium phosphate (200 mM, pH 7.0) was scanned at a rate of 200 nm/min. Concentrations of ligand when present were: FAD (200 μM) and L-lysine (1 mM).

——— *r*lucD
- - - - - *r*lucD + L-lysine
—·—·— *r*lucD + FAD

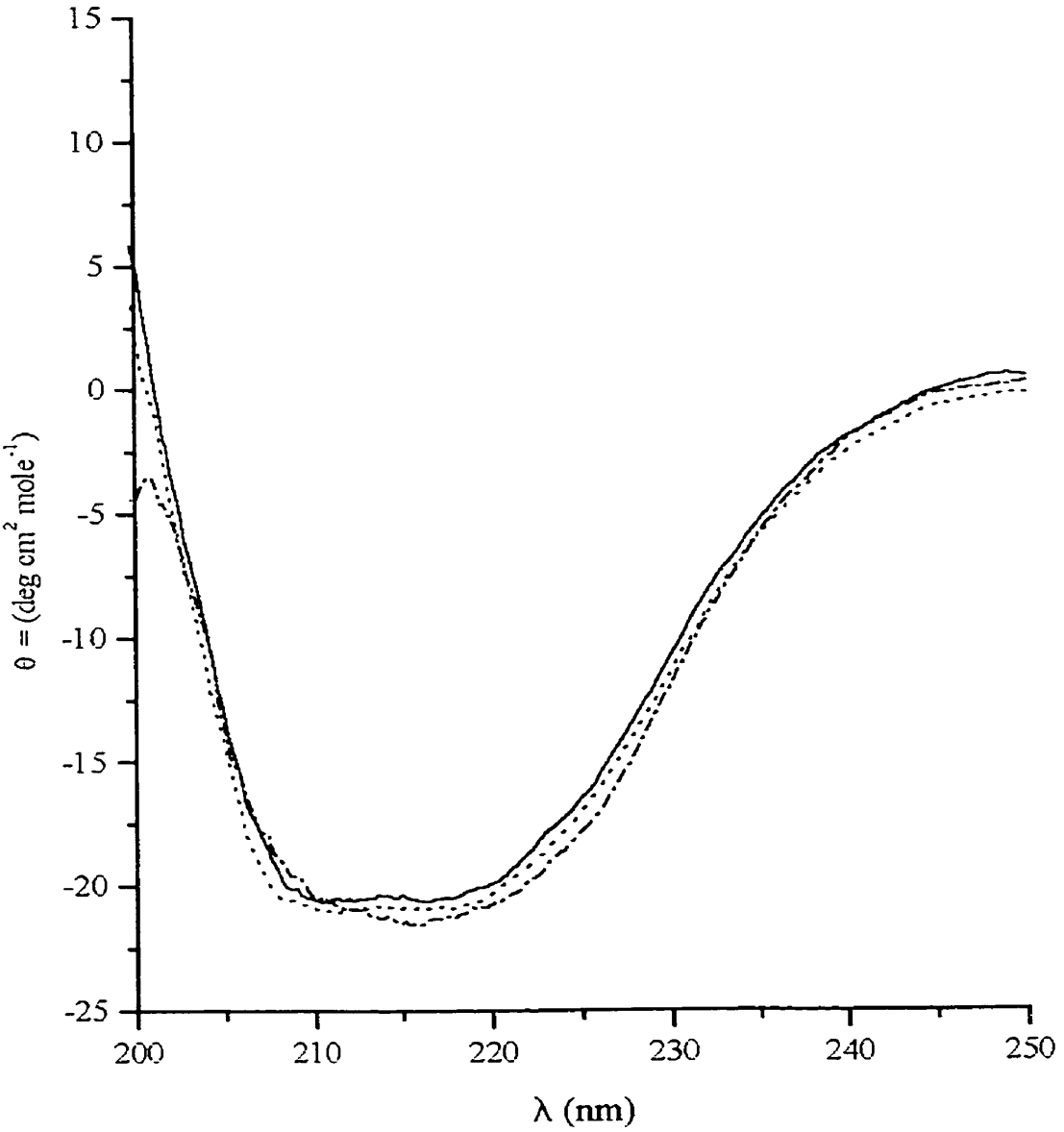
15
10
5
0
-5
-10
-15
-20
-25
200
210
220
230
240
250
θ = (deg cm² mole⁻¹)
λ (nm)

Figure 18: **DSC profile of *rl*ucD**

*rl*ucD (≈1 mg/mL) in potassium phosphate (200 mM, pH 7.0) containing DTT (1 mM) was heated at a rate of 1 K/min. Concentrations of ligands when present: FAD (0.5 mM); ADP (1 mM); and L-lysine (5 mM).

——— *rl*ucD
– – – – – *rl*ucD + ADP
..... *rl*ucD + FAD
–.–.–. *rl*ucD + L-lysine

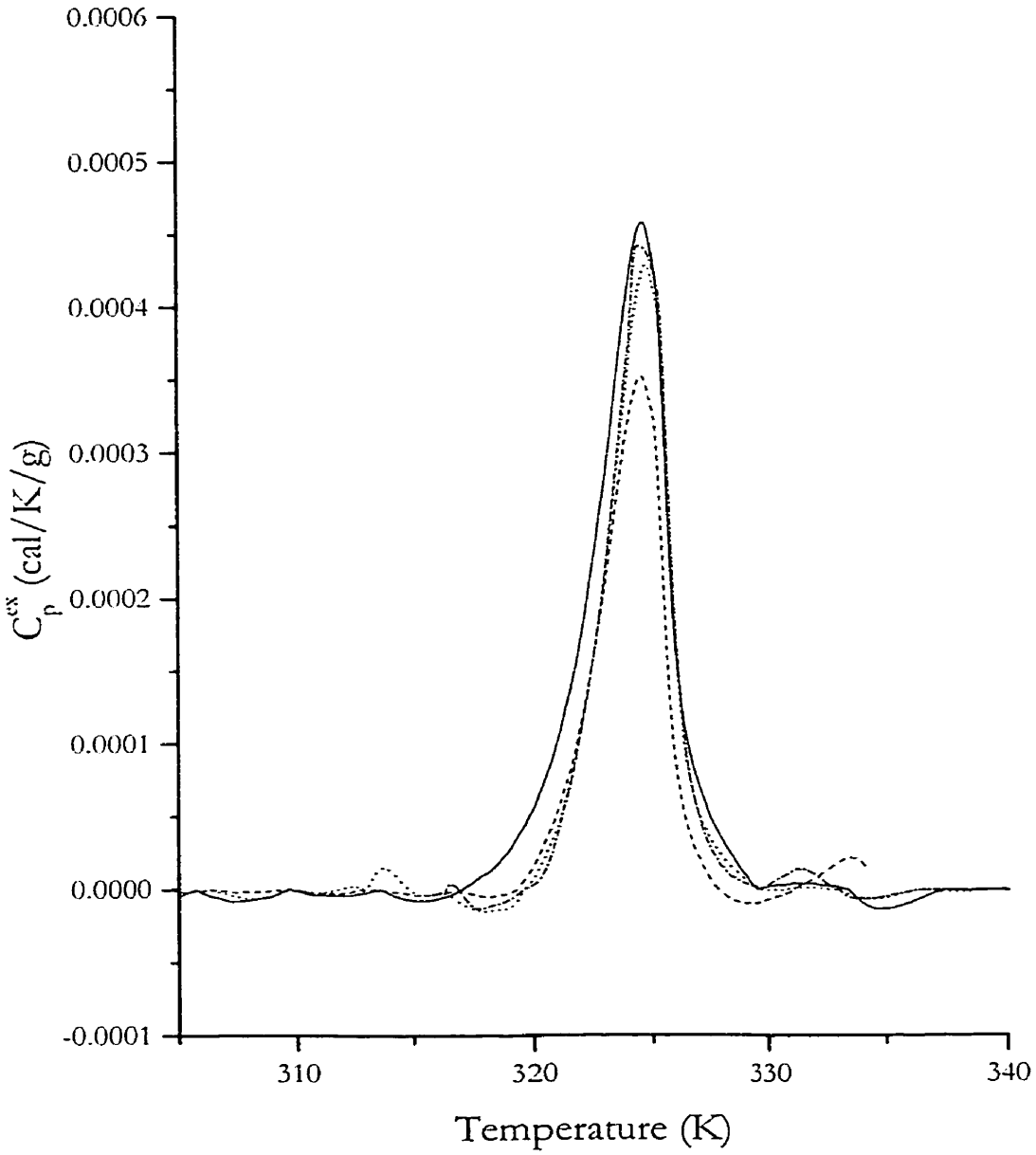
0.0006
0.0005
0.0004
0.0003
0.0002
0.0001
0.0000
-0.0001
C_p^{ex} (cal/K/g)
310
320
330
340
Temperature (K)

4.4.1 Susceptibility to endopeptidases

Treatment of *r*lucD with TPCK-trypsin (see pp. 39-41 for details) resulted in rapid degradation of the protein with concomitant loss of its monooxygenase activity. Similar studies performed in the presence of FAD (0.5 mM) revealed the absence of such adverse action by the protease as indicated by the total retention of *r*lucD's structural integrity and catalytic function. Further investigations performed over a range of FAD concentrations indicated that a cofactor concentration of 200 μM was adequate to protect *r*lucD from proteolytic degradation. Interestingly, ADP (1mM) was also found to shield *r*lucD from tryptic digestion as indicated by the preservation of the protein's structural integrity and catalytic function. Of the other two obligatory participants in the catalytic process mediated by *r*lucD, NADPH and L-lysine, the former was partially effective while the latter (5mM) was totally ineffective in protecting the protein from degradation by trypsin. Thus, in the presence of NADPH (1mM), approximately 50% *r*lucD was degraded by the protease as indicated by SDS-PAGE analysis and measurement of lysine:N^{6}-hydroxylase activity. These results are presented in Figure 19.

In view of the partial (≈50%) protection observed at 1 mM concentration of NADPH, an experiment was performed to determine the concentration of the cofactor capable of conferring *r*lucD total protection from degradation by trypsin. The cofactor concentration used in these studies ranged from 1 to 7 mM. Increases in the concentration of NADPH resulted in enhanced protection from degradation by the protease, with the maximum value (≈80%) of lysine:N^{6}-hydroxylase activity being retained at a cofactor concentration of 7 mM (data not shown). Thus NADPH, even at a concentration of 7 mM was incapable of providing *r*lucD total protection from degradation by proteases.

Figure 19: **(A) SDS-PAGE profile of *r*IucD samples treated with TPCK-trypsin**

*r*IucD (14 μM) was incubated (25°C, 12 min) with TPCK-trypsin (7 μM) in the presence of cofactors and substrate indicated. The reaction was stopped by the addition of SBTI (15 μM) prior to analysis. Lanes: 1. FAD (0.5 mM); 2. ADP (1.0 mM); 3. NADPH (1.0 mM); 4. L-lysine (5 mM);5. L-norleucine (5 mM); 6. none; 7. control, trypsin added after SBTI; 8. molecular weight standards expressed in kDa. (phosphorylase b, 94; serum albumin, 67; ovalbumin, 43; carbonic anhydrase, 30; trypsin inhibitor, 20; and α-lactalbumin, 14)

(B) Vertical bar graph representation of lysine:N^6-hydroxlyase activity following treatment with TPCK-trypsin

Lysine:N^6-hydroxlyase activity was determined after addition of SBTI as mentioned above in A. The vertical bars are matched to their corresponding lanes in A. Increase in NADPH concentration has been found to result in an enhanced protection from degradation by the protease, with maximum value (≈80%) being achieved at an NADPH concentration of 7 mM (data not shown). Studies with azocasein as substrate revealed that none of the cofactors even at the highest concentrations, function as inhibitors of the proteases.

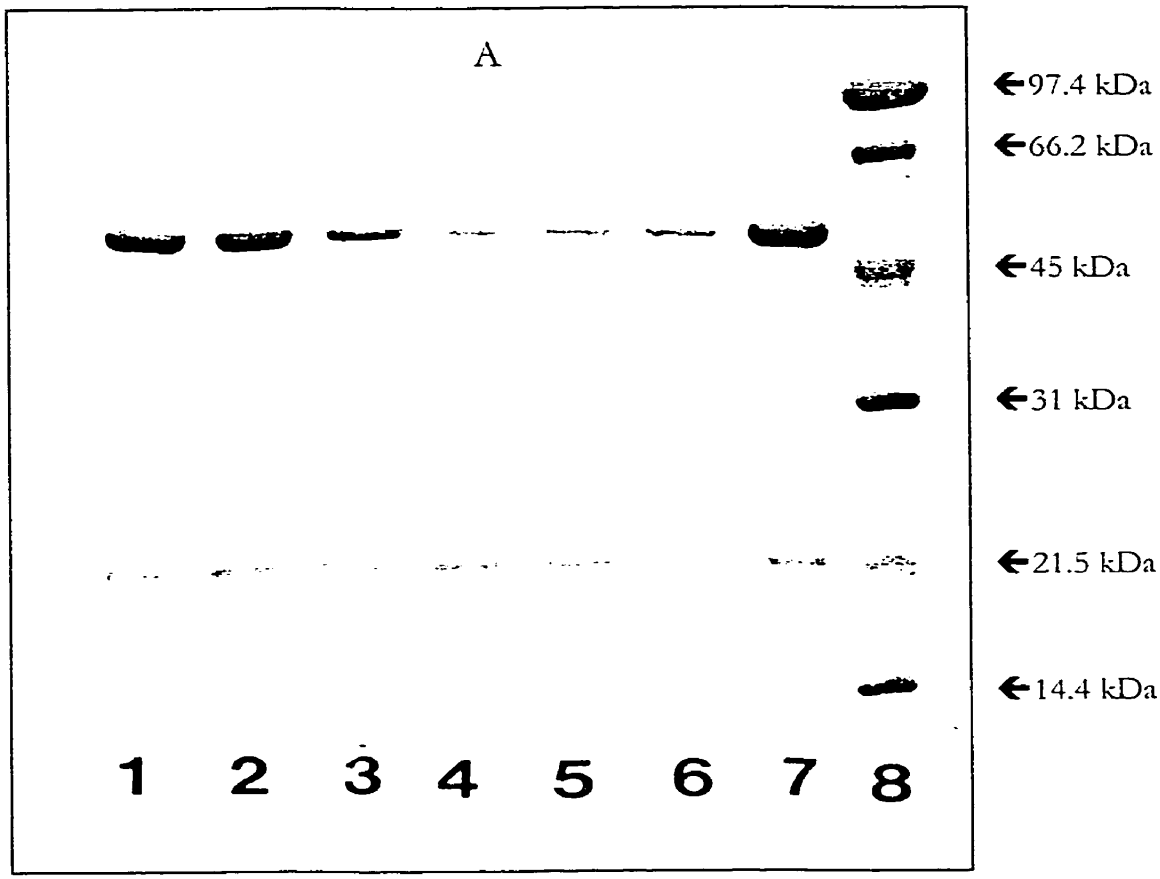
A
97.4 kDa
66.2 kDa
45 kDa
31 kDa
21.5 kDa
14.4 kDa
1
2
3
4
5
6
7
8

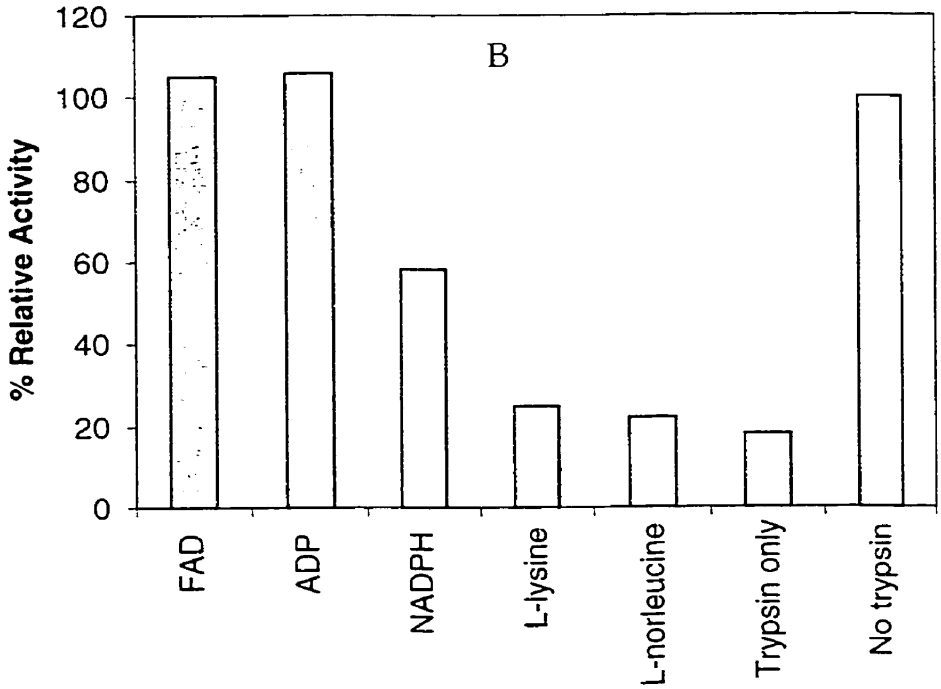
B
% Relative Activity
120
100
80
60
40
20
0
FAD
ADP
NADPH
L-lysine
L-norleucine
Trypsin only
No trypsin

In the experiments with TLCK-chymotrypsin and thermolysin, the observations were similar to those recorded in the studies with TPCK-trypsin. Both FAD and ADP prevented *r*IucD degradation by these proteases while NADPH and lysine were marginally effective and ineffective respectively. The protective effect exerted by FAD and ADP does not appear to be due to their ability to function as inhibitors of the proteases since these compounds, as well as NADPH (at the concentrations used in the study), have no adverse effect in experiments with azocasein serving as a substrate.

4.4.2 Reaction with exopeptidases

Treatment of *r*IucD with exopeptidases CPDA and CPDB, either singly or in combination, did not lead to loss in *r*IucD's monooxygenase activity. Based on the specificity of these enzymes, CPDB should be ineffective in releasing amino acid residues from the C-terminus of *r*IucD. In the case of CPDA, one could expect the release of three C-terminal residues (Figure 20). Treatment of *r*IucD with both exopeptidases can be expected to release only 8 C-terminal residues of the protein in view of their inability to cleave proline, and often the amino acid residue that is preceded by proline. Since there was no appreciable change either in size (by SDS-PAGE) or catalytic function of *r*IucD upon treatment with CPDA and CPDB, characterisation of the truncated form(s) of the protein was not pursued.

The reaction of *r*IucD with CPDY was accompanied by a steady decline in lysine:N^6-hydroxylase activity with approximately 85% activity being lost after 80 minutes of incubation (Figure 21). At this stage of the reaction with CPDY, analyses revealed the release of the following C-terminal amino acids residues from *r*IucD (amounts relative to that of threonine in parentheses): Thr (1.00), Ser (1.20), Gly (1.80), Arg (0.91), Glu (0.25), Ile (0.80), Leu (0.96), Ala (1.10), Pro (1.20), and other amino acid residues ($\leq$ 0.2). Allowing for the loss of tryptophan under strong acidic conditions and the low recovery of glutamic acid, due to

Figure 20: **Extent of cleavage of *r*lucD attainable by exopeptidases**

Amino acid sequence of the C-terminal segment comprising residues 407-425 of *r*lucD. Vertical arrows denote the extent of cleavage attainable by the exopeptidases CPDA and CPDB, either individually or in combination. A horizontal arrow represents the known extent of cleavage of *r*lucD using CPDY. Amino acid residues that have had their triplet codes replaced by a triplet encoding for termination are denoted in bold with asterisks above. These replacements resulted in the production of the following C-terminal truncated muteins: *r*lucD Δ8 (Leu418ter), *r*lucD Δ11 (Pro415ter), *r*lucD Δ14 (Leu412ter), and *r*lucD Δ17 (Leu409ter).

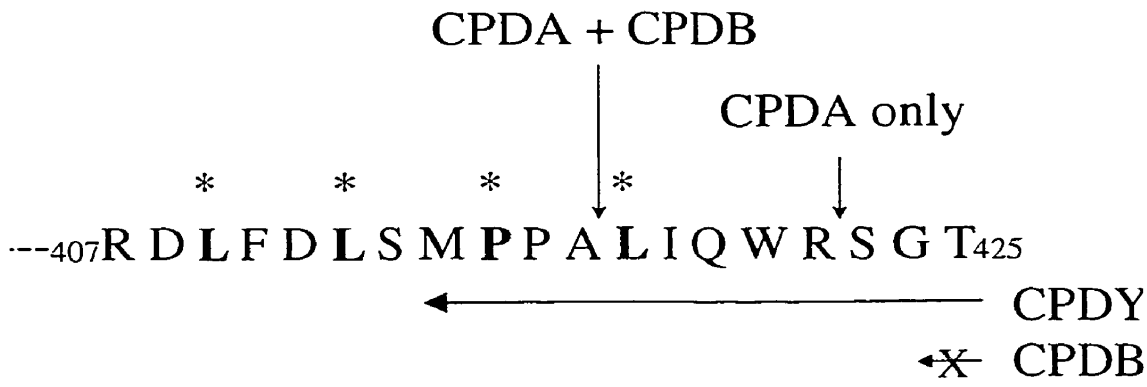
CPDA + CPDB
CPDA only
* * * * *
---407R D L F D L S M P P A L I Q W R S G T425
CPDY
X CPDB

Figure 21: **Effect of CPDY on lysine:N^6-hydroxylase activity of *rl*ucD**

*rl*ucD (10 µM) in 100 mM potassium phosphate, pH 6.0 was treated with CPDY (20 µg) at 37°C. The concentration of other compounds, when included, were: FAD (0.5 mM) and ADP (1.0 mM). Aliquots taken at desired intervals were diluted (1:1000) with 200 mM potassium phosphate buffer, pH 7.0 to stop further degradation and used for the determination of lysine:N^6-hydroxylase activity, O-O none; ●-●, control (no CPDY); ◆-◆ FAD or ADP. L-lysine (5 mM) failed to protect from the adverse action of CPDY (data not shown).

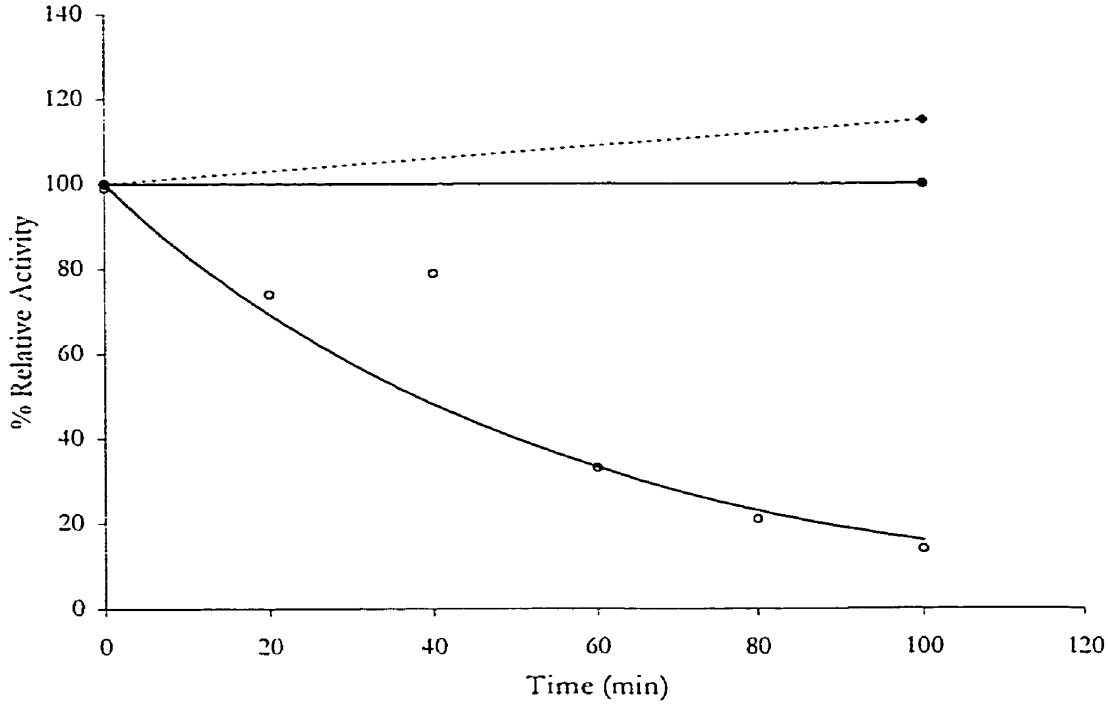
140
120
100
80
60
40
20
0
% Relative Activity
0
20
40
60
80
100
120
Time (min)

its poor retention by the cation exchange resin (in view of the relatively high ionic strength of the CPDY reaction medium), the above data would appear to be consistent with the deletion of 10-11 C-terminal amino acid residues from *r*lucD. Interestingly, both FAD (0.5 mM) and ADP (1mM) offered protection from such deleterious effects as indicated by total retention of *r*lucD's monooxygenase activity even after prolonged exposure to CPDY, while NADPH and lysine were devoid of such beneficial action (Table 12). Finally, FAD and ADP were found to have no adverse effect on the ability of CPDY to mediate the hydrolysis of its typical peptide substrate, furylacryloyl-Phe-Ala (85). Hence, their protective influence observed in the studies with *r*lucD would appear to be due to factors other than functioning as inhibitors of the exoprotease.

The deletion of the C-terminal residues of *r*lucD would appear to result in a disruption of its native conformation as indicated by the development of opalescence in the reaction mixture(s) after prolonged ($\geq$ 75 min) incubation with the exoprotease. Since these observations suggested a crucial role for the C-terminal segment in the maintenance of *r*lucD in its native conformation, the possibility of synthetic peptide mimic(s) compensating for the section deleted by CPDY was explored by performing experiments in the presence of the C-peptide (Pro-Ala-Leu-Ile-Gln-Trp-Arg-Ser-Gly-(D)-Thr, see methods for details). These studies showed that in the presence of the C-peptide (0.5 mM), *r*lucD's monooxygenase activity remained unaffected even after prolonged ($\geq$ 3 hrs) period of reaction with CPDY. Hence, the following three aspects were considered to explain the protective influence exerted by the C-peptide: (i) its ability to compensate for the section of the protein deleted by CPDY; (ii) the possibility of its competing with *r*lucD and serving as a substrate for CPDY; and (iii) its capacity to serve as an inhibitor of CPDY. The first of these three aspects would appear untenable, since addition of C-peptide to *r*lucD preparations

Table 12: **Susceptibility of *r*lucD to degradation by proteases: Influence of substrate, cofactors and analogs**

Effector	% Relative Activity		
	TPCK-Trypsin	TLCK-Chymotrypsin	Carboxypeptidase Y
FAD (0.5 mM)	105	107	139[a]
ADP (1.0 mM)	106	114	114[a]
NADPH (1.0 mM)	58	n.d.	7
L-lysine (5 mM)	25	4	11
none	18	4	8
control	100	100	100

In the case of TPCK-trypsin and TLCK-chymotrypsin, *r*lucD (12-14 μM) in potassium phosphate (100 mM, pH 7.0) was treated with the protease (6-7 μM) at 25°C. After 12 minutes, the reaction was stopped by the addition of SBTI or PMSF prior to determination of lysine:N^6-hydroxylase activity.

In the case of CPDY, *r*lucD (10 μM) in 100 mM potassium phosphate, pH 6.0 was treated with the exopeptidase (0.3 μM) for 2 hours at 37°C prior to determination of lysine:N^6-hydroxylase activity.

The concentration of effector, when included, are as shown in the table. Similar results were obtained with thermolysin.

[a] The apparent increase in the activity of *r*lucD in the presence of FAD and ADP is a reflection of their protective action against the slow inactivation that occurs due to thermal denaturation at 37°C.

pre-treated with the CPDY did not result in the restoration of lysine monooxygenase activity. Concerning the second aspect, HPLC analysis of the C-peptide preparation subsequent to its treatment with CPDY indicated the absence of any degradation, pointing to its inability to serve as a substrate for the exoprotease. This finding is not unexpected in view of the D-configuration of the C-peptide's carboxy terminal residue, a feature deliberately incorporated to minimise its serving as a substrate for CPDY. The ability of the C-peptide to act as an inhibitor of CPDY was confirmed in the studies using furylacryloyl-Phe-Ala. Data presented in Figure 22 show that the C-peptide is an effective inhibitor of CPDY, with approximately 90% inhibition in the hydrolysis of the chromophoric peptide substrate being noted when present in the assay at a concentration of 90 μM.

4.4.3 Studies with C-terminal truncated forms of *r*IucD:

In order to gain an unambiguous insight into structural feature(s) indispensable for the maintenance of *r*IucD in its native conformation, four well-defined *r*IucD variants, differing in the extent of C-terminal deletion, were developed (Table 3). The ability of truncated versions of *iuc*D to encode for a catalytically functional protein was assessed by examining the culture fluids for the presence N^6-hydroxylysine, an inherent feature of cells expressing the catalytically functional form of *r*IucD. Such analyses revealed the presence of N^6-hydroxylysine only in the culture fluid of cells designed to express *r*IucD Δ8 and not in the case of cells transformed to express the other three truncated *iuc*D gene products, namely; *r*IucD Δ17, *r*IucD Δ14, and *r*IucD Δ11. The absence of N^6-hydroxylysine in the case of the latter three cultures could be either due to their inability to express these particular truncated forms of *iuc*D or a reflection of a loss of catalytic function in the three truncated forms of *r*IucD. Analyses of the whole cell lysates of cultures expressing these truncated

Figure 22: **CPDY catalysed hydrolysis of furylacryloyl-Phe-Ala**

Conditions: FA-Phe-Ala (1 mM) in 100 mM potassium phosphate, pH 6.0 with CPDY (10 μg).

(1) in the absence of C-peptide
(2) in the presence of C-peptide (90 μM).

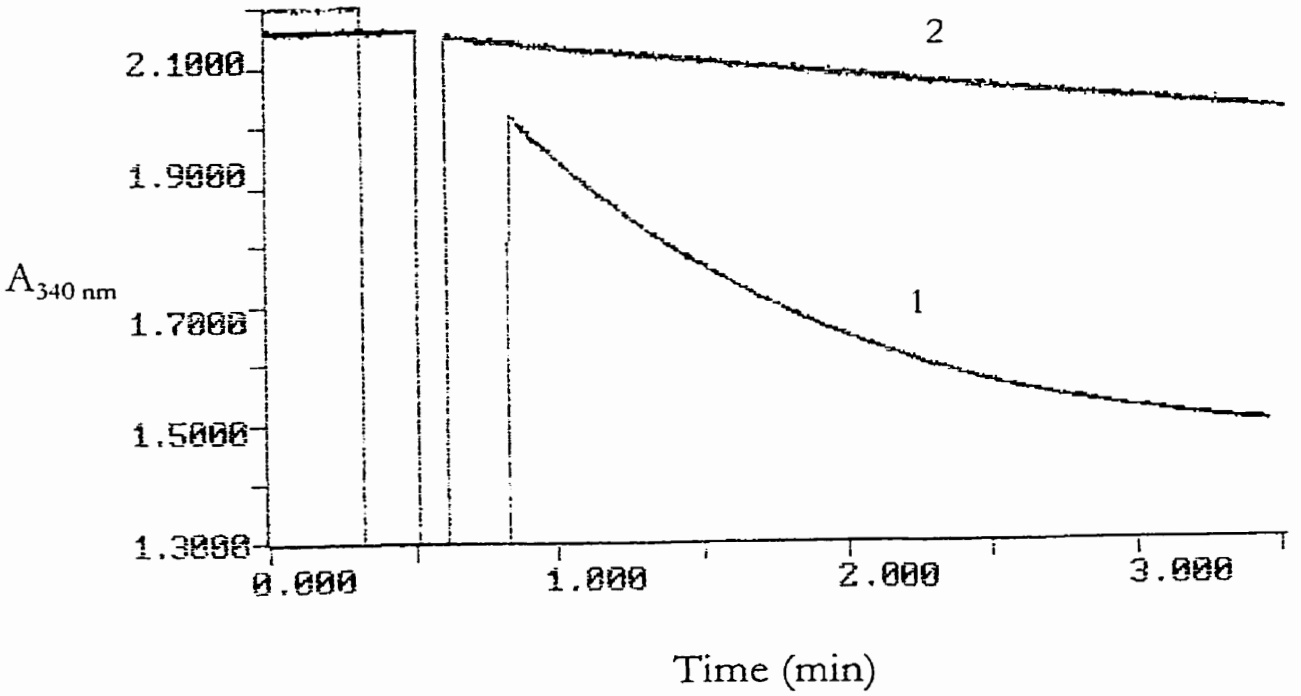
2
1
2.1000
1.9000
1.7000
1.5000
1.3000
$A_{340\ nm}$
0.000
1.000
2.000
3.000
Time (min)

proteins revealed the presence, in all four cases, of a protein with a molecular weight corresponding to that of the *iuc*D gene product, and its identity as such was further confirmed by Western blot analyses using polyclonal antibodies raised against *r*IucD (Figure 23). Thus, all four truncated forms of the *iuc*D gene product would appear to be expressed. However, while *r*IucD Δ8 is capable of lysine N-hydroxylation, the other three mutants (*r*IucD Δ17, *r*IucD Δ14, and *r*IucD Δ11) are devoid of such catalytic activity. Furthermore, during attempts to isolate these truncated *r*IucD preparations, it was noted that their presence could be detected only in the whole cell lysates and the crude cell-free systems, but not in the fractions obtained in subsequent stages of purification. This finding is in distinct contrast with those noted in the case of normal *r*IucD, which is detectable during all stages of purification (46,47,56). The lability of these truncated *r*IucD preparations during later stages of purification would appear to be related to the removal of flavin cofactor(s) normally associated with whole cells and the crude cell-free system. This observation is consistent with the protective action of FAD mentioned in the previous section.

Figure 23: **Western Blot analyses**

The expression of truncated forms of *r*IucD in *E. coli* DH5α and their stability during the protocol for their purification was monitored by Western blot analyses using polyclonal rabbit anti-*r*IucD antibodies (see methods for details). Results obtained with *r*IucD Δ17 are typical of those recorded with other truncated *r*IucD preparations. Similar studies with intact *r*IucD served as a control.

(A) Western blot identification of *r*IucD, from left to right: (1) whole cell lysate; (2) crude cellfree extract; (3) ammonium sulphate (40%) fraction; and (4) pure *r*IucD.

(B) Western blot identification of *r*IucD Δ17, from left to right: (1) whole cell lysate; (2) cell-free extract; and (3) ammonium sulphate (40%) precipitate.

A

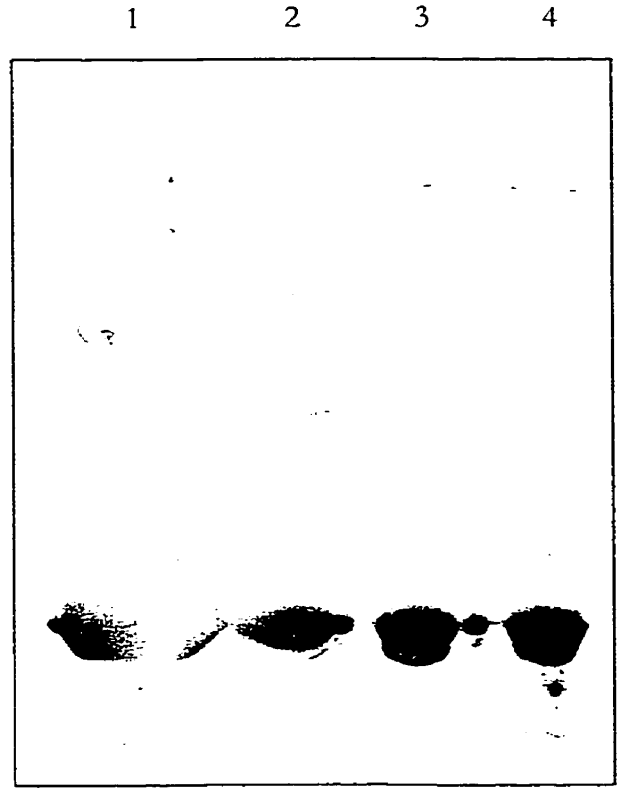

B

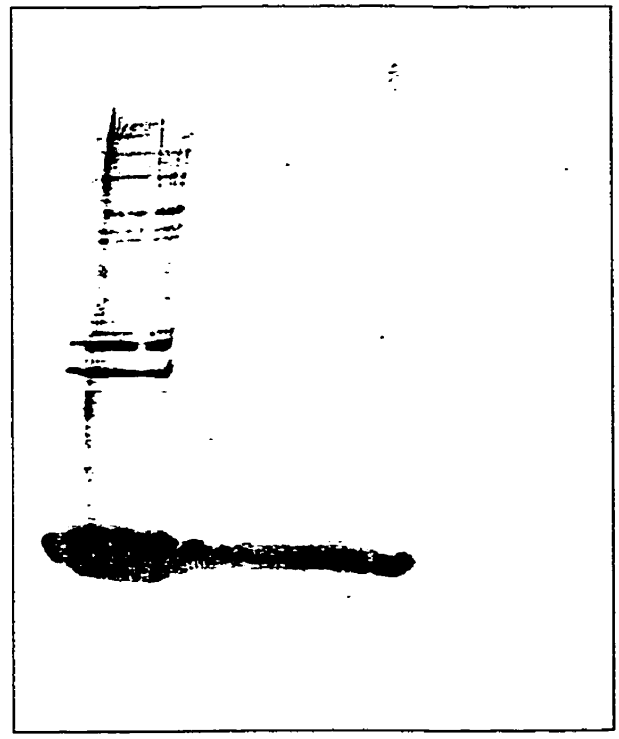

5.0 Discussion

The disparity between the experimentally determined value for the cysteine residues in *r*IucD and that predicted from the nucleotide sequence of *iuc*D, the gene encoding for the protein, had necessitated a redetermination of the latter feature. Such studies led to a revision of the nucleotide sequence of *iuc*D, which predicted the presence of five cysteine residues in its product, a finding in harmony with that observed in *r*IucD (59).

Two observations recorded in the previous investigations, the first pertaining to the progressive loss of monooxygenase function during storage (at ≤ 4°C) and its reversal by mercaptans (DTT), and the second concerning the facile susceptibility to inactivation by thiol group specific reagents (ICH_2COO^- and DTNB) had formed the basis for the notion that cysteine residue(s) play a vital role in *r*IucD's catalytic mechanism (46,47,58,59). The former phenomenon has been shown to be linked, in the current investigations, to the propensity of the protein to assume polytetrameric form(s), stabilised by intertetrameric disulphide bridges. However, the totally unexpected observation, that the alkylatable cysteine residues can be replaced (with alanine) without any adverse effects not only minimised the importance of these residues, but also stressed the need for further studies to determine the basis for the anomaly (59). As a consequence, the early phase of the current investigations concerned the characterisation of S-carboxymethyl-*r*IucD. These studies have revealed the modified *r*IucD to be similar to its unmodified counterpart both in its structural organisation as well as in its ability to promote electron transfer reactions not related to lysine:N^6-hydroxylation. Thus, the basis for the loss of monooxygenase function upon modification of the cysteine residues of *r*IucD still remains to be determined.

A major objective of this study pertains to the identification of the basis underlying the difference noted in the accessibility of *r*IucD's cysteine residues to modification by ICH_2COO^- and DTNB. For the sake of both clarity in presentation as well as convenience, it would appear appropriate to reiterate the observations that were available from prior investigations in our laboratory. These are: treatment of *r*IucD with ICH_2COO^- results in the alkylation of two of its cysteine residues, identified as Cys51 and Cys158, of the protein. This value of cysteine residues modified remains unaltered in spite of the variation (increase the iodoacetate concentration and/or extension of the reaction period from 20 to 60 minutes) in the conditions of treatment. In contrast, treatment of *r*IucD with DTNB results in the modification of three cysteine residues, with the reaction of two of them occurring "fast" (reaction time $\leq$ 20 seconds) and the remaining one "slow" (reaction time $\geq$ 150 seconds). Similar studies with C51A-, C158A-, and C51A/C158A-*r*IucD led to the identification of Cys51 as one of the "fast" and Cys158 as the "slow" residues to undergo modification by DTNB (59). The preceding review of prior literature draws attention to the aspects that need to be resolved. These are: (i) identification of the cysteine residues, other than Cys51, in *r*IucD that participates in the "fast" reaction with DTNB; and (ii) the origin of the additional thiol function detectable in the experiments with DTNB. Replacement of the other three cysteine residues (Cys31, Cys146, and Cys166) of *r*IucD with alanine was performed to address the above cited aspects.

The reaction of C31A-*r*IucD with DTNB yielded results identical with that recorded in the case of parent *r*IucD, thus eliminating Cys31 as a candidate for the yet to be identified residues capable of "fast" reaction with the above thiol modifying agent. Similar studies with C146A-*r*IucD revealed that all four of its cysteine residues were amenable to reaction with DTNB, with three of them reacting "fast" and one "slow" to be modified. This latter residue

is probably Cys158 which, has been shown to be sluggish towards modification. The reaction of C166A-*r*lucD with DTNB showed the presence of two "fast" reacting cysteine residues. Surprisingly no "slow" reacting thiol was found despite the presence of Cys158 in the protein. Hence, it would appear that the effect of Cys166Ala substitution in *r*lucD would be such as to enhance the reactivity of the vicinal Cys158 and render it capable of "fast" reaction with DTNB. This view appears to be consistent with the finding of just one cysteine residue in C51A/C166A-*r*lucD capable of "fast" reaction with DTNB (Table 7). These observations on the reactivities of the cysteine residues in *r*lucD and its muteins suggest that Cys166 is probably the hitherto unidentified residue that is capable of "fast" reaction with DTNB. Thus, of the three cysteine residues of *r*lucD that interact with DTNB, the modification of Cys51 and Cys166 would appear to occur rapidly while that of Cys158 to proceed slowly.

It is evident from the above presentation that cysteine residues in *r*lucD would appear to fall into two distinct categories. One of these groups comprises cysteine residues (Cys31, Cys51, and Cys158) which can be substituted with alanine without any appreciable effect on the reactivity of the remaining such residues in the protein. This feature would imply that such Cys→Ala replacement(s) do not lead to significant alterations in the native conformation of the protein. In contrast, the substitution of cysteine residues in the second category (Cys146 and Cys166) would appear to be accompanied by conformational changes in the protein as reflected in an enhancement of the accessibility of some of the remaining such function(s) to chemical modification. These studies demonstrate the ability of DTNB to serve as an effective and sensitive diagnostic agent for monitoring Cys→Ala induced conformational changes in *r*lucD.

As regards the second aspect, namely the additional cysteine residue noted during the reaction of *r*lucD with DTNB, it would appear that the phenomenon might be related to the mechanism involved in achieving the modification of the thiol function(s). ICH_2COO^- effects alkylation of cysteine residues. This process, being a covalent modification, can not be reversed by mercaptans like DTT. In contrast, the modification of cysteine(s) by DTNB involves disulphide exchange mechanisms resulting in the formation of a mixed disulphide with the concomitant release of 2-nitro-5-thiobenzoate anion. This type of modification is reversible by DTT and other thiol agents (Scheme 6).

The above noted difference in the mechanisms of action of the two thiol modifying agents forms the basis for the following proposal that could account for the third cysteine residue in *r*lucD apparently being capable of reaction only with DTNB. The proposal is based on the premise that two of *r*lucD's cysteine residues that react "fast" with DTNB are in proximity to each other (or induced to such juxtaposition subsequent to modification of one of them) in the three dimensional conformation of the protein. If such a situation were to prevail, the reaction of one of these cysteine residues (likely Cys51 by virtue of its susceptibility to alkylation by ICH_2COO^-) with DTNB will result in its conversion to the mixed disulphide with concomitant release of one equivalent of 2-nitro-5-thiobenzoate anion. In view of the proximity of the second cysteine, this initial event is immediately followed by disulphide exchange process with the formation of an intramolecular disulphide bridge and the concomitant release of another (or second) equivalent of 2-nitro-5-thiobenzoate anion. Finally, the modification of Cys158, slow compared to that of the other two, would result in the release of another (third) equivalent of 2-nitro-5-thiobenzoate anion (Scheme 7). Thus, according to the proposal, only two molecules of DTNB are consumed during the modification of cysteine residues of *r*lucD. However, the process is accompanied

Scheme 6: **Reaction of protein thiol functions with ICH_2COO^- (A) and DTNB (B)**

A)

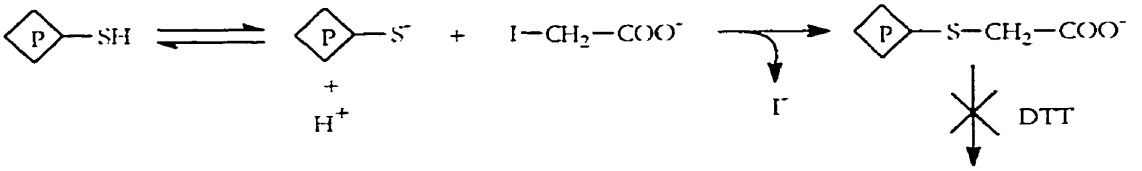
P—SH
P—S⁻
+
H⁺
I—CH₂—COO⁻
I⁻
P—S—CH₂—COO⁻
DTT

B)

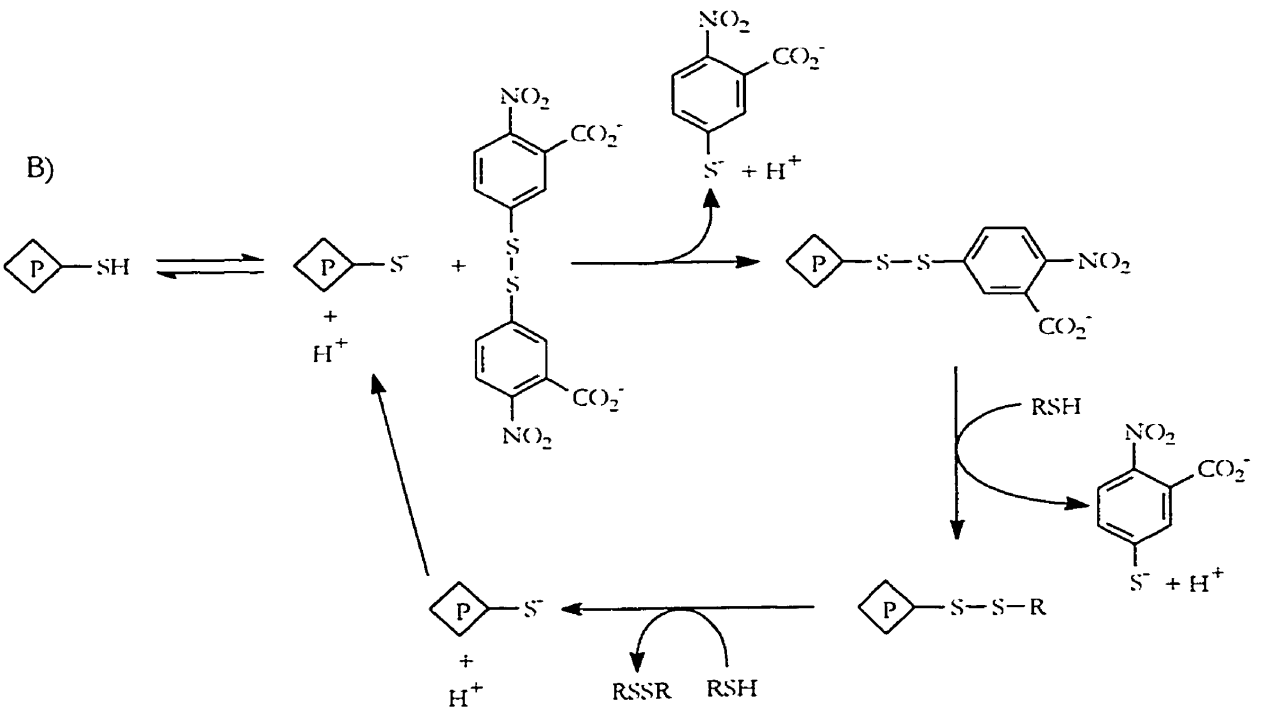
P—SH
P—S⁻
+
H⁺
NO₂
CO₂⁻
S⁻ + H⁺
P—S—S
NO₂
CO₂⁻
RSH
P—S—S—R
P—S⁻
RSSR
RSH

Scheme 7: **A hypothetical sequence of events in the reaction between *r*lucD and DTNB**

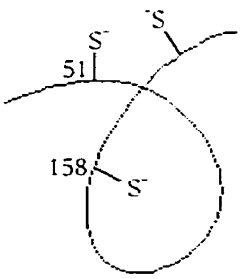

= *r*lucD with three of its DTNB accessible cysteine residues.

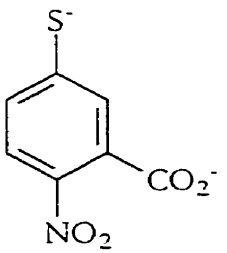

= NTB⁻

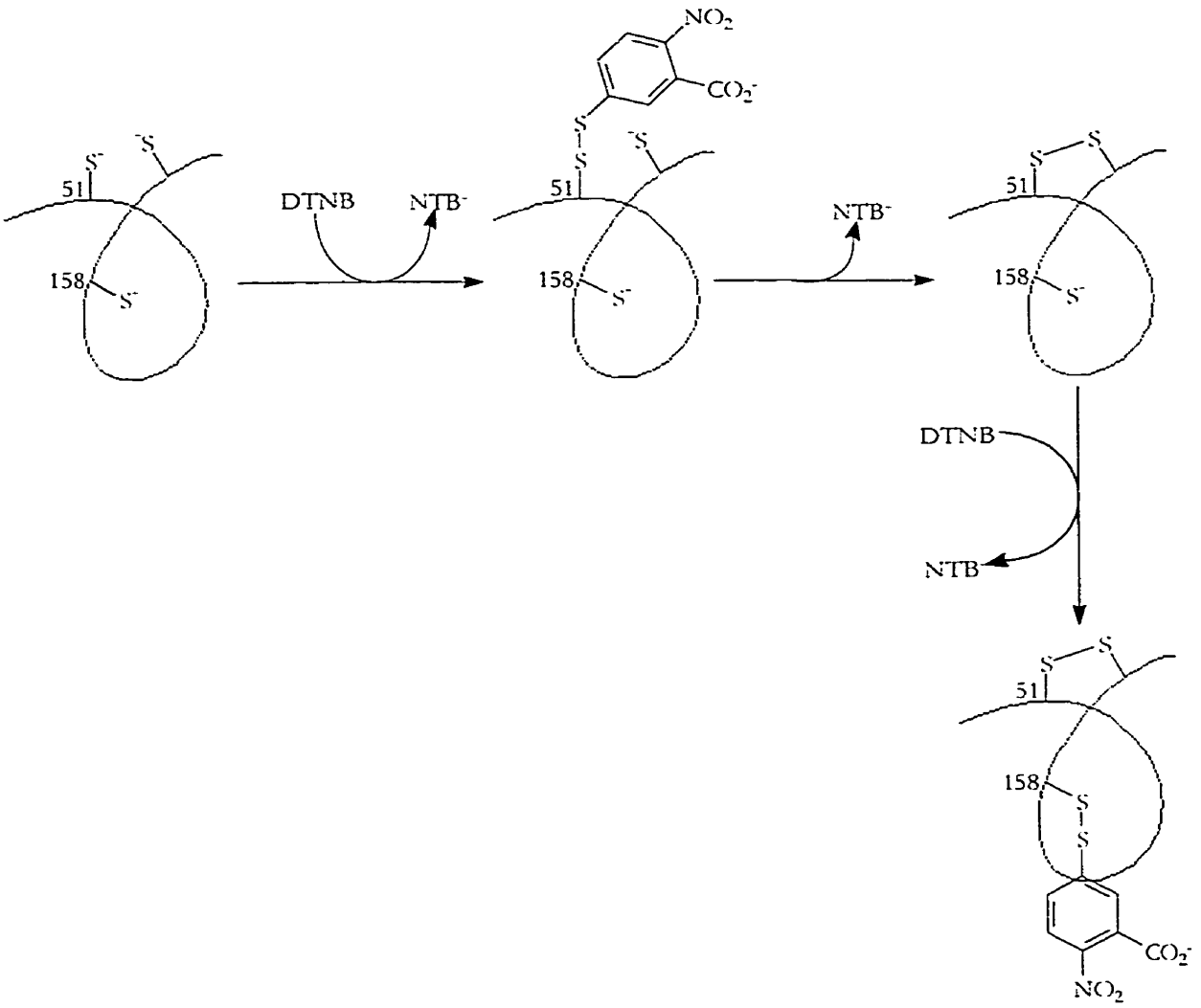
NO2
CO2-
S-
S
51
158
DTNB
NTB-
NTB-
DTNB
NTB

by the release of not two as expected, but three equivalents of 2-nitro-5-thiobenozate anions (as a consequence of intramolecular disulphide linkage) giving the impression that three cysteine residues of the protein have participated in a direct interaction with DTNB. At the present time, the elucidation of the three-dimensional structure of *r*lucD has yet to be realised. In the absence of such information, which can provide insights into the proximity and orientation of the residues in the native conformation of the protein, the proposals pertaining to Cys51 being in the vicinity of another of its kind has to remain in the realm of conjecture.

DPIP, by virtue of its ability to serve as a thiol modifying agent, also proved to be an effective probe for monitoring the mutation induced structural and functional changes in *r*lucD. On the basis of the number of cysteine residues participating in the oxidative addition process and the stoichiometry with respect to the number of mole(s) of covalently bound DPIP per mole of protein, *r*lucD and its muteins can be classified into two distinct categories. These are: (i) proteins that bind one mole of DPIP as a consequence of the participation of two of their cysteine residues in successive oxidative addition reactions with the dye. In this family, which includes *r*lucD, C31A-*r*lucD, C158A-*r*lucD, and C166A-*r*lucD, DPIP is rigidly bound, a feature that prevents the protein from interacting with its flavin cofactor; and (ii) *r*lucD muteins which incorporate one mole of DPIP by covalent attachment to one of their cysteine residues. This group which comprises C51A-*r*lucD, C31A/C51A-*r*lucD, and C51A/C158A-*r*lucD, can accommodate the flavin cofactor in their catalytic function in view of the flexibility in the position of DPIP bound by a single cysteine residue. Finally, C146A-*r*lucD represents a situation where both types of DPIP attachment are encountered. Thus, in this case, three cysteine residues are involved in conjugation with 2 moles of DPIP, one of them being held rigidly by linkage of two thiol functions and the

other attached to a single thiol function. The interaction of *r*lucD and its muteins with DPIP is illustrated in Scheme 8.

The Cys→Ala replacements in *r*lucD would appear to have no significant effect on the monooxygenase function of the protein with the exception of Cys146Ala substitution, which results in approximately 40-50% loss in such activity (Table 11). The reason for such loss of catalytic efficiency in the case of C146A-*r*lucD is not apparent, especially since the affinities for the flavin cofactor (FAD) and the hydroxylatable substrate (L-lysine) are not significantly affected by the amino acid replacement.

The events shown in Scheme 9 represent a superficial overview of the mechanism operative in *r*lucD catalysed reactions. According to this presentation, the reduced form of the flavin cofactor, $FADH_2$, formed in the initial step is rapidly converted to the 4a-peroxyflavin. This species can be channelled towards the production of either N^6-hydroxylysine when lysine is present or H_2O_2 in the absence of the hydroxylatable substrate.

An examination of the stoichiometry between the processes of NADPH oxidation and lysine:N^6-hydroxylation catalysed by *r*lucD and its variants indicated that a considerable (approximately 25%) of the former event is channelled towards production of H_2O_2 (Table 11). This feature, at first glance, could be regarded as a reflection of the degree of uncoupling between the two reactions catalysed by the protein. Such an interpretation would suggest that one out of every four NADPH oxidised by the enzyme may not be linked to the hydroxylation of the substrate. However, other considerations tend to indicate that the process of NADPH oxidation leading to H_2O_2 production may indeed be an inherent feature of *r*lucD, a process distinct from that coupled to N-hydroxylation of lysine. These are: (i) *r*lucD and its muteins catalyse the FAD-dependent process of NADPH oxidation in the absence of L-lysine, the hydroxylatable substrate; and (ii) S-carboxymethyl-*r*lucD, which

Scheme 8: **Reaction of *r*lucD and its muteins with DPIP**

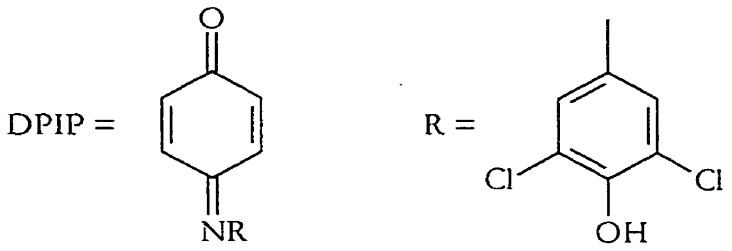

A) Proteins (*r*lucD, C31A-, C158A-, and C166A-*r*lucD muteins) that participate in two successive oxidative addition reactions with the dye.

B) Proteins (C51A-, C31A/C51A-, and C51A/C158A-*r*lucD) that participate in a single oxidative addition to the dye

C) C146A-*r*lucD involved in both type A) and type B) oxidative addition processes.

This assignment of *r*lucD and its muteins was based on: (a) the number of cysteine residues involved in conjugation (Table 9); and (b) the stoichiometry with respect to the number of moles of DPIP conjugated per mole of protein.

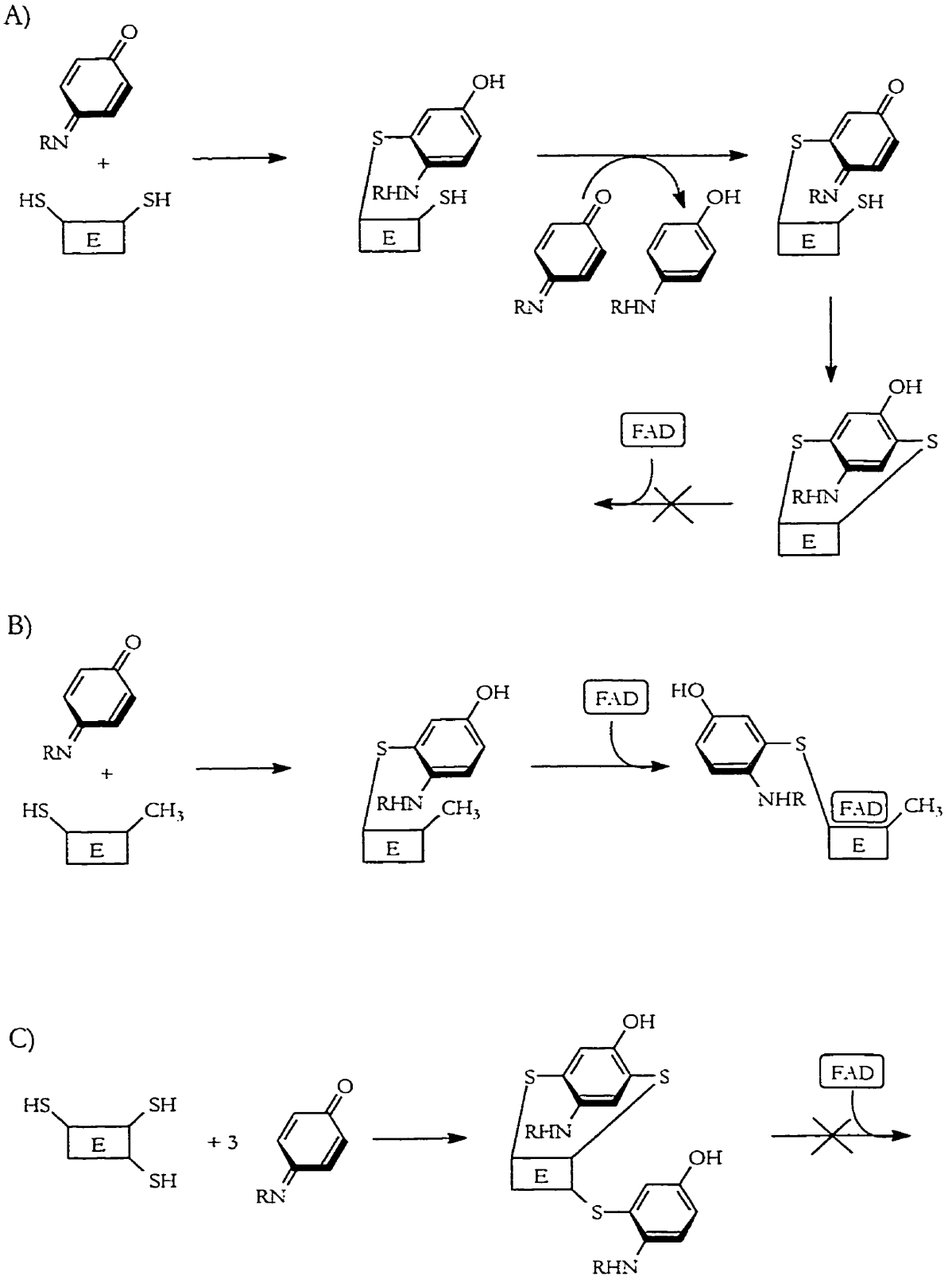
A)
RN
HS
SH
E
OH
RHN
FAD
B)
CH3
NHR
HO
C)
+ 3

Scheme 9: **A proposal for *Rhi*IucD catalysed N^6-hydroxylation of L-lysine and production of H_2O_2 in its absence**

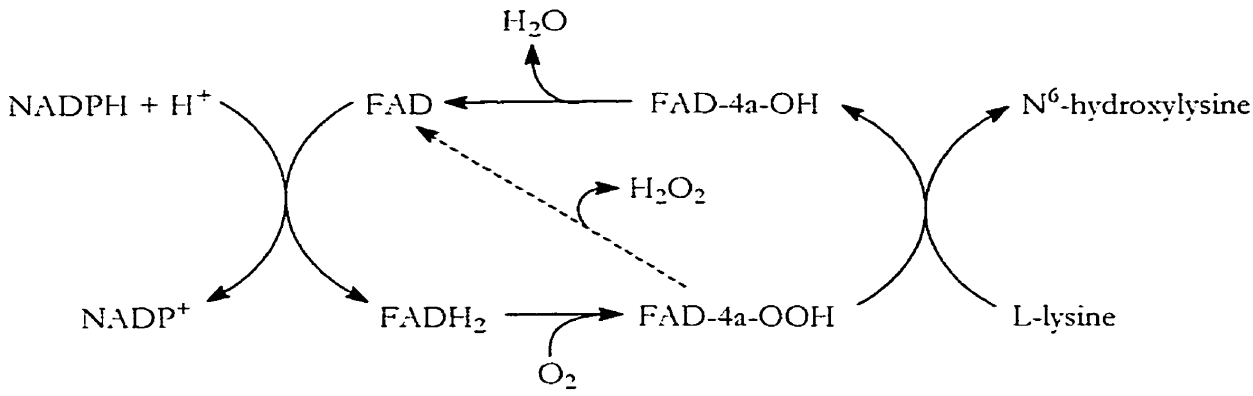
H2O
NADPH + H+
FAD
FAD-4a-OH
N6-hydroxylysine
H2O2
NADP+
FADH2
FAD-4a-OOH
L-lysine
O2

is devoid of monooxygenase function promotes FAD-dependent NADPH oxidation both in the absence as well as in the presence of electron acceptor (Figure 11) as effectively as the parent protein. Thus, it would appear that *r*lucD (or its mutein) is capable of mediating two distinct types of NADPH oxidation reactions, one "lysine-independent" and the other a "lysine-dependent" process. The former reaction results in the generation of H_2O_2 regardless of the presence or absence of the hydroxylatable substrate, while the latter, being tightly coupled to the N^6-hydroxylation process, occurs only in the presence of lysine. In both of the above reactions, NADPH oxidation leads to the formation of the reduced form of the flavin cofactor, $FADH_2$, which by interaction with O_2 generates the 4a-peroxyflavin, FAD-OOH, species. However, in the "lysine-independent" process, peroxyflavin species serves as a precursor for H_2O_2 while in the "lysine-dependent" reaction, it effects hydroxylation of the substrate. Thus, the peroxyflavin species needs to be shielded from the solvent medium in the latter process to prevent its serving as a source of H_2O_2.

In the case of other flavin-dependent monooxygenases such as *p*-hydroxybenzoate hydroxylase (54) and phenol hydroxylase (104), analyses of the three-dimensional structure(s) of the proteins have revealed the occurrence of substrate induced conformational changes that result in the shielding of the red-ox domain (isoalloxazine chromophore) of the flavin cofactor from the solvent medium. Such shielding has been noted to result in a tight coupling of the enzyme mediated processes of NADPH oxidation and hydroxylation of the substrate. In the case of *r*lucD, as noted before, the elucidation of its three-dimensional structure is yet to be achieved. However, neither the CD spectra nor the DSC profile of *r*lucD are appreciably affected in the presence of L-lysine. It is conceivable that subtle substrate induced conformational changes in *r*lucD may not be detectable by the techniques employed to monitor them in the current study.

Interestingly, both L-norleucine as well as L-methionine have been shown to inhibit *r*lucD mediated N-hydroxylation of L-lysine regardless of whether the process is monitored by the determination of N^6-hydroxylysine or by an assessment of NADPH oxidation during the process. These substrate analogs have also been found to exert appreciable (≈40-50%) inhibition of the process of NADPH oxidation occurring in the absence of L-lysine (Table 5). This observation, coupled with that of *r*lucD's ability to bind FAD relatively more tightly in the presence of L-norleucine than in its absence (see p. 60) would suggest that part of the bound flavin cofactor may become shielded from the external medium during the protein's monooxygenase function. In view of the tetrameric organisation of *r*lucD, the possibility of NADPH→FAD electron transfer process occurring either intra- or inter-subunit may have to be considered to explain the observed phenomenon. However, such deliberations have to be deferred until the realisation of the protein's three-dimensional structure and the determination of the size of its catalytically competent unit by radiation inactivation studies of the protein (105,106).

The last phase of these investigations concerns an assessment of ligand induced conformational changes in *r*lucD. The observations recorded in this study have revealed that neither the substrate (L-lysine) nor the cofactor (FAD) elicits significant conformational changes in *r*lucD as is evident from the CD and DSC profiles (Figures 17 and 18). However, when susceptibility to degradation by proteases is employed as a criterion for monitoring the structural changes in *r*lucD, significant differences in the response due to interaction with its various ligands become apparent. Thus, *r*lucD, in the absence of its cofactors or substrate, is susceptible to degradation both by endopeptidases as well as an exopeptidase (CPDY) with concomitant loss of its monooxygenase function. Such adverse action of proteases on *r*lucD is completely prevented when experiments are performed in the presence of low

concentrations of FAD (0.2 mM) or ADP (0.5 mM). Concerning the other two ligands, NADPH (1 mM) has been found to confer partial protection, while the substrate, L-lysine (5 mM), is virtually ineffective in preventing the proteolytic degradation of *r*lucD. The reasons for the inability of L-lysine, the preferred substrate, to protect *r*lucD from the deleterious action of proteases are not clear. In the case of the flavin cofactor, the magnitude of the dissociation constant K_D of the *r*lucD•ligand complex would appear to govern their effectiveness in rendering the protein resistant to the action of proteases. Thus, since *r*lucD's interaction with FAD is characterised by a K_D value of approximately 20 μM (103), cofactor concentrations (200 μM) that ensure the maintenance of the protein in the ligand bound, or the holoenzyme, state are effective in protecting it from proteolytic degradation. The ability of ADP to bind at the flavin cofactor site (103) appears to be responsible for its protective effect.

Under conditions identical with those employed in the studies with FAD, NADPH (1 mM) has been found to be partially effective in preventing the proteolysis of *r*lucD as indicated by the retention of ~50% of the protein's monooxygenase activity (Figure 19). Further increases in the concentration of NADPH result in an enhancement in the degree of protection afforded, with a maximum value ≈80% retention of monooxygenase activity, being observed at cofactor concentrations ≥ 7 mM (data not shown). The reasons for not achieving complete protection are not obvious. The finding may be a reflection of a high K_D value of the *r*lucD•NADPH complex. Although an apparent K_M value of approximately 100 μM for the reduced pyridine nucleotide cofactor has been recorded in experiments with lysine:N^6-hydroxylase activity serving as the criterion for the assessment (46,47), efforts to determine the actual K_D value of the *r*lucD•NADPH complex have been futile. It is not

clear whether this situation is a reflection of the protein's binding of NADPH being contingent upon its initial interaction with FAD. However, the ability of *r*lucD to mediate FAD-dependent NADPH oxidation even in the absence of its substrate (L-lysine) precludes the determination of the dissociation constant for the cofactor under such conditions. The situation appears to be similar to that recorded in the case of *p*-hydroxybenzoate hydroxylase, which utilises FAD and NADPH as cofactors. In the case of this latter enzyme, X-ray crystallographic studies have not been successful in identifying the NADPH-binding domain, in view of the cofactor's propensity to displace FAD from its binding domain in the protein (107). These observations pertaining to the protection of *r*lucD by ligands are analogous to those recorded in the case of glucose oxidase (108), creatine kinase (109), and NADPH quinone reductase (110).

Both the studies with CPDY as well as those with well-defined C-terminal deletion variants of *r*lucD have provided unambiguous evidence for the indispensability of the C-terminal segment for *r*lucD to function as a monooxygenase. The latter approach has also resulted in pinpointing the segment essential for the protein to be catalytically functional. Thus, while *r*lucD Δ11 is incapable of N^6-hydroxylysine production, the *r*lucD Δ8 variant is competent to perform such a function. This observation suggests that the structural feature(s) inherent in this segment, residues 415-417, may be crucial for the maintenance of *r*lucD in its catalytically active conformation.

Reports concerning the importance of the C-terminal domain for the structural integrity and/or catalytic function of proteins have been widely documented (111-119). The observations recorded in the case of lipoamide dehydrogenase from *Azotobacter vinelandii* would appear to be especially relevant since this protein, like *r*lucD, is both oligomeric and utilises FAD for its catalytic function (120). The function of the C-terminus of this protein

has been investigated by deletion of 5, 9, and 14 C-terminal residues respectively. Deletion of 5 residues has no adverse effects, that of 9 residues led to decreased conformational stability, and the removal of 14 residues was accompanied by complete loss of catalytic function (121). Furthermore, these studies also demonstrated the presence of intersubunit interaction involving a tyrosine residue at the N-terminus of one subunit and a histidine at the C-terminus of the second subunit. This structural feature, which is proposed to be involved in mediating the red-ox properties of the flavin cofactor via the conformation of the C-terminal segment, is not present in preparations of enzyme with deletion of either 9 or 14 C-terminal residues (121). As noted before, further studies are needed, especially the elucidation of the three-dimensional structure of the protein, to determine whether a similar situation as above prevails in *r*IucD.

Finally, the basis for the ability of FAD (and ADP) to protect *r*IucD from proteolytic degradation needs to be addressed. This feature is truly remarkable in view of the multitude of targets (47 scissile sites for trypsin and a similar number for the other two proteases used in this study) potentially available for cleavage by the endopeptidases. An examination of the following aspects may provide an insight into the factor(s) contributing to this process: (i) specificity of the phenomenon; (ii) susceptibility of proteins in their native conformation to proteolysis; and (iii) structural features that are indispensable for the maintenance of proteins in their stable, native conformation.

Concerning the first of these aspects, the protective effect of FAD (and ADP) does not extend to every protein but is restricted to *r*IucD (as demonstrated in this study) and to others which require this flavin cofactor for their function (108,110). The phenomenon appears to be stringently specific to proteins containing ADP binding domain(s), since other nucleotide diphosphates (GDP, CDP, etc.) have been found to be devoid of such protective

influence. Furthermore, total protection from proteolytic degradation has been found to require the presence of the flavin cofactor at concentrations ≥ 10 x K_D of the *r*IucD•FAD complex. This finding implies that the maintenance of *r*IucD in the holoenzyme (FAD bound) state is a prerequisite for the protein's acquisition of resistance to proteolysis. This view draws further support by the finding that glucose oxidase in its holoenzyme form (with just one mole of FAD bound per mole of protein) is totally refractory to the action of proteases, while its apoform, under identical experimental conditions, requires a relatively large molar excess (≥ 100 fold) of the flavin cofactor to preserve its structural integrity (108).

Concerning the second aspect, proteins in their native conformations have long been known to be less susceptible to proteolytic degradation than their denatured counterparts (122). Studies with synthetic peptides and ester substrates have led to the identification of minimal structural features that meet the specificity requirements in the case of both endo- as well as exopeptidases (123). However, in the case of polypeptide substrates the complementary interactions between the amino acid residues on either side of the scissile peptide bond and those present in the corresponding locations in the enzyme's active site have been shown to play an important role in the action of proteases (124). These complementary interactions between the polypeptide substrate and the active site of a protease are shown in Figure 24. Needless to note that such complementary interactions, as mentioned above, depends on the flexibility of the polypeptide strand. However, the secondary and tertiary structural features inherent in the native conformation of a protein impose constraints of the flexibility of the polypeptide chain preventing its effective interaction with proteases. The above mentioned considerations may provide the basis for the observed low susceptibility of native proteins to proteolytic degradation. However, it should be noted that they are not totally immune to the action of proteases. Since the native

Figure 24: **Schecter and Berger nomenclature for protease subsites** (124)

The protease is represented as the shaded area. P1 ... P1´ are the side chains of six amino acids, and S1 ... S1´ are the corresponding subsites on the enzyme.

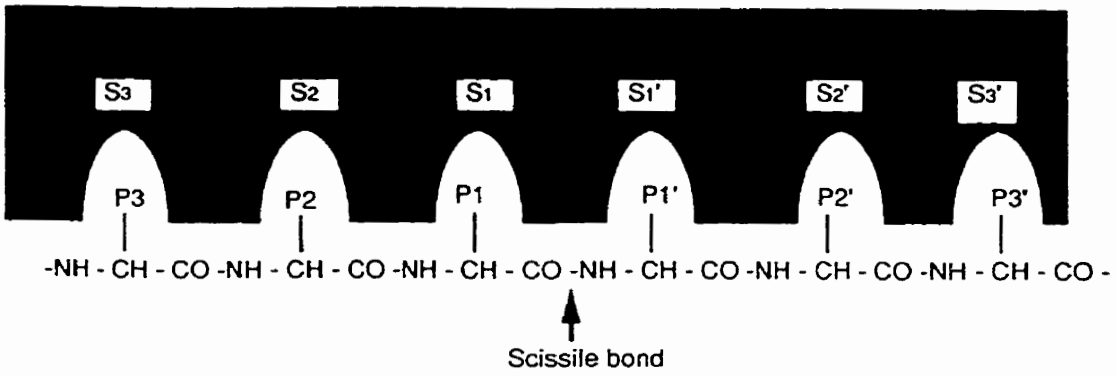
S3
S2
S1
S1'
S2'
S3'
P3
P2
P1
P1'
P2'
P3'
-NH - CH - CO -NH - CH - CO -NH - CH - CO -NH - CH - CO -NH - CH - CO -NH - CH - CO -
Scissile bond

conformation of a protein is not synonymous with the entire population of its molecules being in the most stable conformational state. In contrast, a protein in its "native" state needs to be visualised as a heterogeneous population of molecules with the predominant majority in the most stable conformation in equilibrium with a small number of others in less stable conformations. The transient relief from the earlier noted structural constraints in these latter less stable conformers serves as the basis for the observed low level of susceptibility of "native" proteins to the action of proteases. In the case of *r*lucD, the presence of FAD would appear to suppress even this tendency towards proteolytic degradation. Whether this is a consequence of the flavin cofactor stabilising a unique structural feature that is pivotal to the maintenance of the protein in its most stable, native conformation remains to be determined. As noted earlier, the peptide segment in *r*lucD comprising amino acid residues 415-417 appears to be crucial for the maintenance of *r*lucD in its native conformation. Elucidation of such aspects as whether this peptide segment derives its unique feature by virtue of the presence of a *cis*-peptide bond, a feature commonly encountered with peptide bonds of proline (125), and whether it serves as a recognition point for the flavin cofactor depend on the determination of the three-dimensional structure of the protein.

In summary, of the five cysteine residues present in *r*lucD, individual replacement of three of them (Cys31, Cys 51 and Cys158) with alanine has no significant effect either on the susceptibility of the remaining residues to reaction with DTNB or on the catalytic function of the protein. Such substitution of Cys146 and Cys166 results in the enhancement of the reactivity of other cysteine residue(s) to modification by DTNB and, in the former instance significant diminution in the protein's monooxygenase function. Concerning the interaction of *r*lucD with its ligands, only FAD (and its analog ADP) would appear to induce

conformational changes capable of rendering the protein totally resistant to proteolytic degradation.

The need for further investigations to establish the chemical basis of *r*lucD's catalytic function has been made apparent. The following lines of pursuit would appear to be most appropriate for achieving the above objective: (i) elucidation of the three-dimensional structure of *r*lucD; (ii) determination of the size of the catalytically functional unit of the protein by radiation inactivation experiments; and (iii) further physico-chemical characterisation of Cys146-*r*lucD to identify the structural basis for its monooxygenase function.

6.0 Appendix

Bio-Rad SDS-PAGE molecular weight standards

Kaleidoscope prestained

Myosin	Blue	207 kDa
β-galactosidase	Magenta	123 kDa
Bovine serum albumin	Green	86 kDa
Carbonic anhydrase	Violet	44.6 kDa
Soybean trypsin inhibitor	Orange	31.4 kDa
Lysozyme	Red	18.7 kDa
Aprotinin	Blue	7.2 kDa

SDS-PAGE markers, low range

Phosphorylase b	97.4 kDa
Serum albumin	66.2 kDa
Ovalbumin	45 kDa
Carbonic anhydrase	31 kDa
Trypsin inhibitor	21.5 kDa
Lysozyme	14.4 kDa

Pharmacia SDS-PAGE molecular weight standards

Low molecular weight electrophoresis calibration kit

Phosphorylase b	97 kDa
Albumin	66 kDa
Ovalbumin	45 kDa
Carbonic anhydrase	30 kDa
Trypsin inhibitor	20.1 kDa
α-lactalbumin	14.4 kDa

Composition of growth media and transformation buffer

Nutrient agar

One liter of LB nutrient agar contained the following:

Bacto agar	15 g
Bacto tryptone	10 g
Yeast extract	5 g
NaCl	10 g

The solution was adjusted to pH 7.2 with NaOH and the preparation was autoclaved for 20 minutes at 121°C. When the solution had cooled to 50°C ampicillin, if necessary, was added to a final concentration of 100 µg/ml and aseptically distributed to sterile petri plates and cooled to room temperature.

LB medium

The composition of the LB medium was similar to that described above except for the omission of Bacto agar. Alternatively, EZMix™ LB broth (Sigma) was used.

2X YT medium

One liter of 2X YT medium contained the following:

Bacto tryptone	16 g
Yeast extract	10 g
NaCl	5 g

The solution was adjusted to pH 7.0 with NaOH and the preparation was autoclaved for 20 minutes at 121°C. LB and 2X YT medium were used interchangeably for both liquid media and nutrient agar.

Modified version of Monod minimal medium

One liter of the modified minimal medium contained the following:

Ampicillin	100 mg
Ammonium sulfate	2 g
Calcium chloride, dihydrate	10 mg
Casamino acids	1 g
Glucose	5 g
Magnesium sulfate, heptahydrate	200 mg
Potassium phosphate, dibasic	13.8 g
Potassium phosphate, monobasic	2.73 g
Yeast extract	1 g

The glucose, yeast extract, and casamino acids were autoclaved separately from the salt solution and were added prior to inoculation. Ampicillin was either filter sterilized or added directly to the medium prior to inoculation.

SOC medium

One liter of SOC medium contained:

Bacto tryptone	20 g
Yeast extract	5 g
NaCl	0.5 g

Add the ingredients to 950 mL of H_2O and stir until completely dissolved. Add 10 mL of a 250 mM solution of KCl and adjust the pH to 7.0 with 5N NaOH. Make to 980 mL with H_2O and autoclave for 20 minutes at 121°C. Allow the medium to cool to 60°C and add 20 mL of a sterile 1 M glucose solution.

Transformation buffer

$CaCl_2$	100 mM
MOPS	10 mM
Glucose	0.5 % (w/v)
Glycerol	sterilized separately and added to the transformation when applicable.

SDS-PAGE stock solutions

Acrylamide/Bis (30%T, 2.67% C)

29.2 g	acrylamide
0.8 g	N',N'-bis-methylene-acrylamide

Add these components to ~70 mL of H_2O, stir until dissolved and then make to 100 mL with H_2O.

1.5 M Tris-HCl, pH 8.8

18.15 g	Tris

Add to ~60 mL H_2O, pH to 8.8 with 6N HCl and make to 100 mL with H_2O.

0.5 M Tris-HCl, pH 6.8

6 g	Tris

Add to ~60 mL H_2O, pH to 6.8 with 6N HCl and make to 100 mL with H_2O.

10 % SDS (w/v)

10 g	SDS

Add to ~ 90 mL of H_2O, stir unti lcompletely dissolved, and then make to 100 mL with H_2O.

10% APS (w/v)

20 mg	APS

Add to 200 µL of H_2O and mix until dissolved.

TEMED

Standard solution (BDH)

SDS-PAGE gel formulas

Separating Gel (12%)

	Bio-Rad	Hoefer
H_2O	3.35 mL	8.375 mL
1.5 M Tris, pH 8.8	2.5 mL	6.25 mL
10% SDS (w/v)	100 µL	250 µL
Acrylamide/Bis	4.0 mL	10.0 mL
10% APS (w/v)	50 µL	125 µL
TEMED	5 µL	12.5 µL

Stacking Gel

H_2O	6.1 mL
0.5 M Tris, pH 6.8	2.5 mL
10 % SDS (w/v)	100 µL
Acrylamide/Bis	1.33 mL
10% APS (w/v)	50 µL
TEMED	10 µL

Western blotting buffers

Electroblotting buffer

3.03 g	Tris
14.4 g	Glycine
200 mL	Methanol

Add the compounds to 700 mL H_2O and stir until completely dissolved. Adjust the pH to 8.3 and make to 1 L with H_2O.

Amino acid and nucleic acid sequences of the IucD gene

Met Lys Lys Ser Val Asp Phe Ile Gly Val[10] Gly Thr Gly Pro Phe Asn[16]
ATG AAA AAA AGT GTC GAT TTT ATT GGT GTA GGG ACA GGG CCA TTT AAT

Leu Ser Ile Ala[20] Ala Leu Ser His Gln Ile Glu Glu Leu Asp[30] Cys Leu[32]
CTC AGC ATT GCT GCG TTG TCA CAT CAG ATC GAA GAA CTG GAC TGT CTC

Phe Phe Asp Glu His Pro His Phe[40] Ser Trp His Pro Gly Met Leu Val[48]
TTC TTT GAT GAA CAT CCT CAT TTT TCC TGG CAT CCG GGT ATG CTG GTA

Pro Asp[50] Cys His Met Gln Thr Val Phe Leu Lys Asp[60] Leu Val Ser Ala[64]
CCG GAT TGT CAT ATG CAG ACC GTC TTT CTG AAA GAT CTG GTC AGT GCT

Val Ala Pro Thr Asn Pro[70] Tyr Ser Phe Val Asn Tyr Leu Val Lys His[80]
GTT GCA CCT ACA AAT CCC TAC AGT TTT GTT AAC TAT CTG GTG AAG CAC

Lys Lys Phe Tyr Arg Phe Leu Thr Ser Arg[90] Leu Arg Thr Val Ser Arg[96]
AAA AAG TTC TAT CGC TTC CTT ACA AGC AGA CTA CGT ACA GTA TCC CGT

Glu Glu Phe Ser[100] Asp Tyr Leu Arg Trp Ala Ala Glu Asp Met[110] Asn Asn[112]
GAA GAG TTT TCT GAC TAC CTC CGC TGG GCT GCT GAA GAT ATG AAT AAC

Leu Tyr Phe Ser His Thr Val Glu[120] Asn Ile Asp Phe Asp Lys Lys Arg[128]
CTG TAT TTC AGT CAT ACC GTT GAA AAC ATT GAT TTC GAT AAA AAA CGT

Arg Leu[130] Phe Leu Val Gln Thr Ser Gln Gly Glu Tyr[140] Phe Ala Arg Asn[144]
CGA TTG TTT CTG GTG CAA ACC AGC CAG GGA GAA TAT TTT GCC CGC AAT

Ile Cys Leu Gly Thr Gly[150] Lys Gln Pro Tyr Leu Pro Pro Cys Val Lys[160]
ATC TGC CTT GGT ACA GGA AAA CAA CCT TAT TTA CCA CCC TGT GTG AAG

His Met Thr Gln Ser Cys Phe His Ala Ser[170] Glu Met Asn Leu Arg Arg[176]
CAT ATG ACA CAA TCC TGT TTC CAT GCC AGT GAA ATG AAT CTT CGT CGG

Pro Asp Leu Ser[180] Gly Lys Arg Ile Thr Val Val Gly Gly Gly[190] Gln Ser[192]
CCG GAC CTT AGT GGA AAA CGG ATA ACC GTG GTT GGT GGA GGA CAG AGT

Gly Ala Asp Leu Phe Leu Asn Ala[200] Leu Arg Gly Glu Trp Gly Glu Ala[208]
GGT GCA GAC CTG TTC CTT AAT GCA TTA CGC GGG GAA TGG GGA GAA GCG

Ala Glu[210] Ile Asn Trp Val Ser Arg Arg Asn Asn Phe[220] Asn Ala Leu Asp[224]
GCG GAA ATA AAC TGG GTC TCC CGG CGT AAT AAT TTT AAC GCA CTG GAT

Glu Ala Ala Phe Ala Asp[230] Glu Tyr Phe Thr Pro Glu Tyr Ile Ser Gly[240]
GAG GCT GCT TTT GCT GAT GAG TAT TTT ACA CCT GAA TAT ATT TCA GGC

Phe Ser Gly Leu Glu Glu Asp Ile Arg His[250] Gln Leu Leu Asp Glu Gln[256]
TTC TCC GGA CTG GAG GAA GAT ATT CGC CAT CAG TTA CTG GAT GAG CAG

Lys Met Thr Ser[260] Asp Gly Ile Thr Ala Asp Ser Leu Leu Thr[270] Ile Tyr[272]
AAA ATG ACA TCG GAT GGC ATC ACT GCC GAT TCT TTA CTG ACC ATT TAT

Arg Glu Leu Tyr His Arg Phe Glu[280] Val Leu Arg Lys Pro Arg Asn Ile[288]
CGT GAG TTG TAC CAC CGT TTT GAA GTT CTG AGA AAA CCA AGA AAT ATC

Arg Leu[290] Leu Pro Ser Arg Ser Val Thr Thr Leu Glu[300] Ser Ser Gly Pro[304]
CGT CTG CTA CCC AGC CGC TCG GTA ACA ACT CTG GAA AGT AGT GGT CCT

Gly Trp Lys Leu Leu Met[310] Glu His His Leu Asp Gln Gly Arg Glu Ser[320]
GGC TGG AAG TTG CTG ATG GAG CAT CAT CTG GAT CAG GGC AGG GAG AGC

Leu Glu Ser Asp Val Val Ile Phe Ala Thr[330] Gly Tyr Arg Ser Ala Leu[336]
CTG GAA AGT GAT GTG GTG ATT TTC GCC ACA GGT TAC CGT TCT GCG TTG

Pro Gln Ile Leu[340] Pro Ser Leu Met Pro Leu Ile Thr Met His[350] Asp Lys[352]
CCA CAA ATA CTT CCC TCA CTG ATG CCC CTG ATC ACC ATG CAC GAT AAG

Asn Thr Phe Lys Val Arg Asp Asp[360] Phe Thr Leu Glu Trp Ser Gly Pro[368]
AAC ACC TTT AAA GTG CGT GAT GAC TTC ACT CTG GAA TGG AGT GGC CCG

Lys Glu[370] Asn Asn Ile Phe Val Val Asn Ala Ser Met[380] Gln Thr His Gly[384]
AAA GAG AAC AAC ATC TTC GTG GTC AAC GCC AGT ATG CAA ACC CAT GGC

Ile Ala Glu Pro Gln Leu[390] Ser Leu Met Ala Trp Arg Ser Ala Arg Ile[400]
ATC GCC GAA CCC CAG CTC AGC CTG ATG GCA TGG AGA TCT GCA CGT ATT

Leu Asn Arg Val Met Gly Arg Asp Leu Phe[410] Asp Leu Ser Met Pro Pro[416]
CTT AAT CGC GTA ATG GGA CGT GAT TTA TTC GAT CTC AGT ATG CCG CCC

Ala Leu Ile Gln[420] Trp Arg Ser Gly Thr[425] ter
GCC CTG ATT CAG TGG CGC AGC GGC ACC TAG

7.0 References

1. Neilands, J.B., Konopka, K., Schwyn, B., Coy, M., Francis, R.T., Paw, B.H., and Bagg, A. (1987) in *Iron Transport in Microbes, Plants and Animals* (Winkelmann, G., van der Helm, D., and Neilands, J.B., eds) pp. 3-33, VCH Press, Weinhelm.

2. Neilands, J.B. (1981) *Ann. Rev. Nutr.* **1**, 27-46.

3. Neilands, J.B. (1984) in *Structure and Bonding* **58**, 1-24, Springer-Verlag Publications, Berlin.

4. Neilands, J.B. (1994) in *The Development of Iron Chelators for Clinical Use* (Bergeron, R.J., and Brittenham, G.M., eds) pp. 151-168, CRC Press, Boca Raton.

5. Emery, T. (1982) *Amer. Scientist* **70**, 626-632.

6. Winkelmann, G., and Huschka, H-G. (1987) in *Iron Transport in Microbes, Plants and Animals* (Winkelmann, G., van der Helm, D., and Neilands, J.B., eds) pp. 317-336, VCH Press, Weinhelm.

7. Neilands, J.B. (1952) *J. Am. Chem. Soc.* **74**, 4846-4847.

8. Garibaldi, J.A., and Neilands, J.B. (1955) *J. Am. Chem.Soc.* **22**, 2429-2430.

9. McMurray, T.J., Raymond, K.N., and Smith, P.H. (1989) *Science* **244**, 938-943.

10. Raymond, K.N., Muller, G., and Matzanke, B.F. (1984) in *Topics in Current Chemistry; Structural Chemistry* (Boschke, F.L. ed.) pp. 49-102, Springer-Verlag, Berlin.

11. Raymond, K.N., and Carrano, C. (1979) *Acc. Chem. Res.* **12**, 183-190.

12. Ankenbauer, R.G., Toyokuni, T., Staley, A., Rinehart, K.L., Jr., and Cox, C.D. (1988) *J. Biol. Chem.* **170**, 5344-5351.

13. Roosenberg, J.M.,2nd, Lin, Y.M., Lu, Y., and Miller, M.J. (2000) *Curr. Med. Chem.* **7**, 159-97.

14. Maurer, P.J., and Miller, M.J. (1981) *J. Org. Chem.* **46**, 2835-2836.

15. Maurer, P.J., and Miller, M.J. (1982) *J. Am. Chem. Soc.* **104**, 3096-3101.

16. Peterson, T., Falk, K-E., Leong, S.A., Klein, M.P., and Neilands, J.B. (1980) *J. Am. Chem. Soc.* **102**, 7715-7718.

17. Corey, E.J., and Battacharyya, S. (1977) *Tetrahedron Lett.* **45**, 3919-3922.

18. Isowa, Y., Ohmori, M., and Kurita, H. (1974) *Bull. Chem. Soc. Japan* **47**, 215-220.

19. Fujii, T., and Hatanaka, Y. (1973) *Tetrahedron* **29**, 3825-3831.

20. Gibson, F. and Magrath, D.T. (1969) *Biochim. Biophys. Acta* **192**, 175-184.

21. Williams, P.H. (1979) *Infect. Immun.* **26**, 925-932.

22. Williams, P.H., and Warner, P.J. (1980) *Infect. Immun.* **29**, 411-416.

23. Neilands, J.B. (1992) *Can. J. Microbiol.* **38**, 728-733.

24. Gross, R., Engelbrecht, F., and Braun, V. (1984) *Mol. Gen. Genet.* **196**, 74-80.

25. Gross, R. Engelbrecht, F., and Braun V. (1985) *Mol. Gen. Genet.* **201**, 204-212.

26. de Lorenzo, V., Bindereif, A., Paw, B.H., and Neilands, J.B. (1986) *J. Bacteriol.* **165**, 570-578.

27. de Lorenzo, V., and Neilands, J.B. (1986) *J. Bacteriol.* **167**, 350-355.

28. Murray, G.J., Clark, G.E.D., Parniak, M.A., and Viswanatha, T. (1977) *Can. J. Biochem.* **55**,625-629.

29. Appana, D.L., Grundy, B.J., Szczepan, E.W., and Viswanatha, T. (1984) *Biochim. Biophys. Acta* **801**, 307-320.

30. de Lorenzo, V., Giovannini, F., Herrero, M., and Neilands, J.B. (1988) *J. Mol. Biol.* **203**, 875-884.

31. Neilands, J.B. (1995) *J. Biol. Chem.* **270**, 26723-26726.

32. Litwin, M., and Calderwood, S. (1993) *Clin Microbiol. Rev.* **6**, 137-149.

33. Tardat, B., and Touati, D. (1993) *Mol. Microbiol.* **9**, 53-63.

34. Zheng, M., Doan, B., Schneider, T.D., and Storz, G. (1999) *J. Bacteriol.* **181**, 4639-4643.

35. Hall, H.K., and Foster, J.W. (1996) *J. Bacteriol.* **178**, 5683-5691.

36. Hantke, K. (1987) *Mol. Gen. Genet.* **210**, 135-139.

37. Coy, M., and Neilands, J.B. (1991) *Biochemistry* **30**, 8201-8210.

38. Neilands, J.B. (1990) in *Advances in Inorganic Biochemistry* (Eichorn, G.L., and Marzilli, L.G., eds) **8**, 63-90, Elsevier, New York.

39. Althaus, E.W., Outten, C.E., Olson, K.E., Cao, H., and O'Halloran, T.V. (1999) *Biochemistry* **38**, 6559-6569.

40. Parniak, M.A., Jackson, G.E.D., Murray, G.J., and Viswanatha, T. (1979) *Biochim. Biophys. Acta* **569**, 99-108.

41. Goh, C.J., Szczepan, E.W., Wright, G., Menhart, N., Honek, J.F., and Viswanatha, T. (1989) *Bioorg. Chem* **17**, 13-27.

42. Szczepan, E.W., Kaller, D., Honek, J.F., and Viswanatha, T. (1987) *FEBS Lett.* **211**, 239-242.

43. Jackson, G.E.D., Parniak, M.A., Murray, G.J., and Viswanatha, T. (1984) *J. Cell. Biochem.* **24**, 395-403.

44. Herrero, M., de Lorenzo, V., and Neilands, J.B. (1988) *J. Bacteriol.* **170**, 56-64.

45. Goh, C.J., Szczepan, E.W., Menhart, N., and Viswanatha, T. (1989) *Biochim. Biophys. Acta* **990**, 240-245.

46. Thariath, A.M., Socha, D., Valvano, M.A., and Viswanatha, T. (1993) *J. Bacteriol.* **175**, 589-596.

47. Thariath, A.M., Fatum, K.L., Valvano, M.A., and Viswanatha, T. (1993) *Biochim. Biophys. Acta* **1203**, 27-35.

48. Yanisch-Peron, C., Vieira, J., and Messing, J. (1985) *Gene* **33**, 103-119.

49. Wierenga, R.K., Terpstra, P., and Hol, W.G.J. (1986) *J. Mol. Biol.* **187**, 101-107.

50. Schreuder, H.A., van der Laan, J.M., Hol, W.G.J., and Drenth, J. (1990) *in Chemistry and Biochemistry of Flavoenzymes* (Muller, F. ed) **2**, 31-60, CRC Press, Boca Raton.

51. Stehr, M., Diekmann, H., Smau, L., Seth, O., Ghisla, S., Singh, M., and Macheroux, P. (1998) *Trends Biochem. Sci.* **23**,56-57.

52. Stehr, M., Smau, L., Singh, M., Seth, O., Macheroux, P., Ghisla, S., and Diekmann, H. (1999) *Biol. Chem.* **380**, 47-54.

53. Dick, S., Marrone, L., Thariath, A.M., Valvano, M.A., and Viswanatha, T. (1998) *Trends Biochem. Sci.* **23**, 414.

54. Gatti, D.L., Palfey, B.A., Lah, M.S., Entsch, B., Massey, V., Ballou, D.P., and Ludwig, M.L. (1994) *Science* **266**, 110-114.

55. Doussiere, J., Laporte, F., and Vignais, P.V. (1986) *Biochem. Biophys. Res. Comm.* **139**, 85-94.

56. Thariath, A.M., Valvano, M.A., and Viswanatha, T. (1994) in *The Development of Iron Chelators for Clinical Use* (Bergeron, R.J., and Brittenham, G.M., eds) pp. 169-186, CRC Press, Boca Raton.

57. Viswanatha, T. Szczepan, E.W. and Murray, G.J. (1987) in *Iron Transport in Microbes, Plants and Animals* (Winkelmann, G., van der Helm, D., and Neilands, J.B., eds) pp. 117-132, VCH Press, Weinhelm.

58. Marrone, L., Beecorft, M., and Viswanatha, T. (1996) *Bioorg. Chem.* **24**, 304-317.

59. Marrone, L., and Viswanatha, T. (1997) *Biochim. Biophys. Acta* **1343**, 263-277.

60. Hadler, H.I., Erwin, M.J., and Lardy, H.A. (1963) *J. Am. Chem. Soc.* **85**, 458-461.

61. Hadler, H.I., and Erwin, M.J. (1963) *Biochemistry* **2**, 954-957.

62. Hadler, H.I., Alt, S.K., and Falcone, A.B. (1966) *J. Biol. Chem.* **241**, 2886-2890.

63. Hille, R., and Nishino, T. (1995) *FASEB J.* **9**, 995-1003.

64. Hille, R. (1996) *Chem. Rev.* **97**, 2757-2816.

65. Massey, V., and Harris, C.M. (1997) *Biochem. Soc. Trans.* **25**, 750-755.

66. Nishino, T., Nishino, T., Schopfer, L.M., and Massey, V. (1989) *J. Biol. Chem.* **264**, 2518-2527.

67. Hille, R. (1992) in *Chemistry and Biochemistry of Flavoenzymes* (Muller, F., ed) 2, 21-62, CRC Press, Boca Raton.

68. Della Corte, E., and Stripe, F. (1972) *Biochem. J.* **126**, 739-745.

69. QIAprep Miniprep Handbook (July, 1999) Qiagen Inc., Chatsworth, CA.

70. QIAGEN Plasmid Purification Handbook (November, 1998) Qiagen Inc., Chatsworth, CA.

71. QIAquick Spin Handbook (January, 1999) Qiagen Inc., Chatsworth, CA.

72. MabTrap GII Instruction Manual, Edition AB (1999) Amersham Pharmacia Biotech AB, Uppsala, Sweden.

73. Sambrook, J., Fritsch, E.F., and Maniatis, T. (1989) in *Molecular Cloning: A Laboratory Manual, 2nd Edition* p. 1.78, Cold Spring Harbor Press, Cold Spring Harbor.

74. Sambrook, J., Fritsch, E.F., and Maniatis, T. (1989) in *Molecular Cloning: A Laboratory Manual, 2nd Edition* p. B.24, Cold Spring Harbor Press, Cold Spring Harbor.

75. Cohen, S.N., Chang, A.C.Y., and Hsu, L. (1972) *Proc. Natl. Acad. Sci. USA* **69**, 2110-2114.

76. Thariath, A.M. (1993) Ph.D. Thesis, University of Waterloo.

77. *E. coli* Pulser Transformation Apparatus Operating Instructions and Applications Guide (1992) p. 8-9, BioRad Laboratories, Inc., Hercules, CA.

78. Sambrook, J., Fritsch, E.F., and Maniatis, T. (1989) in *Molecular Cloning: A Laboratory Manual, 2nd Edition* p. 6.1-6.26, Cold Spring Harbor Press, Cold Spring Harbor.

79. QuickChange™ Site Directed Mutagenesis Kit, Intruction Manual, Catalog #200518, Revision #125001 (1995) Stratagene Cloning Systems, La Jolla, CA.

80. Davis, A.L., Skinner, G.G., and Shive, W. (1961) *J. Am. Chem. Soc.* **83**, 2279-2281.

81. Mizusaki, K., Sugahara, Y., Tsunematsu, H., and Makisumi, S. (1986) *J. Biochem.* **100**, 21-25.

82. Martin, B., Svendsen, I., and Ottesen, M. (1977) *Carlsberg Res. Commun.* **42**, 99-102.

83. Spackman, D.H., Stein, W.H., and Moore, S. (1958) *Anal. Chem.* **30**, 1190-1206.

84. Cowen, D.A., and Daniel, R.M. (1982) *Biotech. Bioeng.* **24**, 2053-2061.

85. Breddam, K. (1986) *Carlsberg Res. Commun.* **51**, 83-128.

86. Laemmli, U.K. (1970) *Nature* **227**, 680-685.

87. Bradford, M.M. (1976) *Anal. Biochem.* **72**, 248-254.

88. Sambrook, J., Fritsch, E.F., and Maniatis, T. (1989) in *Molecular Cloning: A Laboratory Manual, 2nd Edition* pp. C1, E5, Cold Spring Harbor Press, Cold Spring Harbor.

89. Tomlinson, G., Cruickshank, W.H., and Viswanatha, T. (1971) *Anal. Biochem.* **44**, 670-679.

90. Marquart, D.W. (1963) *J. Soc. Ind. Appl. Math.* **11**, 431-441.

91. Hildebrandt, A.G., Roots, L., Tjoe, M., and Heinemeyer, G. (1978) *Methods in Enzymol.* **52**, 342-350.

92. Ellman, G.L. (1959) *Arch Biochim. Biophys.* **82**, 70-77.

93. Riddles, P.W., Blakely, R.L., and Zerner, B. (1979) *Anal. Biochem.* **94**, 75-81.

94. Massey, V. (1958) *Biochim. Biophys. Acta* **30**, 205-206.

95. Trimboli, A.J., Quinn, G.B., Smith, E.T., and Barber, M.J. (1996) *Arch. Biochem. Biophys.* **331**, 117-126.

96. Blake, M.S., Johnston, K.H., Russell-Jones, G.J., and Gotshlich, E.C. (1984) *Anal. Biochem.* **136**, 175-179.

97. Monod, J., Changeux, J.P., and Jacob, F. (1963) *J. Mol. Biol.* **6**, 306-329.

98. Monod, J., Wyman, J., and Changeux, J.P. (1965) *J. Mol. Biol.* **12**, 88-118.

99. Marrone, L., Siemann, S., Beecroft, M., and Viswanatha, T. (1996) *Bioorg. Chem.* **24**, 401-416.

100. Claiborne, A., Yeh, J.I, Mallett, T.C., Luba, J., Crane, E.J., 3rd, Charrier, V., and Parsonage, D. (1999) *Biochemistry* **38**, 15407-16

101. Benitez, L.V., and Allison, W.S. (1974) *J. Biol. Chem.* **249**, 6234-6243.

102. Allison, W.S. (1976) *Acc. Chem. Res.* **9**, 293-299.

103. Marrone, L. (1996) Ph.D. Thesis, University of Waterloo.

104. Enroth, C., Neujahr, H., Schneider, G., and Lindquist, Y. (1998) *Structure* **6**, 605-617.

105. Harman, J.T., Nielsen, T.B., and Kempner, E.S. (1985) *Methods Enzymol.* **117**, 65-94.

106. Kempner, E.S. (1988) *Adv. Enzymol.* **61**, 107-147.

107. van der Laan, J.M., Schreuder, H.A., Swarte, M.B.A., Wierenga, R.K., Kalk, K.H., Hol, W.G.J., and Drenth, J. (1989) *Biochemistry* **28**, 7199-7205.

108. Swoboda, P.E. (1969) *Biochim. Biophys. Acta* **175**, 365-379.

109. Jacobs, G., and Cunningham, L.W. (1968) *Biochemistry* **7**, 143-151.

110. Chen, S., Deng, P.S., Bailey, J.M., and Swiderek, K.M. (1994) *Protein Sci.* **3**, 51-57.

111. Yu, M., Souaya, J., and Julin, D.A. (1998) *Proc. Natl. Acad. Sci. USA* **95**, 981-986.

112. Dai, Y. and Wang, C. (1997) *J. Biol. Chem.* **272**, 27572-27576.

113. Albalat, R., Valls, M., Fibla, J., Atrian, S., and Gonzalez-Duarte, R. (1995) *Eur. J. Biochem.* **233**, 498-505.

114. Walter, R.A., Nairn, J., Duncan, D., Price, N.C., Kelly, S.M., Rigden, D.J., and Fothergill-Gilmore, L.A. (1999) *Biochem. J.* **337**, 89-95.

115. Nechustan, A., Smith, C.L., Hsu, Y.T., and Youle, R.J. (1999) *EMBO J.* **18**, 2330-2341.

116. Shimada, Y., Makamura, M., Naito, Y., Nomura, K., and Ohno-Iwashita, Y. (1999) *J. Biol. Chem.* **274**, 18536-18542.

117. Criado, M., Gil, A., Viniegra, S., and Gutirrez, L.M. (1999) *Proc. Natl. Acad. Sci. USA* **96**, 7256-7261.

118. Mata, L., Gripon, J.C., and Mistou, M.Y. (1999) *Protein Eng.* **12**, 681-686.

119. Allardyce, C.S., McDonagh, P.D., Lian, L.Y., Wolf, C.R., and Roberts, G.C.K. (1999) *Biochem. J.* **343**, 525-531.

120. Mattevi, A., Schierbeck, A.J., and Hol, W.G.J. (1991) *J. Mol. Biol.* **220**, 975-994.

121. Benen, J., van Berkel, W., Veeger, C., and de Kok, A. (1992) *Eur. J. Biochem.* **207**, 499-505.

122. Linderstrøm-Lang, K. (1949) Cold Spring Harbor Symposia *Quant. Biol.* **14**, 117.

123. *Proteolytic Enzymes: a practical approach* (1990) (Benyon, R.J., and Bond, J.S., eds.) IRC Press, New York.

124. Schechter, I., and Berger, A. (1967) *Biochem. Biophys. Res. Commun.* **27**, 157-162.

125. Pal, D., and Chakrabarti, P. (1999) *J. Mol. Biol.* **294**, 271-288.